Lattice Boltzmann methods for CFD

Manfred Krafczyk
kraft@irmb.tu-bs.de
http://www.cab.bau.tu-bs.de
contributors:
B. Ahrenholz, S. Freudiger, S. Geller, B. Nachtwey, M. Stiebler, J. Tölke,
IRMB, TU Braunschweig

A. Düster, LS Bauinformatik, TU Munich

Overview

- **Lattice Gases:**
  A short trip back to the roots of physics of fluids
- **The mesoscopic picture:**
  The Lattice-Boltzmann equation
- **hydrodynamic limits and moments of distributions**

continuous fluid

particle ensemble (real gas)

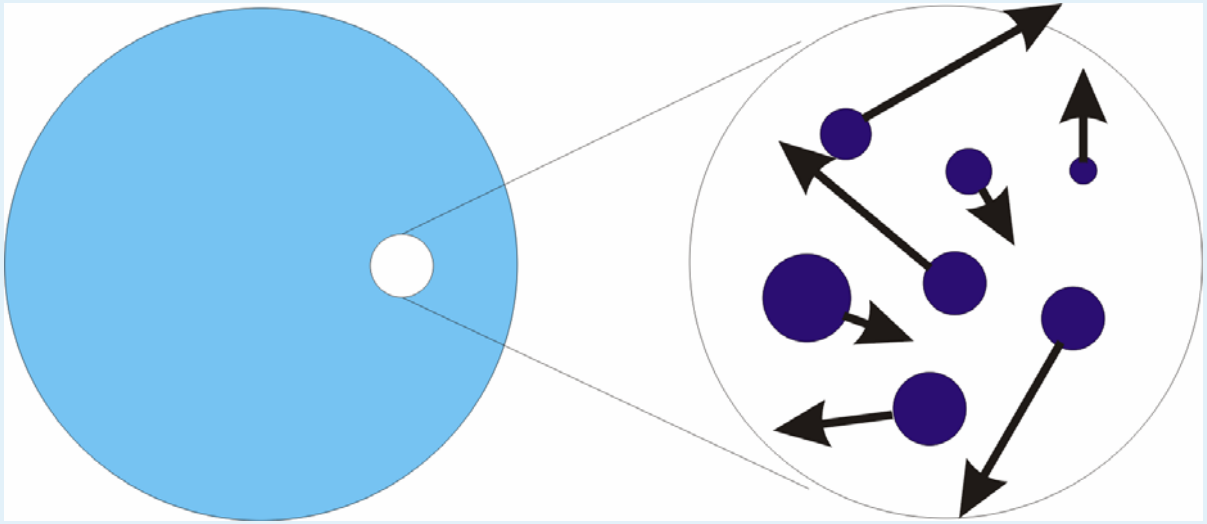

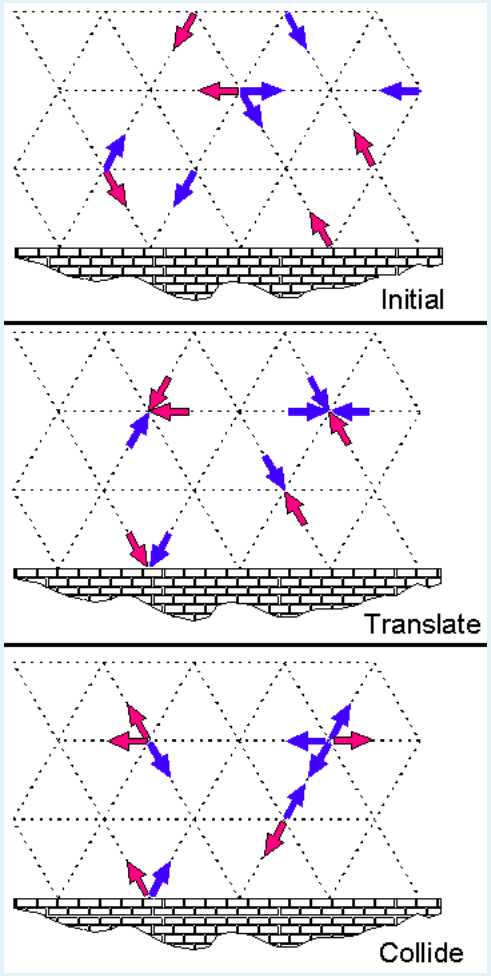

$$\mathrm{p}, \nu, \vec{\mathrm{v}}(\vec{\mathrm{r}}, \mathrm{t}), \rho$$

$$\mathrm{m_i}, \omega, \vec{\mathrm{v}}_\mathrm{i}(\vec{\mathrm{r}}, \mathrm{t})$$

$$\frac{\partial \vec{u}}{\partial t} + \vec{u}\nabla \otimes \vec{u} = -\nabla p^* + \nu \Delta \vec{u}$$

$$m_i \frac{\partial v_i}{\partial t} = \sum_{i \neq j} \frac{\partial V(\|\vec{r}_i - \vec{r}_j\|)}{\partial \vec{r}_j}$$

$$\vec{\mathrm{e}}_\mathrm{i}(\vec{\mathrm{r}}, \mathrm{t})$$

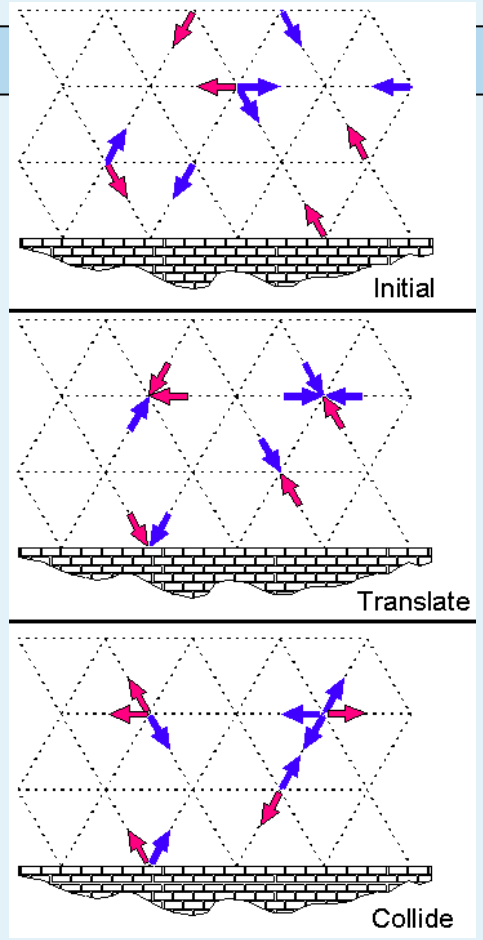

Evolution equation for ‚digital' particles:

$$n_i\left(\vec{x}+\vec{e}_i\delta t, t+\delta t\right)-n_i\left(\vec{x},t\right)=\Omega_i$$

Coupling to ‚real world properties' via moments:

$$\rho=\sum_{i=0}^{m-1} n_i \qquad \vec{u}=\frac{1}{\rho}\sum_{i=1}^{m-1} n_i\vec{e}_i \qquad p_\infty = c_s^2(\rho-\rho_0)$$

Chapman-Enskog expansion shows:

Dynamics of velocity and pressure is (for Kn,Ma→0) equivalent to that given by the Navier-Stokes equations:

$$\frac{\partial\rho}{\partial t}+\nabla\vec{u}=0 \qquad \frac{\partial\vec{u}}{\partial t}+\vec{u}\nabla\vec{u}=-\frac{1}{\rho_0}\nabla p_\infty+\nu\nabla^2(\rho\vec{u})$$

Problems

- Lack of Galilean Invariance
- Anomalous velocity dependence of the fluid pressure

$$\left\langle n_i^{eq} \right\rangle = \frac{\rho}{b}(1 + e_{i\alpha}u_\alpha / c_s^2 + GQ_{\alpha\beta}u_\alpha u_\beta / 2c_s^4)$$

$$G(\rho) = \frac{1 - 2\frac{\rho}{b}}{1 - \frac{\rho}{b}} \neq 1$$

$$\sum_i \left\langle n_i^{eq} \right\rangle e_{i\alpha}e_{i\beta} = \rho(gu_\alpha u_\beta + c_s^2(1 - gMa^2)\delta_{\alpha\beta})$$

$$g(\rho) = \frac{D}{D+2}G(\rho) \neq 1$$

- Statistical noise
- High viscosity (low „element Re“)
- Exponential complexity of collision operator
- Spurious invariants

from Boltzmann to Navier Stokes and LBGK

small Knudsen number

Boltzmann equation

$$\frac{\partial f}{\partial t} + \vec{\xi}\frac{\partial f}{\partial \vec{x}} = \Omega(f, f)$$

Chapman-Enskog-Expansion

BGK-Approximation (Bhatnagar, Gross, Krook)

Navier Stokes equations

$$\frac{\partial \vec{v}}{\partial t} + (\vec{v}\nabla)\vec{v} = -\frac{1}{\rho}\nabla p + \frac{\eta}{\rho}\Delta\vec{v}$$

continuity equation

$$\frac{\partial \rho}{\partial t} + \nabla(\rho\vec{u}) = 0$$

$$\frac{\partial f}{\partial t} + \vec{\xi}\frac{\partial f}{\partial \vec{x}} = -\frac{1}{\tau}\left(f - f^{(0)}\right)$$

discretization in space and time

Lattice Boltzmann equation (LBGK)

$$f_i(t+\Delta t, \vec{x}+\xi_i\Delta t) = f_i(t,\vec{x}) - \frac{\Delta t}{\tau}\left(f_i(t,\vec{x}), f_i^{(0)}(t,\vec{x})\right)$$

small Knudsen number
small Mach number

Chapman-Enskog-Expansion

Lattice-Bhatnagar-Gross-Krook (LBGK) models for Navier-Stokes problems

Starting with the Boltzmann equation

$$\frac{\partial f}{\partial t} + \vec{\upsilon}\nabla f = \Omega$$

the phase space can be discretized resulting in

$$\frac{\partial f_i(\vec{x},t)}{\partial t} + \vec{e}_i \nabla f(\vec{x},t) = \Omega_i\left(\left\{f_j(\vec{x},t)\right\}\right), i, j \in \{1,\ldots,n\} \qquad (1)$$

Additional simplification (Bhatnagar Gross-Krook):

Ω is described by a 'Single Time Relaxation Approximation' (STRA) of the form

$$\Omega_i = -\frac{1}{\tau}(f_i - f_i^{eq})$$

Macroscopic flow variables and can be defined as moments of f_i

$$\rho = \sum_{i=0}^{m-1} f_i \qquad \vec{u} = \frac{1}{\rho} \sum_{i=1}^{m-1} f_i \vec{e}_i$$

Equations (1) can be solved e.g. by FD schemes

$$f_i\left(\vec{x} + \vec{e}_i \delta t, t + \delta t\right) - f_i\left(\vec{x}, t\right) = -\frac{1}{\tau}\left(f_i\left(\vec{x}, t\right) - f_i^{eq}\left(\vec{x}, t\right)\right)$$

The kinematic viscosity can be identified as $\nu = \frac{2\tau - 1}{6} \frac{\delta h^2}{\delta t}$

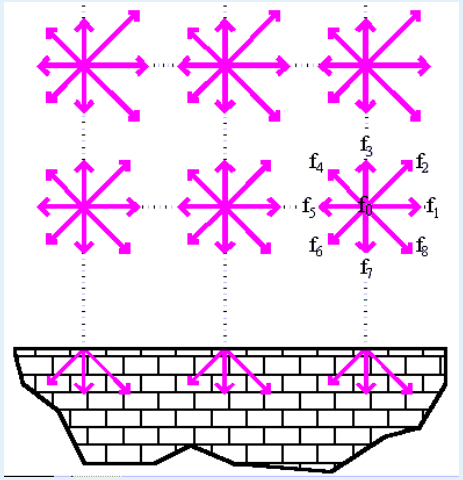

D3Q19 model

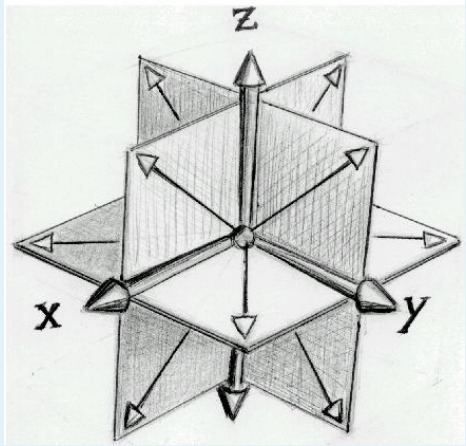

The LB-equation $$f_i\left(\vec{x}+\vec{e}_i\delta t, t+\delta t\right)-f_i\left(\vec{x},t\right)=\Omega_i\left(\{f_j\left(\vec{x},t\right)\}\right)$$

Typical claims (prejudices ??) found in the literature:

- suited for flows in complex geometries
- efficient for complex fluids (especially multiphase problems)
- easy to vectorize
- very good scaling on parallel machines
- no numerical scheme („cellular automata“)
- easy to program

Do LB methods really do a better job than ‚conventional' approaches ?
or
are they numerically efficient ?

structural advantages:

- ***Linear*** and ***exact*** advection operator
- conservative scheme for mass and momentum
- no numerical viscosity
- local shear stress tensor

$$S_{\alpha\beta} = \left(\frac{\Delta t}{2\tau} - 1\right) \sum_i \mathrm{v}_{i\alpha} \mathrm{v}_{i\beta} f_i^{(neq)}$$

structural disadvantages:

- conditionally stable
- cartesian grids
- inherently transient scheme
- more DOF per node than Navier-Stokes CFD solvers (3/9 in 2D, 13-27/4 in 3D)

Chapman-Enskog expansion in a nutshell:

rescaling

$$\Theta = \frac{\partial \hat{f}}{\partial \hat{t}} + \hat{\vec{\upsilon}} \nabla \hat{f} = -\frac{1}{\varepsilon}(\hat{f}_i - \hat{f}_i^{eq}), \varepsilon = \frac{c_r \tau}{L_r}$$

expansion:

$$f = \sum_{k=0}^{\infty} \varepsilon^k f^{(k)}, f^{(0)} = f^{(eq)}$$

Definition of moments:

$$\rho = \int f d\vec{v} = \int f^{(0)} d\vec{v} \qquad \rho u_\alpha = \int v_\alpha f d\vec{v} = \int v_\alpha f^{(0)} d\vec{v}$$

$$D_{\alpha\beta} = \int v_\alpha v_\beta f d\vec{v}$$

Taking into account terms for k=0,1,2, ... results in a hierarchy of equations

$$\Theta^0(\hat{f}^{(0)}) = 0$$
$$\Theta^1(\hat{f}^{(0)}, \hat{f}^{(1)}) = 0$$
$$\Theta^2(\hat{f}^{(0)}, \hat{f}^{(1)}, \hat{f}^{(2)}) = 0$$

Analysis of the first order terms $\{\hat{f}^{(0)}, \hat{f}^{(1)}, \hat{f}^{(2)}\}$ shows, that the dynamics of the hydrodynamic moments of f (ρ and u) in the limit of low Mach- und Knudsen numbers is described by the Navier-Stokes equations

$$\frac{\partial \rho}{\partial t} + \nabla(\rho \vec{u}) = 0$$

$$\frac{\partial \rho \vec{u}}{\partial t} + \nabla(\rho \vec{u} \vec{u}) = -\nabla p + \nabla \overline{\overline{\tau}}$$

$$\overline{\overline{\tau}} = \mu(\nabla \vec{u} + (\nabla \vec{u})^T) - \frac{2}{3}\mu(\nabla \vec{u})\overline{\overline{I}}$$

Computational aspects

- no Poisson equation is solved for the pressure
- Boundary conditions of Dirichlet and Neumann type can (have to) be set via f
- Convergence properties:
  LBE can be tuned to second-order accuracy with respect to the corresponding solution of one-phase Navier-Stokes flow
- Because of their explicit nature LBGK models are optimally suited for vectorization and parallelization
- For many practical applications LBGK's computational efficiency has been shown to be comparable to state-of-the-art FV, FE or FD discretizations of the corresponding Navier-Stokes problem
- Implicit and multigrid discretizations or FEM and FV variants can be constructed

NS = LB + O(Kn^2) + O(Ma^2) + O(dt*Ma) + O(dx^2)

→ test case: Taylor vortex

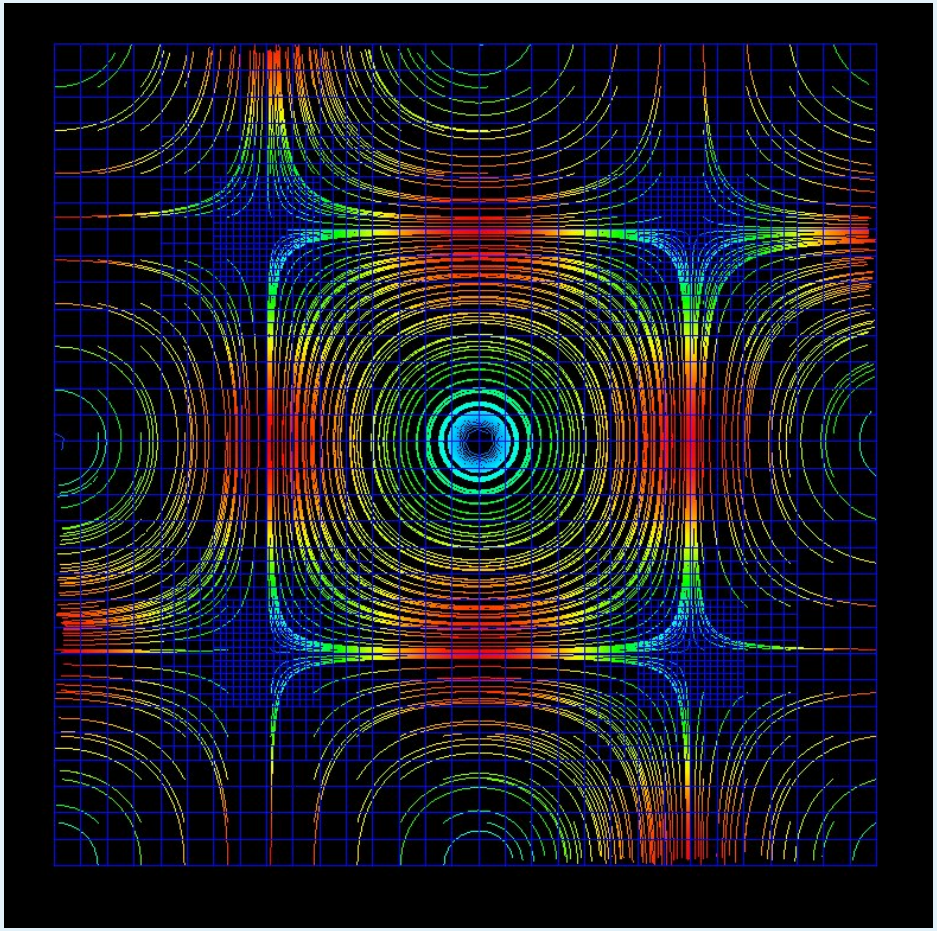

$$E2(T) = \frac{\sqrt{\sum_i (u(\vec{x},t) - u_{ex}(\vec{x},t))^2}}{\sum_i u_{ex}(\vec{x},t)^2}$$

Re=50
periodic BCs

level	Ma	E2	exponent
5	0,026041	0,002272	-2,075082
6	0,013020	0,000550	-1,904702
7	0,006501	0,000140	-1,973622
8	0,003250	0,000034	-1,989559
9	0,001625	0,000008	-2,001034

- Chapman-Enskog Analysis
- Derivation of the discrete Boltzmann equation
- Finite Difference Discretisation
- Multi-Relaxation-Time

The Boltzmann equation

$$\frac{\partial f(t,\mathbf{v},\mathbf{x})}{\partial t} + \mathbf{v} \bullet \nabla f(t,\mathbf{v},\mathbf{x}) = \Omega(t,\mathbf{v},\mathbf{x})$$

f	Particle distribution function
Ω	collision operator
$\mathbf{v}$	microscopic velocity
$\mathbf{x}$	Position

Macroscopic quantities are moments with respect to **v** :

Dichte $$\rho(t,\mathbf{x}) = \int_{-\infty}^{+\infty} f(t,\mathbf{v},\mathbf{x})\, d\mathbf{v}$$

Impuls $$\mathbf{u}(t,\mathbf{x}) = \int_{-\infty}^{+\infty} \mathbf{v}\, f(t,\mathbf{v},\mathbf{x})\, d\mathbf{v}$$

pressure tensor (scalar pressure +shear stresses):

$$P_{\alpha\beta}(t,\mathbf{x}) = \int_{-\infty}^{+\infty} (v_\alpha - u_\alpha)(v_\beta - u_\beta) f(t,\mathbf{v},\mathbf{x})\, d\mathbf{v}$$

$$P_{\alpha\beta}(t,\mathbf{x}) = -\rho\, u_\alpha u_\beta + \int_{-\infty}^{+\infty} v_\alpha\, v_\beta\, f(t,\mathbf{v},\mathbf{x})\, d\mathbf{v}$$

collision operator:

mass conservation:

$$\int_{-\infty}^{+\infty} \Omega(t, \mathbf{v}, \mathbf{x})\, d\mathbf{v} = 0$$

momentum conservation:

$$\int_{-\infty}^{+\infty} \mathbf{v}\, \Omega(t, \mathbf{v}, \mathbf{x})\, d\mathbf{v} = 0$$

uniform state solution: Maxwell distribution

$$f^{eq}(t, \mathbf{v}, \mathbf{x}) = \frac{\rho}{(2\pi c_s^2)^{D/2}} \exp\left(-\frac{(\mathbf{v}-\mathbf{u})^2}{2 c_s^2}\right)$$

continuum limit:

$$Kn = \frac{\lambda_r}{L_r} << 1$$

Kn Knudsen number

λ_r mean free path of particles

L_r macroscopic reference length

continuum limit:

small deviations from equilibrium:

simplified collision operator

$$\Omega = -\frac{1}{\tau}(f - f^{eq})$$

τ relaxation time

Ansatz: solution f should only depend on

macroscopic (i.e. hydrodynamic and beyond) moments

zero order moment of the Boltzmann-equation:

$$\int_{-\infty}^{+\infty} \left(\frac{\partial f(t,\mathbf{v},\mathbf{x})}{\partial t} + \mathbf{v} \bullet \nabla f(t,\mathbf{v},\mathbf{x}) = \Omega(t,\mathbf{v},\mathbf{x}) \right) d\mathbf{v}$$

$$\frac{\partial}{\partial t} \int_{-\infty}^{+\infty} f(t,\mathbf{v},\mathbf{x})\, d\mathbf{v} + \nabla \bullet \int_{-\infty}^{+\infty} \mathbf{v}\, f(t,\mathbf{v},\mathbf{x})\, d\mathbf{v} = 0$$

continuity equation:

$$\Rightarrow \quad \frac{\partial}{\partial t} \rho(t,\mathbf{x}) + \nabla \bullet \rho\, \mathbf{u}(t,\mathbf{x}) = 0$$

first order moment of the Boltzmann-equation:

$$\int_{-\infty}^{+\infty} \mathbf{v}\left(\frac{\partial f(t,\mathbf{v},\mathbf{x})}{\partial t} + \mathbf{v} \bullet \nabla f(t,\mathbf{v},\mathbf{x}) = \Omega(t,\mathbf{v},\mathbf{x})\right) d\mathbf{v}$$

$$\frac{\partial}{\partial t}\int_{-\infty}^{+\infty} v_\alpha \, f(t,\mathbf{v},\mathbf{x})\, d\mathbf{v} + \frac{\partial}{\partial x_\beta}\int_{-\infty}^{+\infty} v_\alpha v_\beta \, f(t,\mathbf{v},\mathbf{x})\, d\mathbf{v} = 0$$

where $$\int_{-\infty}^{+\infty} v_\alpha \, v_\beta \, f(t,\mathbf{v},\mathbf{x})\, d\mathbf{v} = \rho\, u_\alpha u_\beta + P_{\alpha\beta}(t,\mathbf{x})$$

momentum equation:

$$\Rightarrow \quad \frac{\partial}{\partial t}\rho u_\alpha(t,\mathbf{x}) + \frac{\partial}{\partial x_\beta}\rho\, u_\alpha u_\beta(t,\mathbf{x}) + \frac{\partial}{\partial x_\beta} P_{\alpha\beta} = 0$$

Problem:

pressure tensor should be expressed in macroscopic quantities!

first order appr.: $$f(t,\mathbf{v},\mathbf{x}) \approx f^{eq}(\rho(t,\mathbf{x}),u(t,\mathbf{x}),\mathbf{v})$$

$$P^{(0)}_{\alpha\beta}(t,\mathbf{x}) = \int_{-\infty}^{+\infty}(v_\alpha - u_\alpha)(v_\beta - u_\beta) f^{eq}(t,\mathbf{v},\mathbf{x})\,d\mathbf{v} = {c_s}^2 \rho(t,\mathbf{x})$$

Euler equation:

$$\Rightarrow \frac{\partial}{\partial t}\rho u_\alpha(t,\mathbf{x}) + \frac{\partial}{\partial x_\beta}\rho\, u_\alpha u_\beta(t,\mathbf{x}) + \frac{\partial}{\partial x_\alpha}{c_s}^2 \rho(t,\mathbf{x}) = 0$$

Chapman-Enskog expansion (dimensionless):

Knudsen number:

$$\varepsilon = \frac{c_r \tau}{L_r} << 1$$

$$f = \sum_{k=0}^{\infty} \varepsilon^k f^{(k)}$$

Boltzmann equation:

$$\frac{\partial}{\partial t}(f^{(0)} + \varepsilon f^{(1)}) + \boldsymbol{\upsilon} \bullet \nabla (f^{(0)} + \varepsilon f^{(1)}) =$$

$$-\frac{1}{\varepsilon}(f^{(0)} + \varepsilon f^{(1)} - f^{(eq)})$$

sorting the equations order by order:

order	equation
$1/\varepsilon$	$f^{(0)} = f^{(eq)}$
1	$\frac{\partial}{\partial t} f^{(0)} + \mathbf{v} \bullet \nabla f^{(0)} = f^{(1)}$
ε	$\frac{\partial}{\partial t} f^{(1)} + \mathbf{v} \bullet \nabla f^{(1)} = f^{(2)}$

estimation of f^{1} (dimensional):

$$f^{(1)} = -\tau \left(\frac{\partial}{\partial t} f^{(0)} + \mathbf{v} \bullet \nabla f^{(0)} \right) =$$

$$-\tau \left(\frac{\partial f^{(0)}}{\partial \rho} \frac{\partial \rho}{\partial t} + \frac{\partial f^{(0)}}{\partial u} \frac{\partial u}{\partial t} + \mathbf{v} \bullet \nabla f^{(0)} \right)$$

$\frac{\partial \rho}{\partial t}$ ⇒ continuity-equation

$\frac{\partial u}{\partial t}$ ⇒ Euler-equation

$$P_{\alpha\beta} = P_{\alpha\beta}^{(0)} + P_{\alpha\beta}^{(1)} =$$

$$c_s^2 \rho + \int_{-\infty}^{+\infty} (v_\alpha - u_\alpha)(v_\beta - u_\beta) f^{(1)}(t, \mathbf{v}, \mathbf{x})\, d\mathbf{v} =$$

$$c_s{}^2 \rho - c_s{}^2 \rho \tau \left(\frac{\partial u_\alpha}{\partial x_\beta} + \frac{\partial u_\beta}{\partial x_\alpha}\right)$$

⇒ Navier-Stokes equation

$$\frac{\partial}{\partial t} \rho u_\alpha + \frac{\partial}{\partial x_\beta} \rho u_\alpha u_\beta + \frac{\partial}{\partial x_\beta} \left(c_s{}^2 \rho \delta_{\alpha\beta} - \mu \left(\frac{\partial u_\alpha}{\partial x_\beta} + \frac{\partial u_\beta}{\partial x_\alpha}\right)\right) = 0$$

viscosity: $\mu = c_s^2 \rho \tau$

The discrete Boltzmann equation

small Knudsen+
large Mach number

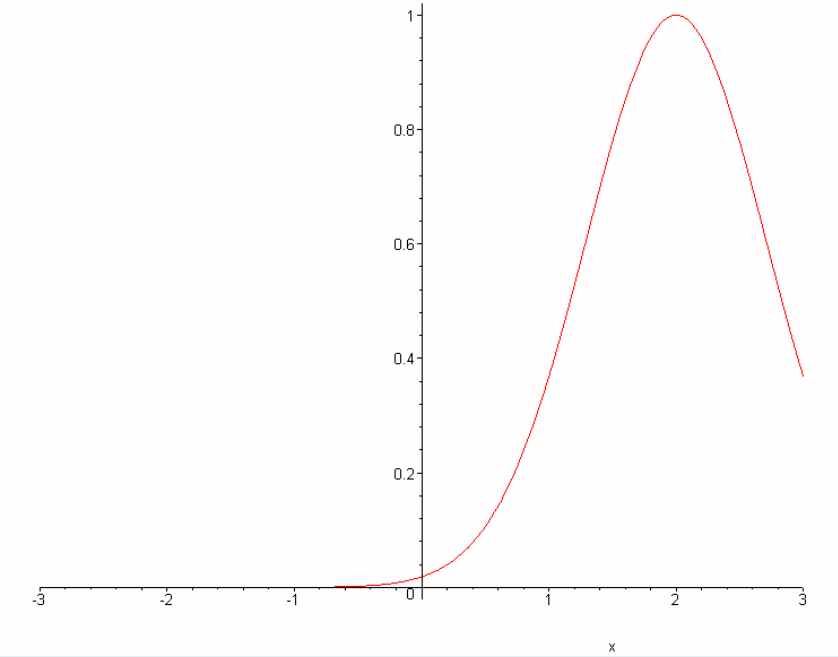

small Knudsen+
small Mach number

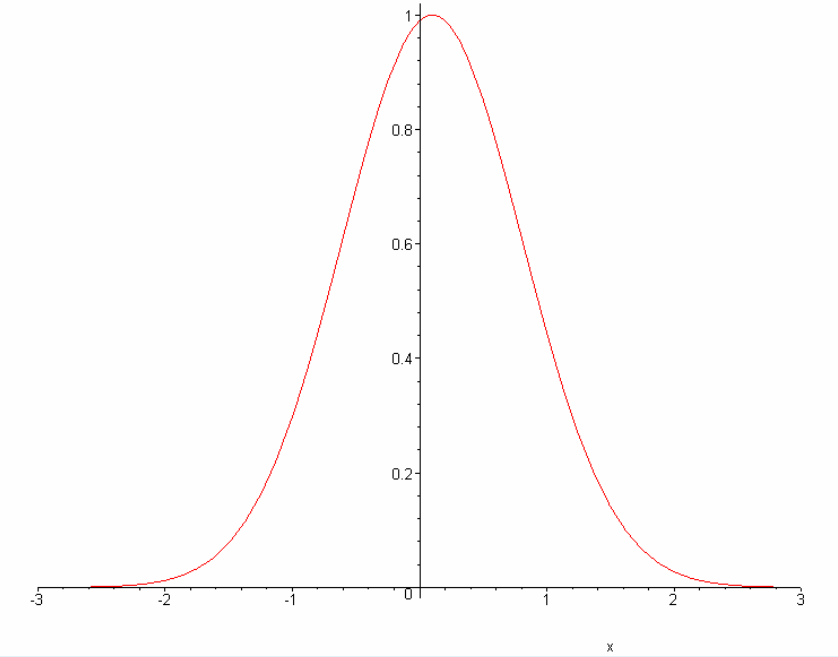

small Knudsen+
large Ma

Expansion about local eq.

⇩

Galerkin Method

⇩

Grad‘s 13 Moment-System

⇩

Elimination of small time scale effects

⇩

Navier-Stokes equation

small Knudsen+
small Mach

Expansion about global eq.

⇩

Collocation

⇩

Discrete Boltzmann equation

Ansatz (in 2D):

$$f^{abs}(t,\mathbf{v}) = \frac{\rho}{(2\pi c_s^{\,2})^{D/2}} \exp\left(-\frac{v_1^{\,2} + v_2^{\,2}}{2 c_s^{\,2}}\right)$$

$$f(t,\mathbf{v},\mathbf{x}) = f^{abs}(t,\mathbf{v}) \sum_{k=0}^{8} a_k(t,\mathbf{x})\theta_k(\mathbf{v})$$

Hermite-Polynomials:

$$\int_{-\infty}^{+\infty} f^{abs}\theta_k\theta_l d\mathbf{v} = \begin{cases} 0, & if\ k \neq l \\ A_k, & if\ k = l \end{cases}$$

$$H_0(x) = 1$$

$$H_1(x) = 2x$$

$$H_2(x) = 4x^2 - 2$$

$\theta_0 = 1$	a_0	density
$\theta_1 = H_1(\mathrm{v}_1)$	a_1	momentum in x
$\theta_2 = H_1(\mathrm{v}_2)$	a_2	momentum in y
$\theta_3 = H_2(\mathrm{v}_1)$	a_3	~pressure tensor xx
$\theta_4 = H_2(\mathrm{v}_2)$	a_4	~pressure tensor yy
$\theta_5 = H_1(\mathrm{v}_1)H_1(\mathrm{v}_2)$	a_5	~pressure tensor xy
$\theta_6 = H_1(\mathrm{v}_1)\cdot(H_2(\mathrm{v}_1)+H_2(\mathrm{v}_2))$	a_6	~heat flux in x
$\theta_7 = H_1(\mathrm{v}_2)\cdot(H_2(\mathrm{v}_1)+H_2(\mathrm{v}_2))$	a_7	~heat flux in y
$\theta_8 = (H_2(\mathrm{v}_1)+H_2(\mathrm{v}_2))^2$	a_8	~higher order moment

Hermite polynomial coefficients

(representation in moment space)

linear transformation

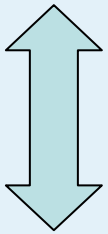

discrete *f*i at collocation points (D2Q9)

(representation in distribution space)

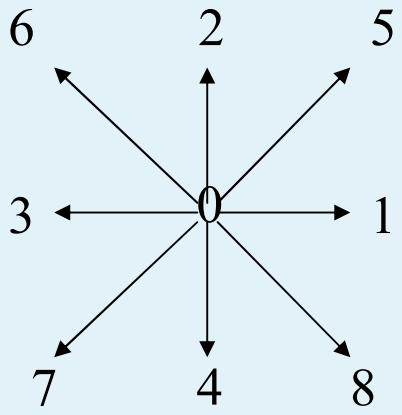

caveat:

equilibrium distribution f^{eq} must be projected into the space spanned by the Hermite-Polynomials (orthogonal projection):

$$\tilde{f}^{eq}(t,\mathbf{x},\mathbf{v}) = f^{abs}(t,\mathbf{v})\sum_{k=0}^{k=8}\tilde{a}_k(t,\mathbf{x})\,\theta_k(\mathbf{v})$$

$$\tilde{a}_k(\rho,\mathbf{u}) = \int_{-\infty}^{+\infty} f^{abs} f^{eq}\theta_k d\mathbf{v} \,/\, \int_{-\infty}^{+\infty} f^{abs}\theta_k\theta_k d\mathbf{v}$$

Quadrature: evaluation of equilibrium distr. at collocation points $\mathbf{v_i}$

$$\tilde{f}^{eq}(\rho,\mathbf{u},\mathbf{v}_i) = \tilde{f}_i^{eq}(\rho,\mathbf{u}) = w_i\rho(1+\frac{3}{2}\mathbf{v}_i\cdot\mathbf{u}+\frac{9}{2}(\mathbf{v}_i\cdot\mathbf{u})^2-\frac{3}{2}\mathbf{u}^2) \quad i=0,\ldots,m$$

As a result we obtain the discrete Boltzmann equation:

$$\frac{\partial f_i(t,\mathbf{x})}{\partial t} + \mathbf{v}_i \cdot \nabla f_i(t,\mathbf{x}) = -\frac{1}{\tau}\left(f_i(t,\mathbf{x}) - \tilde{f}_i^{eq}(t,\mathbf{x})\right) \quad i = 0,\ldots,8$$

macroscopic moments can now be obtained as sums

density $$\rho = \sum_{i=0}^{m} f_i$$

momentum $$\rho\mathbf{u} = \sum_{i=0}^{m} \mathbf{v}_i f_i$$

pressure tensor $$P_{\alpha\beta} = \sum_{i=0}^{m} (\mathrm{v}_{i\alpha} - \mathrm{u}_\alpha)(\mathrm{v}_{i\beta} - u_\beta) f_i$$

strain tensor $$S_{\alpha\beta} \propto \sum_i \mathrm{v}_{i\alpha}\mathrm{v}_{i\beta} f_i^{(neq)}$$

From the discrete BE to LBGK:

Finite Difference discretization

$$\frac{f_i(\vec{x},t+\Delta t)-f_i(\vec{x},t)}{\Delta t}+c\frac{f_i(\vec{x}+\vec{e}_i\Delta t,t+\Delta t)-f_i(\vec{x},t+\Delta t)}{\Delta x}=-\frac{1}{\tau}\left(f_i(\vec{x},t)-f_i^{eq}(\vec{x},t)\right)$$

$$\Downarrow$$

$$\Delta t = c\Delta x$$

$$\Downarrow$$

$$f_i(\vec{x}+\vec{e}_i\Delta t,t+\Delta t)-f_i(\vec{x},t+\Delta t)=-\frac{\Delta t}{\tau}\left(f_i(\vec{x},t)-f_i^{eq}(\vec{x},t)\right)$$

Taylor expansion + Chapman-Enskog analysis:

viscosity: $$\mu = c_s^2\rho\left(\tau-\frac{\Delta t}{2}\right)$$

Multi-Relaxation-time approach

Linear transformation:

$$\vec{m} = \mathbf{M}\,\vec{f}$$

$$\vec{m} = [\rho, e, \varepsilon, j_x, q_x, j_y, q_y, p_{xx}, p_{xy}]$$

$$\vec{m}^{eq} = [0, e^{eq}, \varepsilon^{eq}, 0, q_x^{eq}, 0, q_y^{eq}, p_{xx}^{eq}, p_{xy}^{eq}]$$

collision in moment space:

$$\widetilde{\Omega}_i = s_i (m_i - m_i^{eq}) \quad i \in \{0,\ldots,m\}$$

$$\widetilde{f} = \mathbf{M}^{-1}\,\widetilde{\Omega}_i$$

D. d'Humiéres, I. Ginzburg, M. Krafczyk, P. Lallemand, L. Luo (2002)

Re=2000
(52^3 nodes)

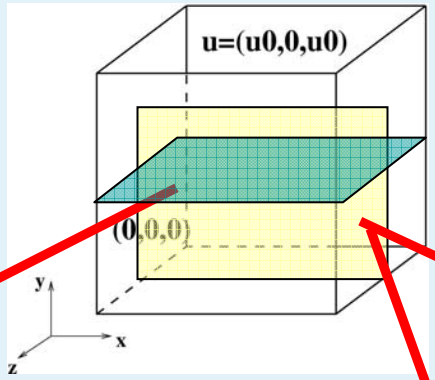

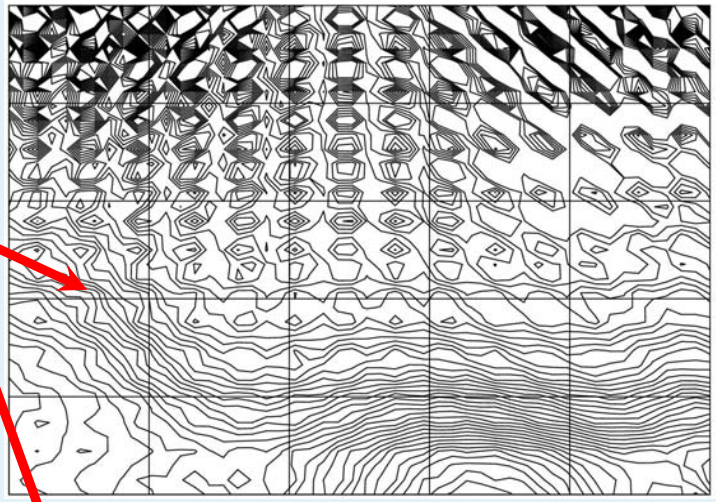

LBGK

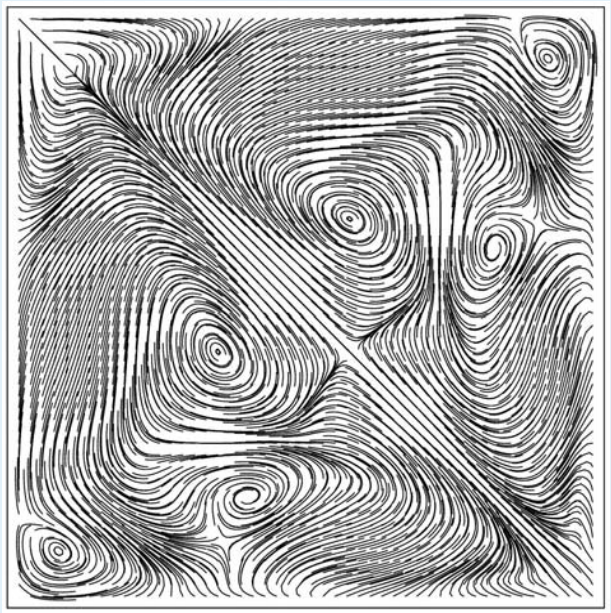

GLBE

efficiency gain
up to ~ 1:100

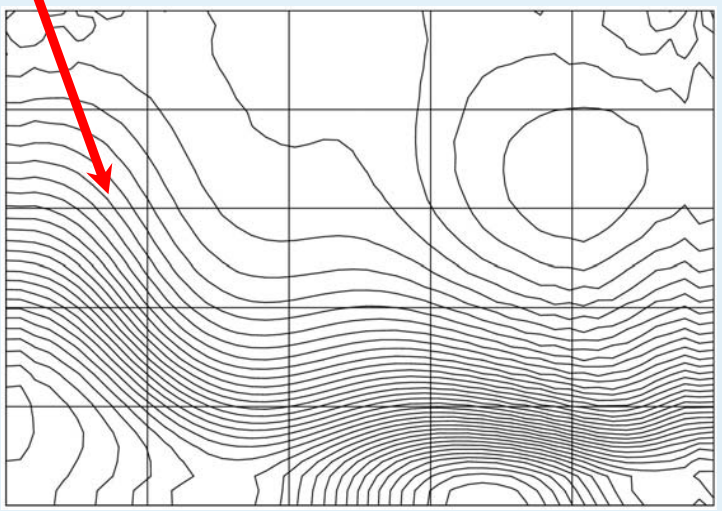

choose free parameter s_i to maximize Galilean invariance, stability and isotropy (dispersion):

Method	*Max. Cell-Reynolds-number*
Navier-Stokes Expl. Euler and centered Differences	2
LBGK	~ 30
MRT	~ 200

flow field simulation with Lattice Boltzmann

LBE $$f_{i,l}(t+\Delta t_l,\ \vec{x}+\vec{e}_i\Delta t_l) = f_{i,l}(t,\vec{x}) + \Omega_{i,l}(t,\vec{x})$$

$$\rho = \sum_i f_i \qquad \rho\vec{u} = \sum_i \vec{e}_i f_i$$

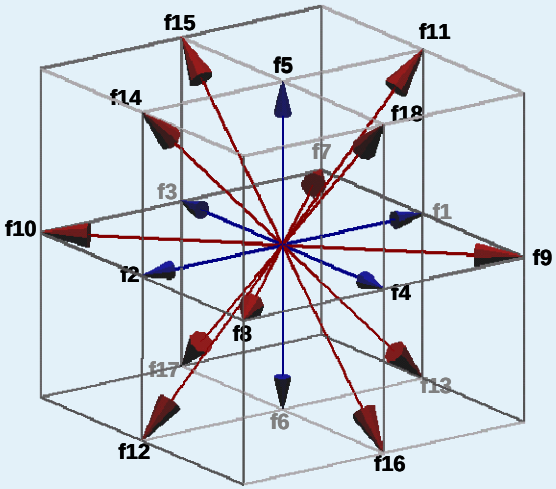

collision:

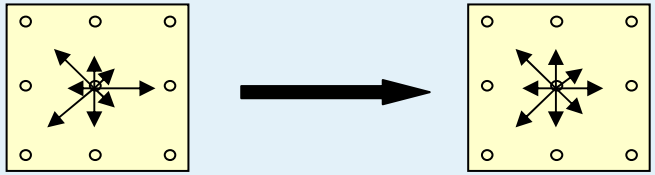

$$\tilde{f}_i(t,\vec{x}) = f_i(t,\vec{x}) + \Omega_{i,l}(t,\vec{x})$$

- ***STR***: $\Omega_{i,l}(t,\vec{x}) = -\dfrac{\Delta t_l}{\tau_l}\left(f_i(t,\vec{x}) - f_i^{eq}(t,\vec{x})\right), \quad \tau_l = 3\dfrac{\nu}{c^2} + \dfrac{1}{2}\Delta t_l$
  (Quian, 1992)
- ***MRT***: $\Omega_{i,l}(t,\vec{x}) = M^{-1}S_l\left[\underbrace{(Mf(t,\vec{x}))}_{m} - m^{eq,l}(t,\vec{x})\right]$
  (d'Humiéres, 1992)

propagation:

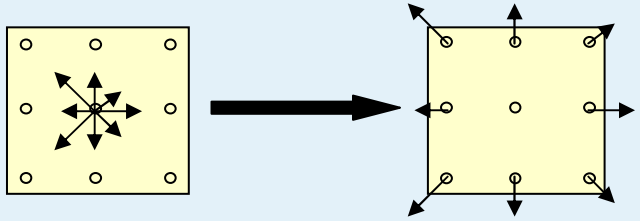

$$f_{i,l}(t+\Delta t_l,\ \vec{x}+\vec{e}_i\Delta t_l) = \tilde{f}_{i,l}(t,\vec{x})$$

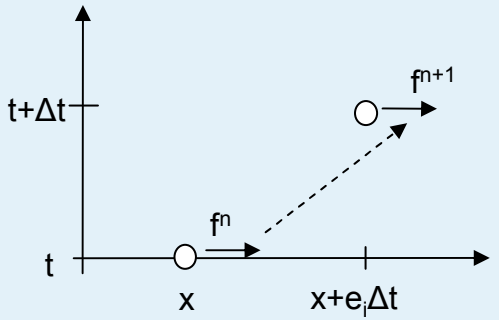

Single phase LB: Boundary & Initial Conditions, Force evaluation and Fluid-Structure Interaction

Manfred Krafczyk

contributors:
B. Ahrenholz, S. Freudiger, S. Geller, B. Nachtwey, M. Stiebler, J. Tölke

kraft@cab.bau.tu-bs.de

http://www.cab.bau.tu-bs.de

Overview

- **No-slip BC: from bounce back to Multi-Reflection**
- **Initialization: a semi-Poisson LB-solver**
- **Force evaluation**
- **FSI**

Sources of accuracy degradation due to bounday conditions

The LB bulk scheme (fluid nodes) can be shown to be second order accurate in space. Boundary conditions potentially decrease the order of convergence. Two different effects have to be distinguished:

- geometric approximation of curved boundaries by a Cartesian voxel grid
  -> consideration of subgrid distances between lattice links and surfaces

- kinetic boundary layer (error terms) produce a shift
  of the effective boundary location.
  This problem cannot be cured for BGK models !
  (see the work of I. Ginzburg and D. d'Humieres)

Boundary Conditions (no slip)

- **Simple Bounce-Back**

$$f_{inversDirection}(x, t+\Delta t) = \tilde{f}_{Direction}(x,t)$$

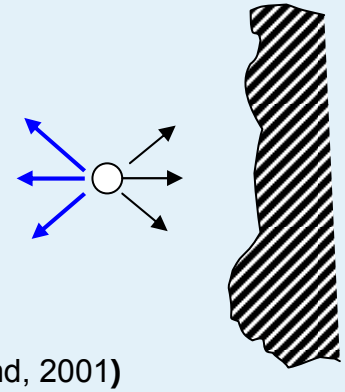

- **Second Order Bounce-Back** (Bouzidi, Firdaouss, Lallemand, 2001)

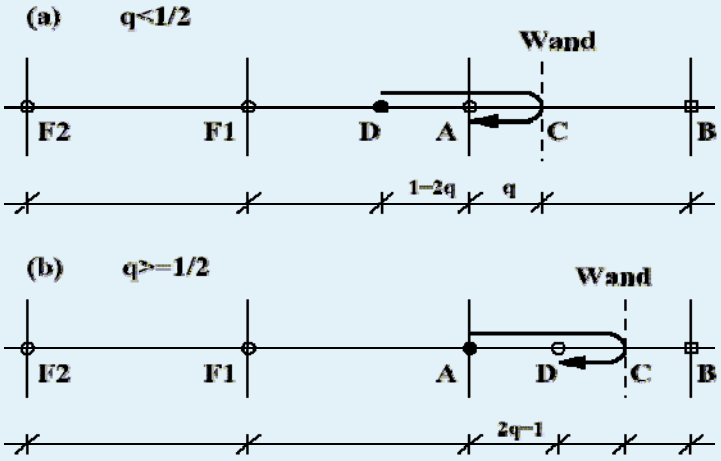

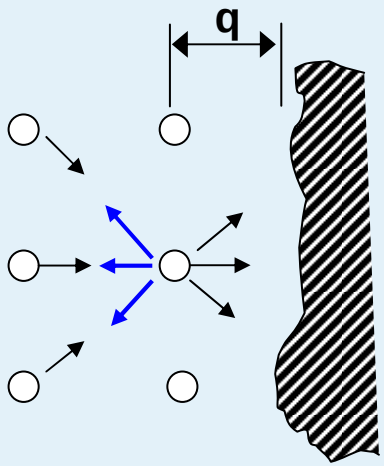

- **Multi-Reflection BCs** (Ginzburg, d'Humiéres, 2003)

Dirichlet Boundary Conditions

Velocity boundary (first order):

$$f_i^{t+1} = f_{invers} + \frac{2}{c_s^2}\rho w_i \vec{e}_i * \vec{u}_0$$ (Ladd, 92)

pressure has to evolve

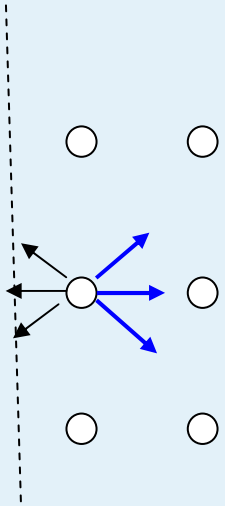

Pressure/Density boundary:

$$f^{t+1} = -f_{invers} + f^{eq}_{invers}(P_o, \vec{u}) + f^{eq}(P_o, \vec{u})$$

simple outflow:
equ. distributions from computed velocity and desired pressure (~zero gradient)

Velocity boundary (second order):

(Bouzidi, Firdaouss, Lallemand, 2001)

$$f_{IA}^{t+1} = (1-2q)\cdot f_{iF}^{t} + 2q\cdot f_{iA}^{t} - 6\frac{\mathbf{e}_i \mathbf{u}_w}{c^2}, \quad 0.0 < q < 0.5$$

$$f_{IA}^{t+1} = \frac{2q-1}{2q}\cdot f_{IA}^{t} + \frac{1}{2q}\cdot f_{iA}^{t} - 3\frac{\mathbf{e}_i \mathbf{u}_w}{qc^2}, \quad 0.5 \le q \le 1.0$$

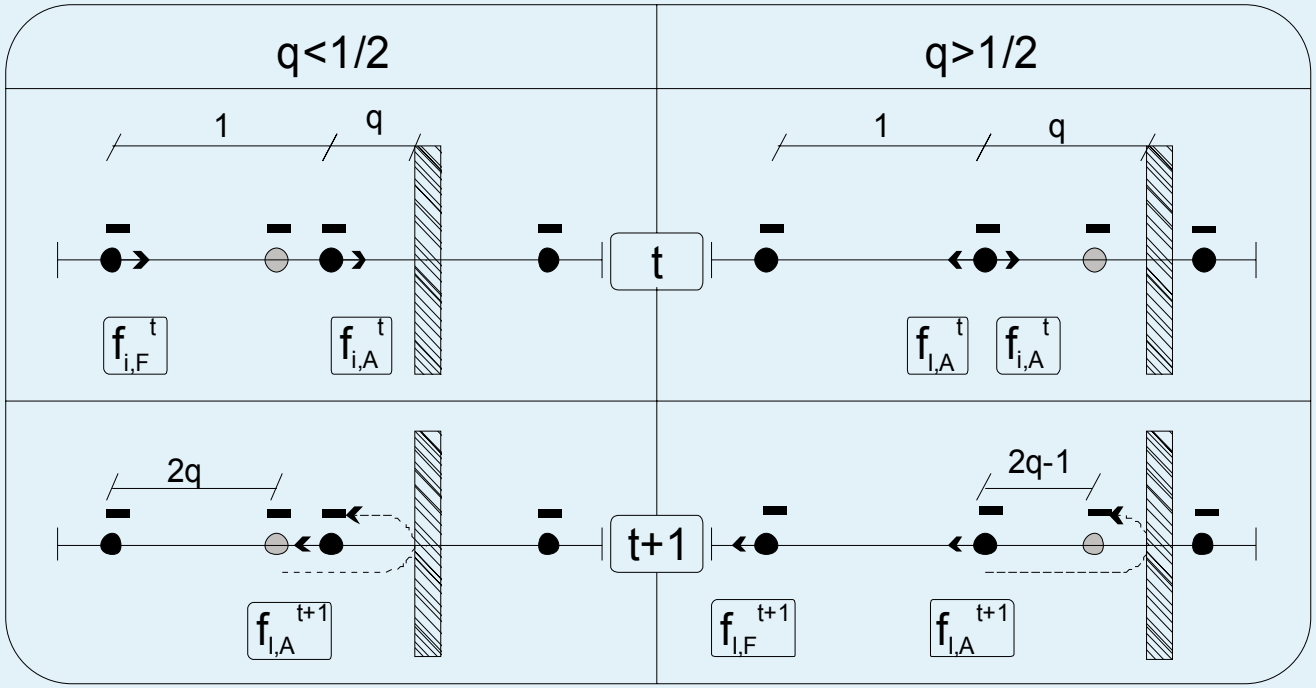

Moving Boundaries

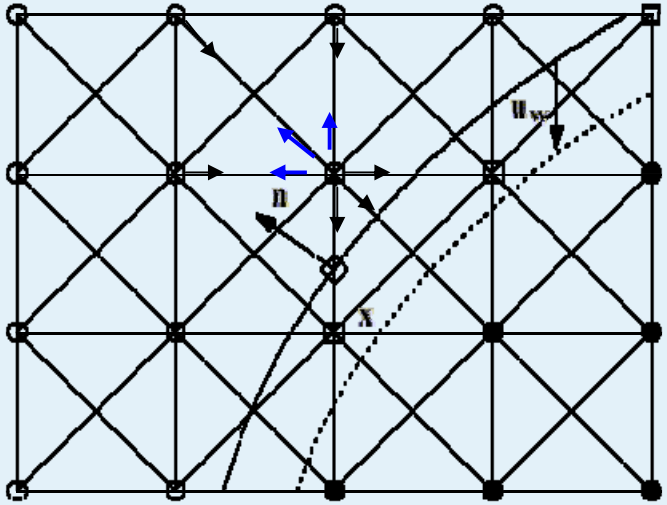

- **initialization of new fluid nodes**

  → **local Poisson type iteration**

Problem: Given an initial velocity field, determine a consistent pressure field and consistent non-equilibrium distributions.

Idea: Iterate the collision and propagation cycle starting from u0 and p0, but let the pressure evolve and keep the velocity field fixed to the initial value until convergence.
The use of BGK may (for small viscosities) result in large iteration numbers.
As usual, one can speed up convergence using the MRT version. (R. Mei, L. Luo, P. Lallemand, D. d'Humieres, 2006)

After convergence, the resulting pressure field can be shown to obey the Poisson equation and the resulting non-equilibrium distribution will be consistent in terms of higher order moments (e.g. stresses).

Grid generation

Calculation of subgrid distances q‘s

D2Q9-Model

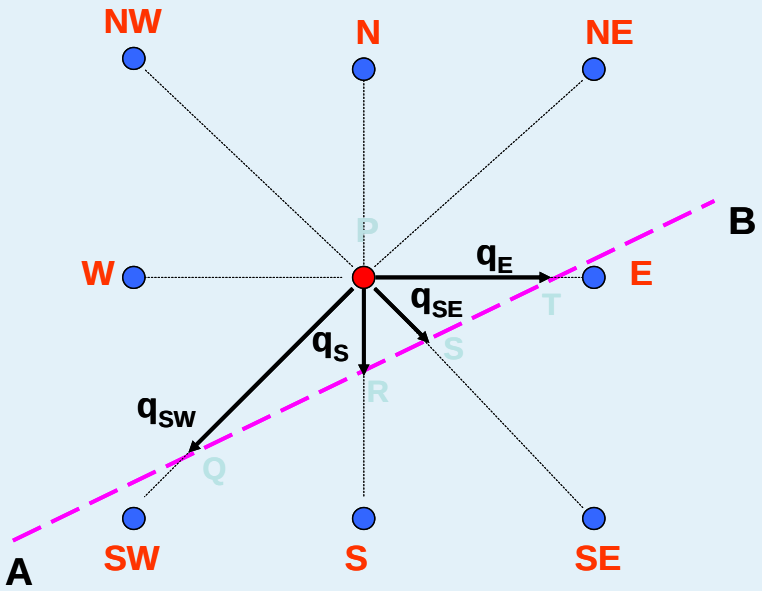

D3Q19-Model

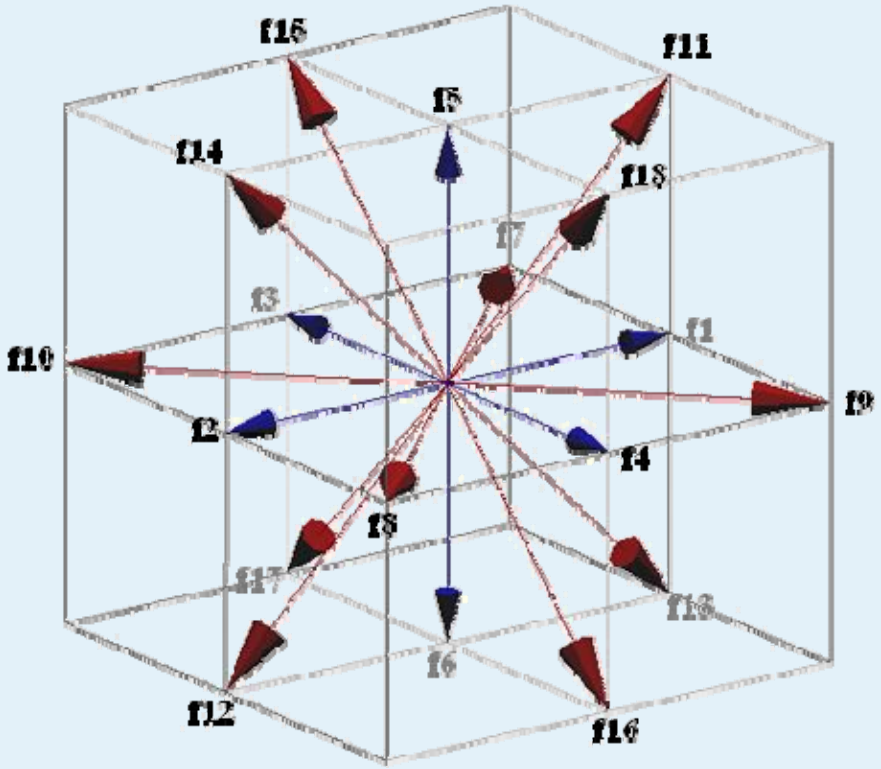

3D grid generation

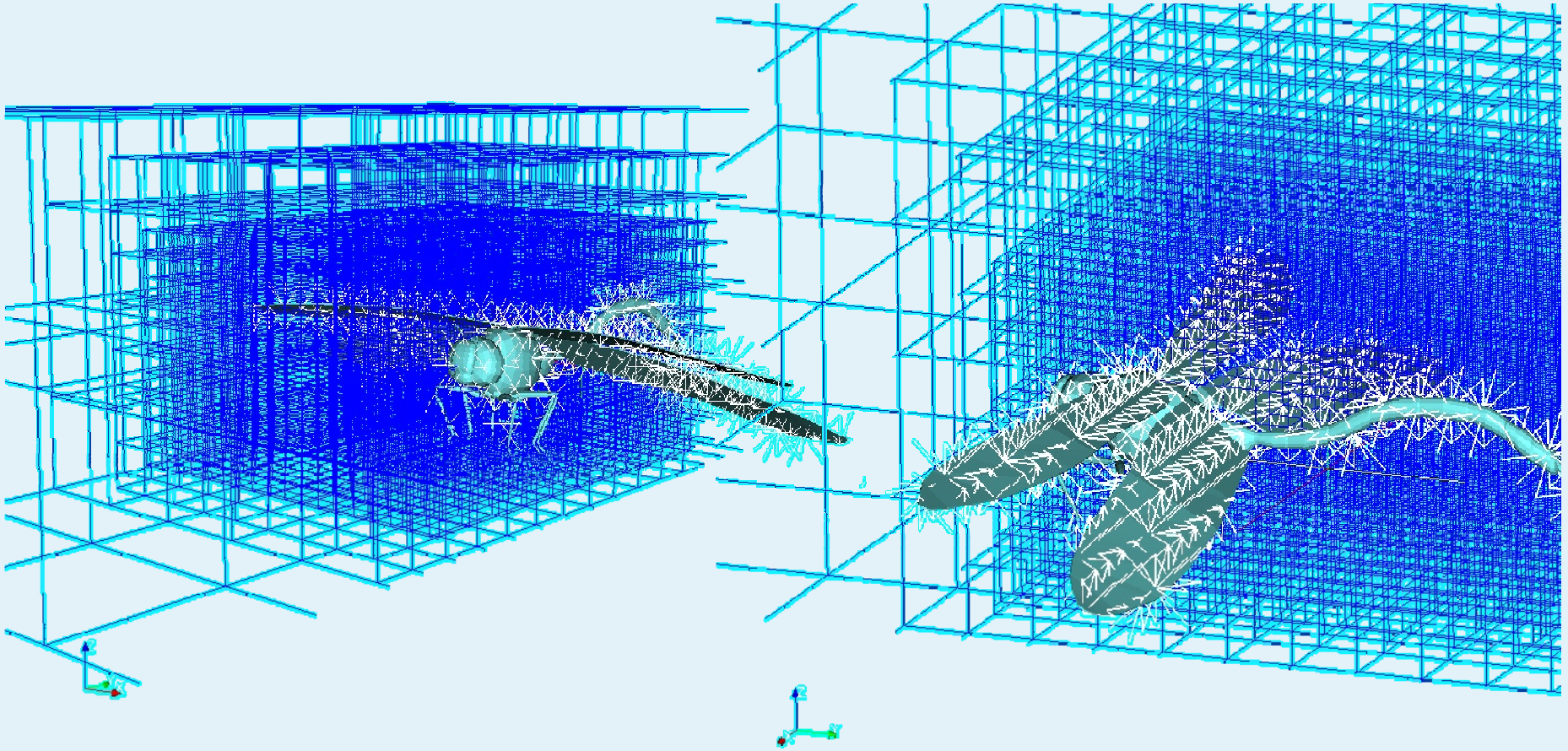

Preprocessing of subgrid links for high resolution porous media tomographic data is tedious (> 500.000.000 Voxel)

(tomographic data courtesy of A. Kästner, P. Lehmann, ETH Zürich)

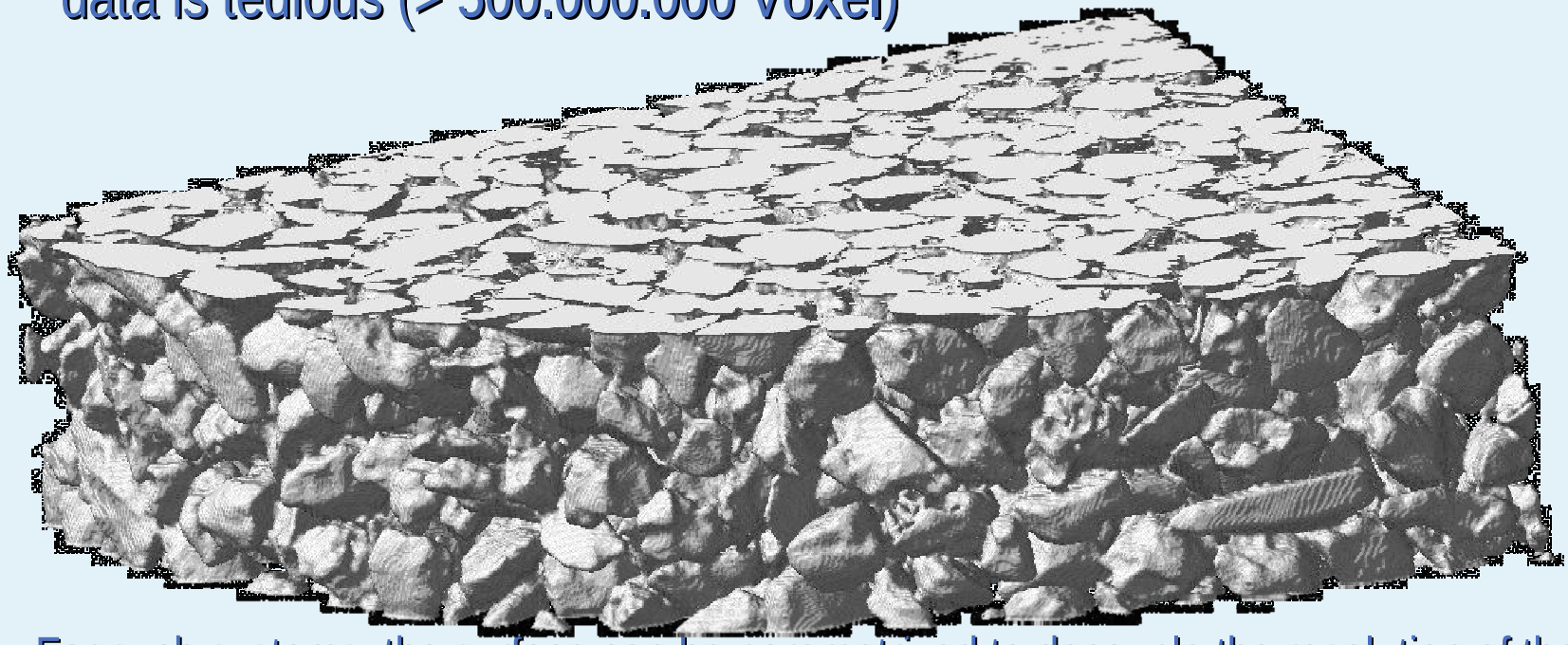

For such systems, the surface can be parametrized to decouple the resolution of the tomography data from the resolution of the numerical grid
(Ahrenholz, Tölke, Krafczyk, preprint)
Applications: soil physics, particle filters, fuel cells etc.

Second-order accurate slip boundary conditions

- Velocity boundary conditions

$$f_{IA}^{t+1} = (1-2q)\cdot f_{iF}^{t} + 2q\cdot f_{iA}^{t} - 6\frac{\mathbf{e}_i \mathbf{u}_w}{c^2}, \quad 0.0 < q < 0.5$$

$$f_{IA}^{t+1} = \frac{2q-1}{2q}\cdot f_{IA}^{t} + \frac{1}{2q}\cdot f_{iA}^{t} - 3\frac{\mathbf{e}_i \mathbf{u}_w}{qc^2}, \quad 0.5 \le q \le 1.0$$

- Calculation of the velocity component
  - Calculate the amplitude from local velocity and the wall normal
  - Calculate the velocity at the wall using the normal, the local velocity and the amplitude

$$amplitude = \mathbf{u}_w \mathbf{n}$$

$$\mathbf{u}_w = \mathbf{u}_w - amplitude\mathbf{n}$$

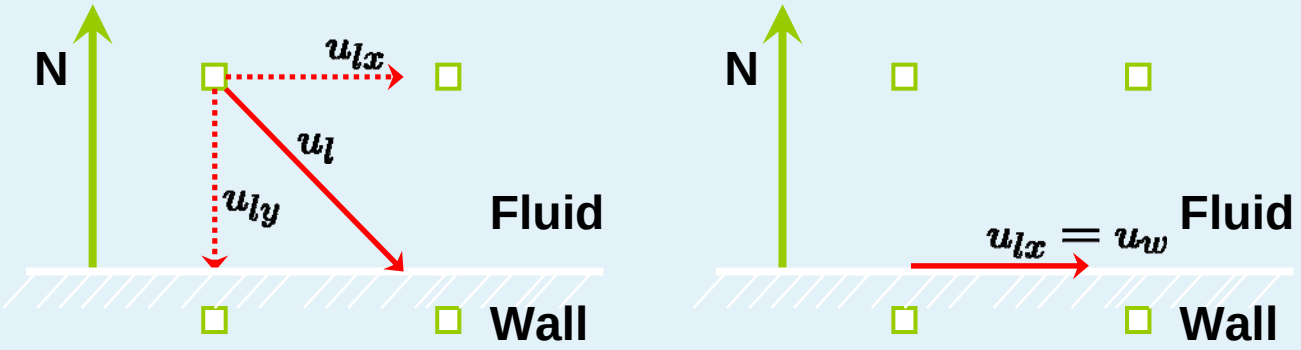

- works for arbitrary geometries
  (in contrary to specular reflection)
- only prerequisite is the local normal vector of the wall and the subgrid distances.

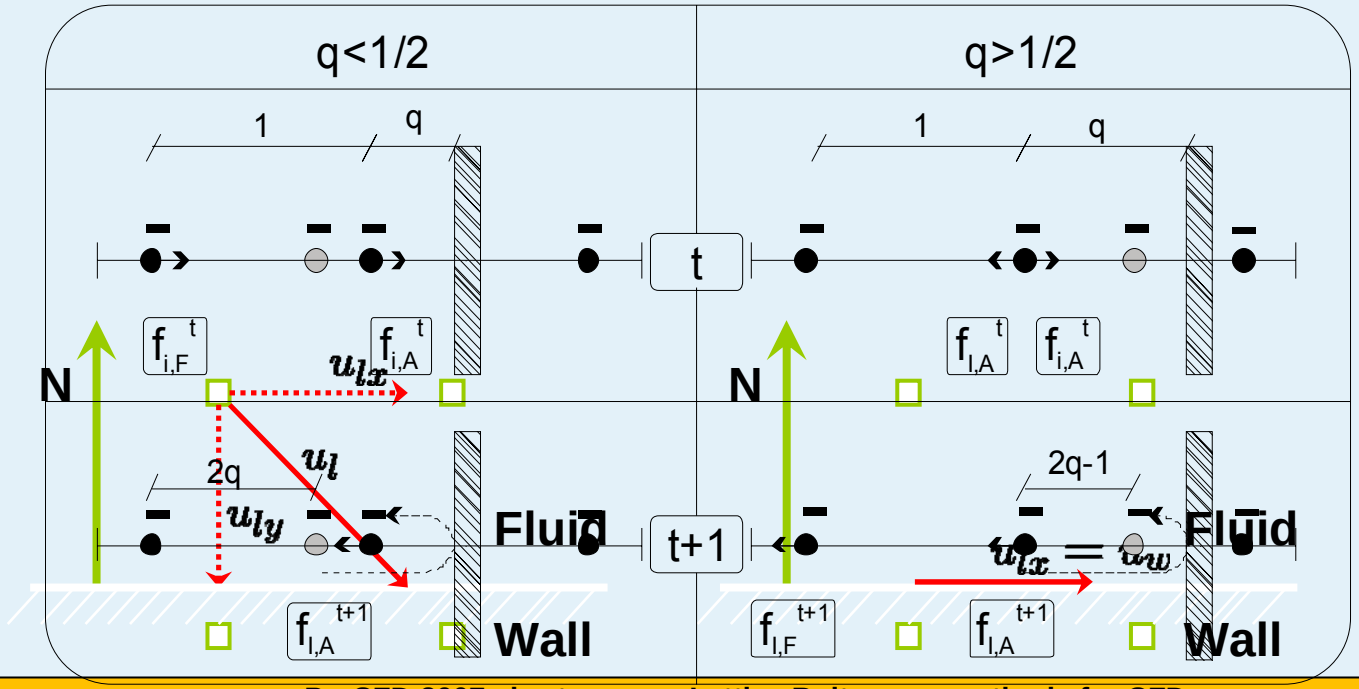

Validation II

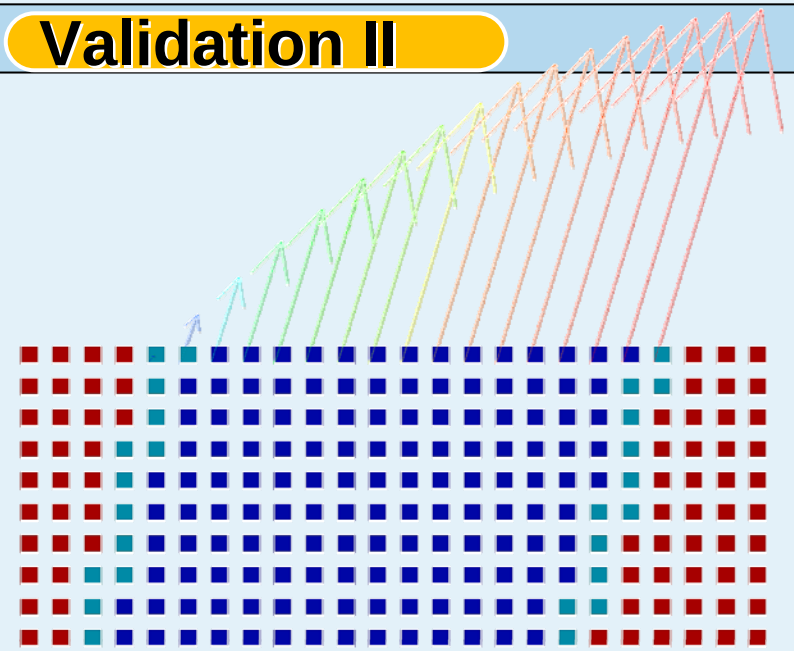

Velocity profile and discretized node grid

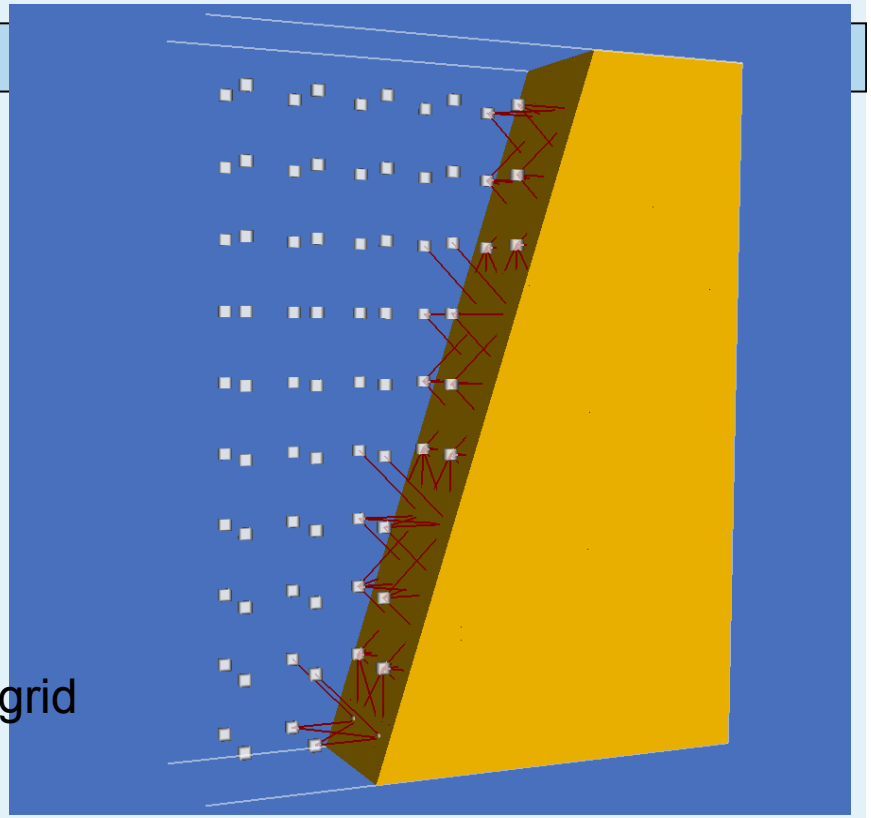

Node grid with q-links to the wall

- **Results:**
  - **order of accuracy for simple bounce back for grid aligned walls is N^{-2}**
  - **order of accuracy for simple bounce back for inclined walls is N^{-1}**
  - **order of accuracy for linear interpolated bounce back for inclined walls is close to N^{-2}**

Validation III

- Results:

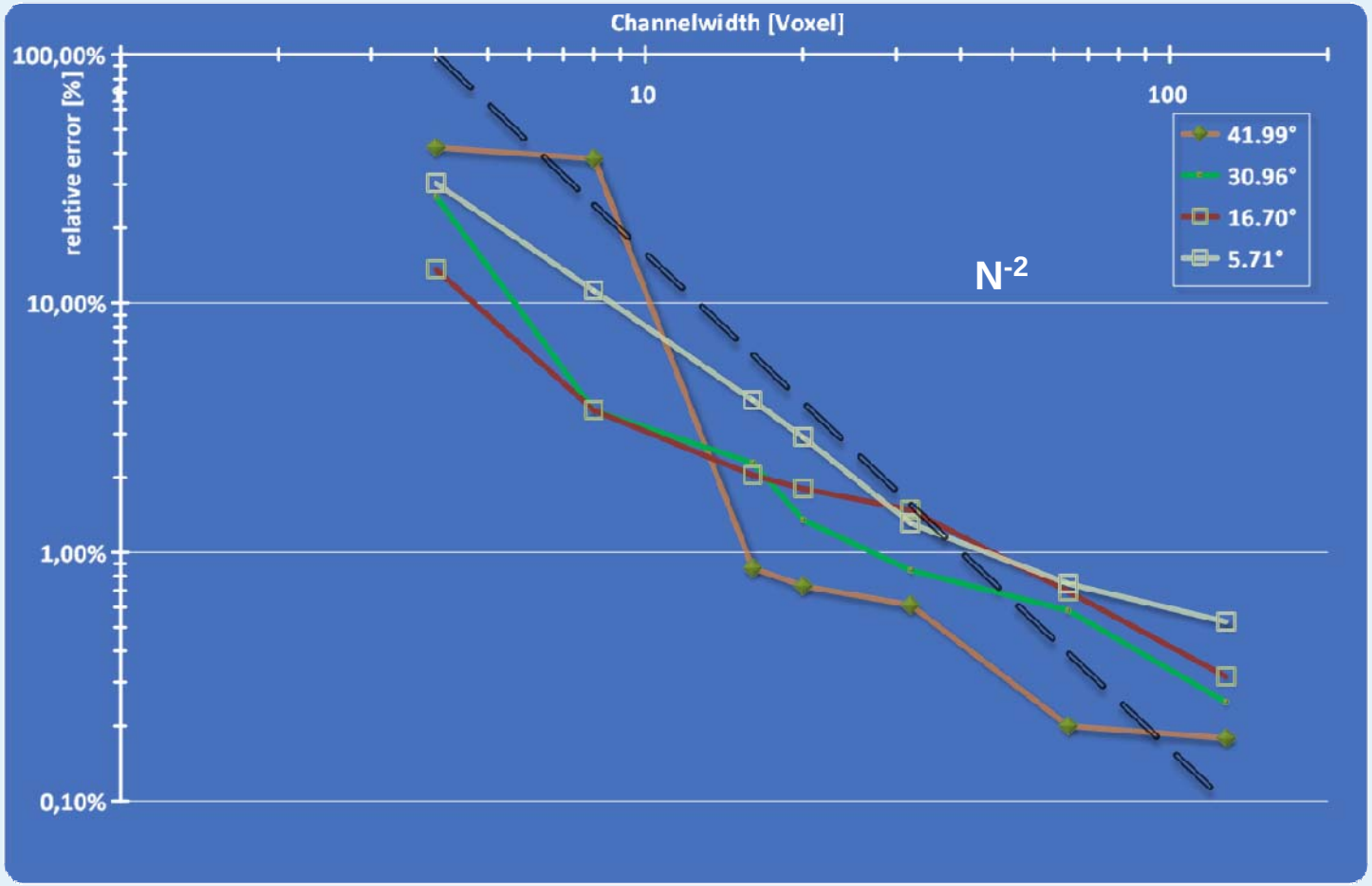

Relative error of the 2-dimensional Poiseuille Flow compared to the analytical solution at different inclination angles

Can LB be regarded as an efficient approach for CFD ?

Ingredients:

- **2nd order BCs**
- **MRT**
- **grid refinement (to be discussed)**
- **efficient data structures**

S. Geller, M. Krafczyk, J. Tölke, S. Turek, J. Hron:
Benchmark computations based on Lattice-Boltzmann,
Finite Element and Finite Volume Methods for laminar Flows,
Computers and Fluids 35, pp. 888-897 (2006)

Benchmark stationary (Ergun Re=1) and transient (Ergun Re=200)

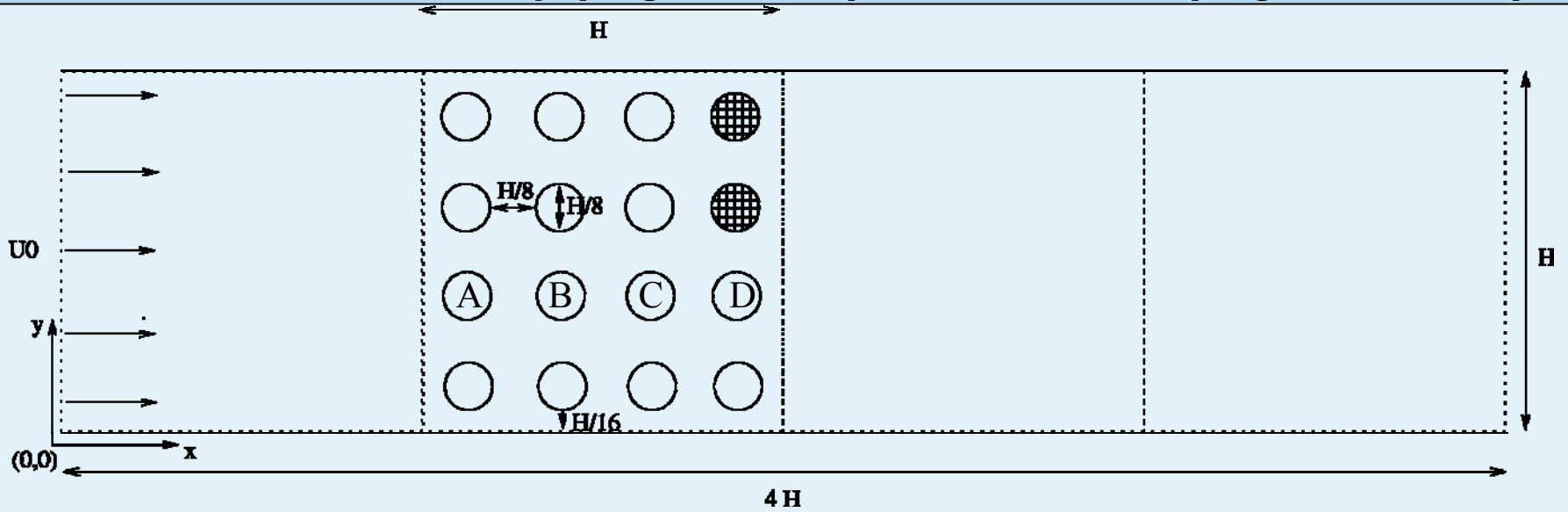

Re 1: pressure plots for y=0.5/0.625H

drag & lift coefficients for obstacle „A“

Re 200: drag & lift for obstacle „D“

FE-solver: „Featflow“, Prof. Turek, TU Dortmund
www.featflow.de

Pressure (Ergun Re=1)

y = 0.5 H

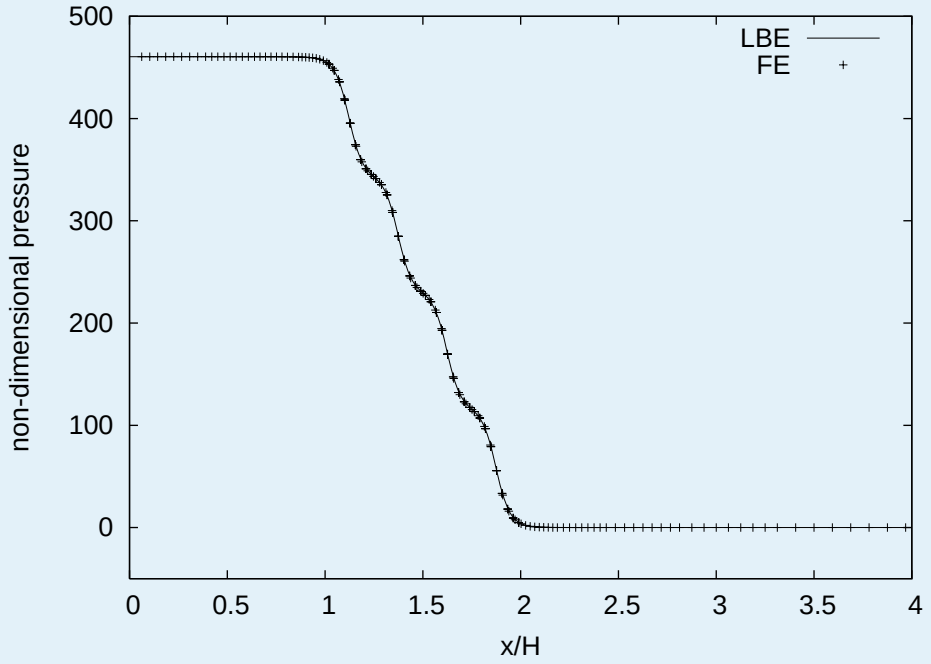

y = 0.625 H

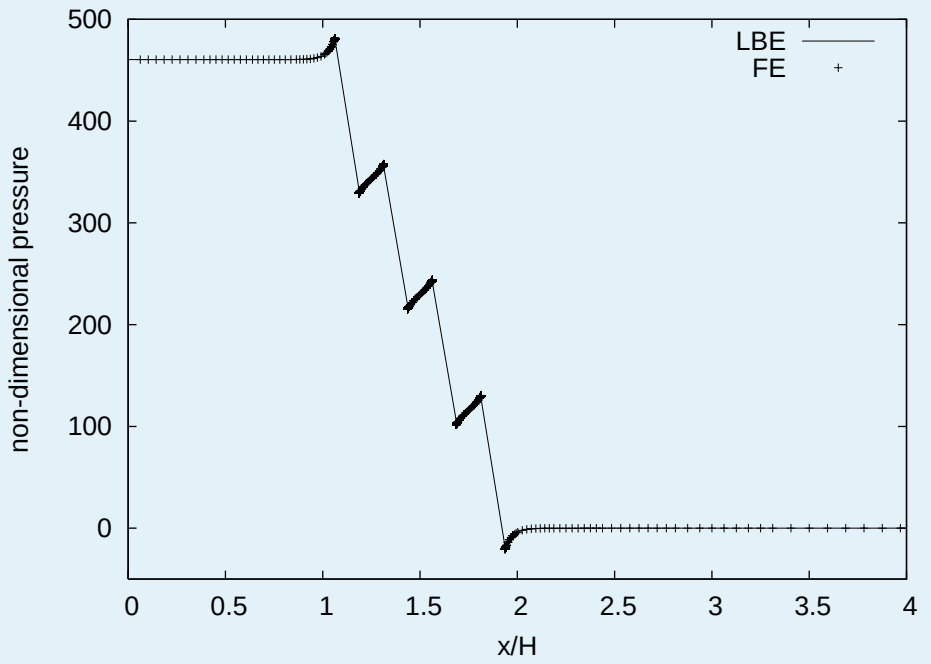

cylinder A, Re_E=1
reference: drag = 465.58, lift = 0.958

		rel.error [%]		
scheme	#dof	drag	lift	time [s]
LB, 4-6	48096	1.03	1.07	10
LB, 4-7	**141696**	**0.43**	**0.70**	**93**
FF, 0+2	11774	0.77	5.50	6
FF, 1+2	**26922**	**0.58**	**1.04**	**53**
FF, 2+0	30642	1.34	0.19	33
FF, 2+1	43314	0.37	0.10	38

convergence study: LBE, Re=1, circle A, drag

min	max	Ma	#DOF	#drag	rel. error[%]	#timesteps	time [s]
4	5	0,0173205	15264	450,7688527	3,183	3900	3
4	6	0,0086603	40320	470,4550817	1,045	2000	9
4	7	0,0043301	141696	467,5764449	0,427	2900	93,2
4	8	0,0021651	549936	465,9428266	0,076	4900	1140
4	9	0,0010825	2182608	465,6574185	0,014	7900	14703
9	9	0,0010825	8976960	465,5861301	0,000	152300	45352

reference value: 465,58

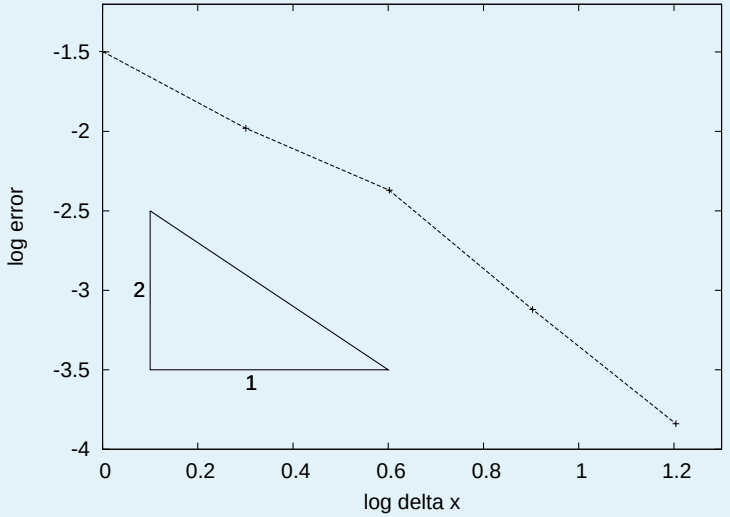

LBE grid: level 6 to 9

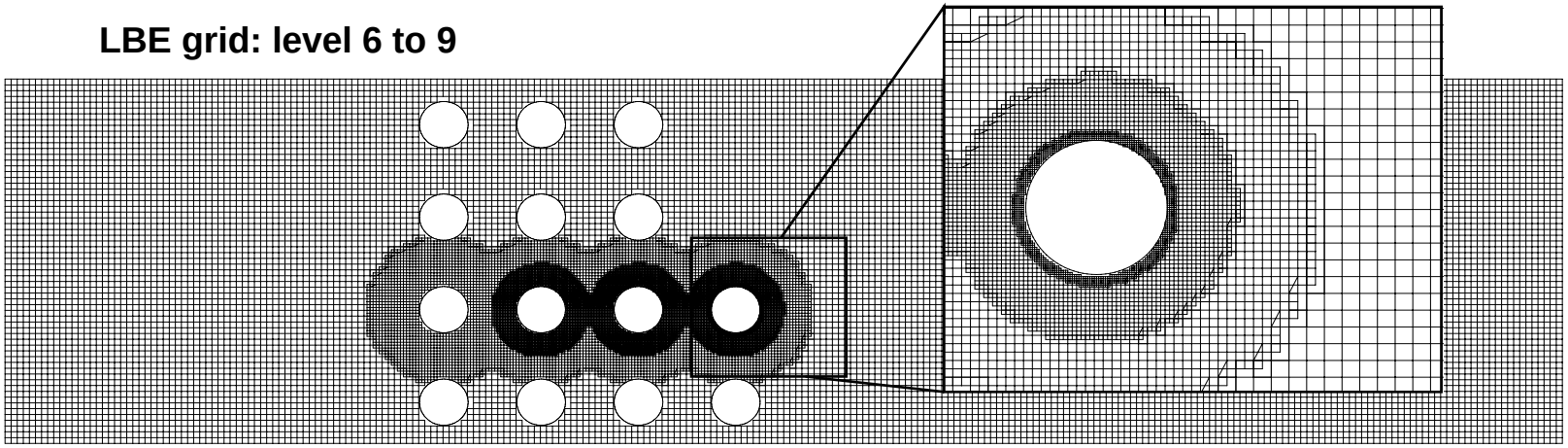

FE-mesh: level 5

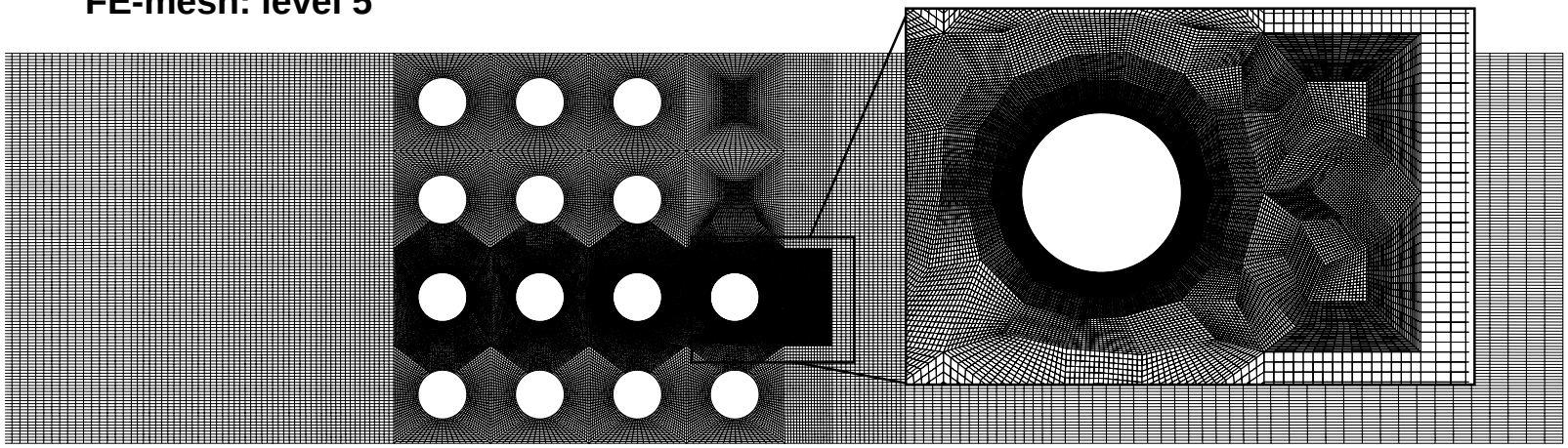

results for the transient case (Ergun Re = 200, cylinder D):

scheme	#dof	cd[%]	cl[%]	Tref [%]	CPU-time[s] / Tref
LB (6-8)	199.656	2.4	0.4	0.5	30
LB (6-9)	243.774	0.3	1.6	0.5	46
FEM(4)	113.264	1.3	0.3	9.2	22
FEM(5)	450.528	0.1	1.5	0.1	265
CFX	385.485	1.6	2.5	0.2	2856
CFX	917.616	0.5	1.3	0.2	6594
CFX	1.807.428	0	0	0	13440

Ma = 0.02
reference: cd = 2.0548
cl = 0.9150
Tref = 4.2327

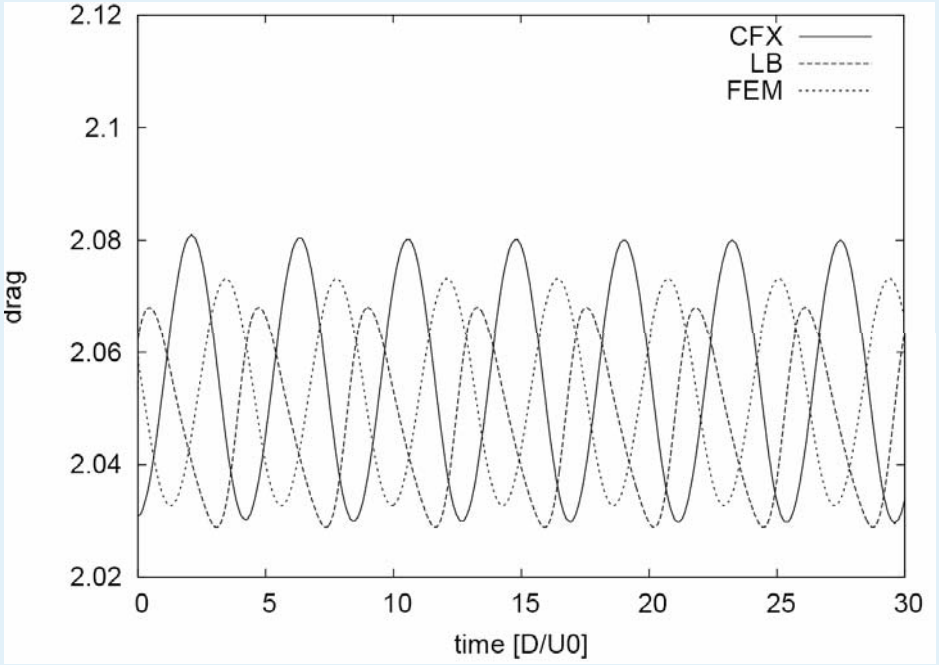

results for the transient case (Ergun Re = 200, cylinder D):

scheme	#dof	Ma	CPU-time[s] / Tref
LB (6-8)	318.123	0.1	12
LB (6-8)	318.123	0.05	25
LB (6-8)	318.123	0.02	61
CFX	385.485	0.1	2730
CFX	385.485	0.05	2814
CFX	385.485	0.02	2772
CFX	1.807.428	0	2856

compressibility effect
- Ma number effect

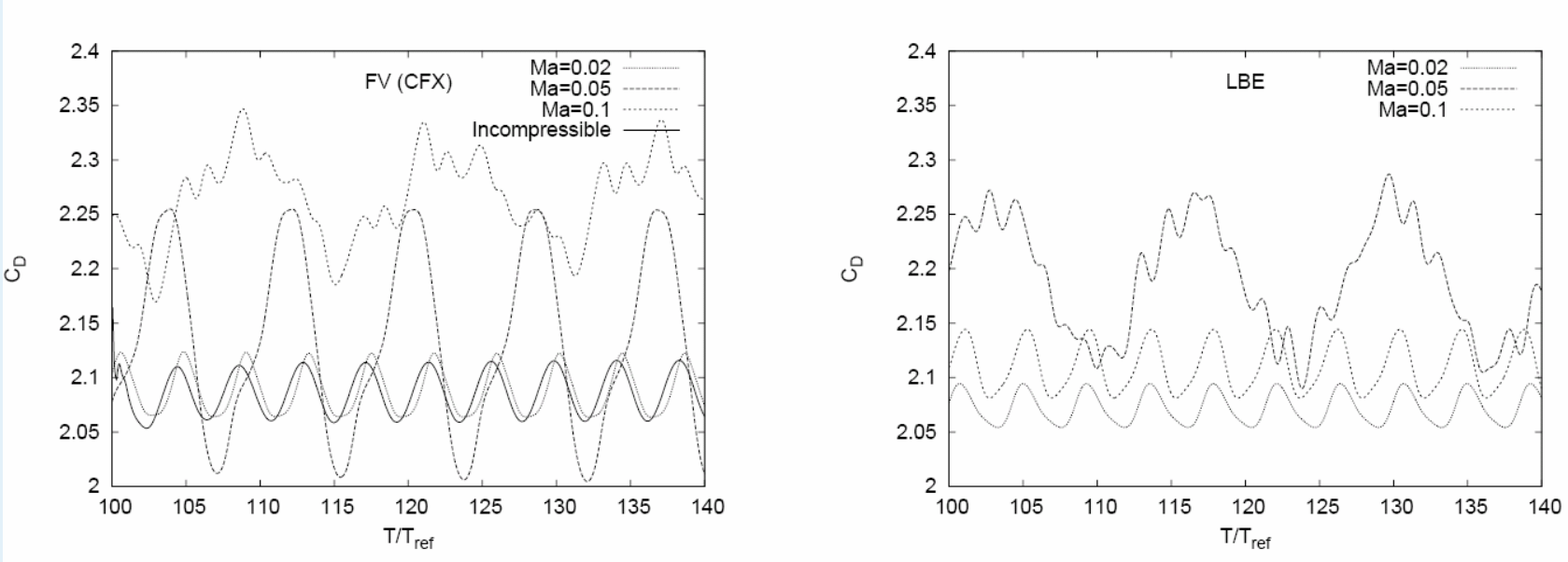

Force evaluation

- **momentum exchange:** (Ladd, 1992, 2002)

$$dI = f_{inversDir}(x, t + \Delta t) + \tilde{f}_{Dir}(x, t)$$

- **forces:**

$$F_i = \sum_i e_i \cdot [f_{inversDir}(x, t + \Delta t) + \tilde{f}_{Dir}(x, t)] \cdot \frac{\Delta x^2}{\Delta t}$$

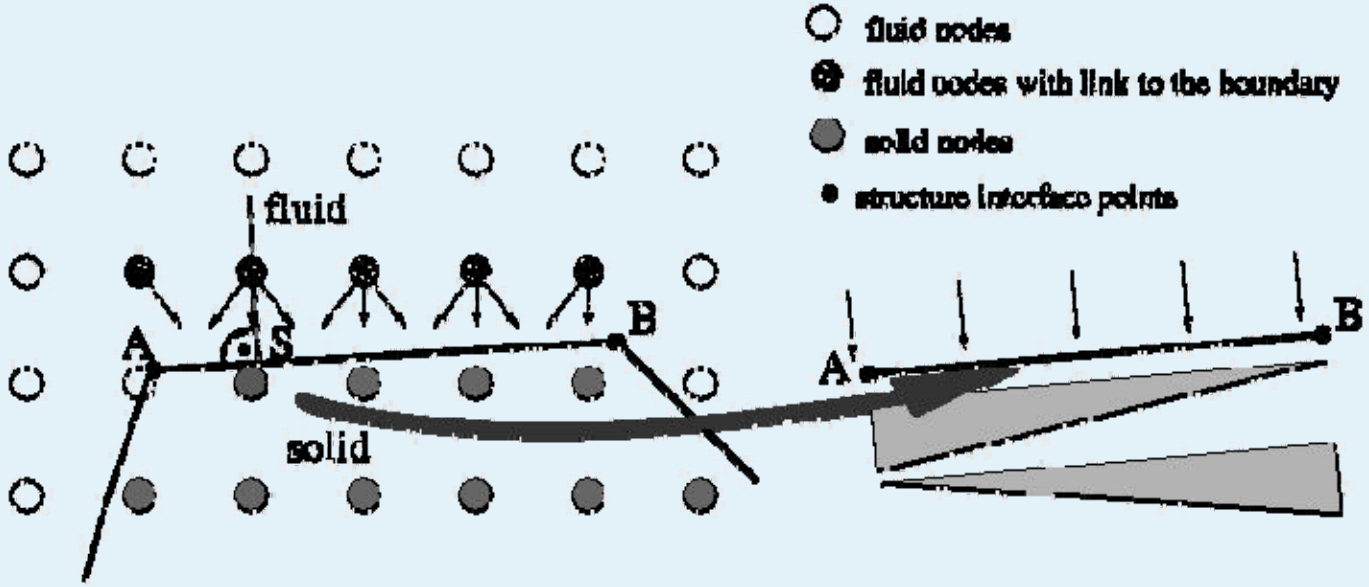

Force evaluation

- **stress integration:**

$$P_{\alpha\beta} = c_s^{\,2}\rho\,\delta_{\alpha\beta} + (1-\frac{\Delta t}{2\tau})\sum_k f_k^{neq} e_{i\alpha} e_{i\beta}$$

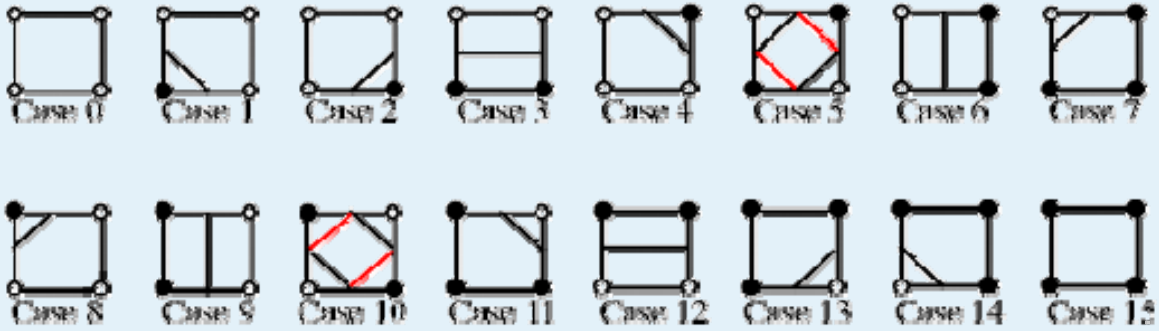

- **forces:**

$$F_B = (\frac{1}{4}\sigma_A + \frac{3}{4}\sigma_B) n_{AB} \frac{1}{2} l_{AB} + (\frac{3}{4}\sigma_B + \frac{1}{4}\sigma_C) n_{BC} \frac{1}{2} l_{BC}$$

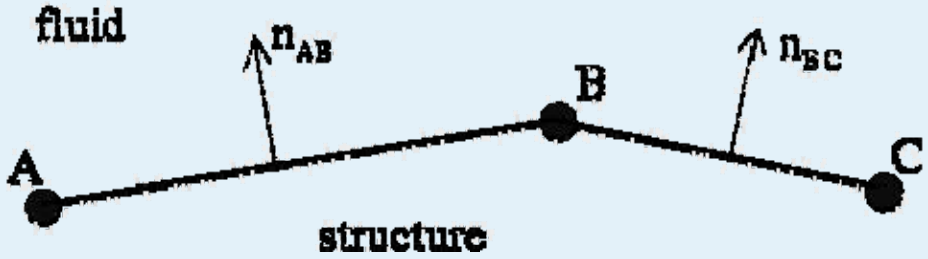

Force evaluation

- simple example:

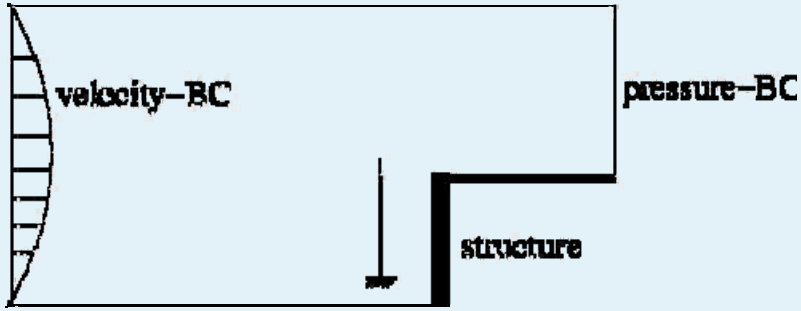

- momentum exchange

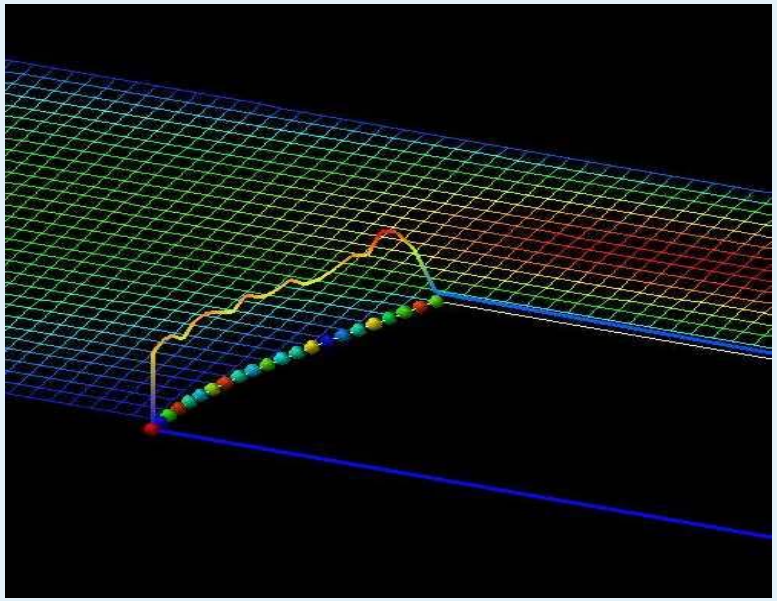

- stress integration

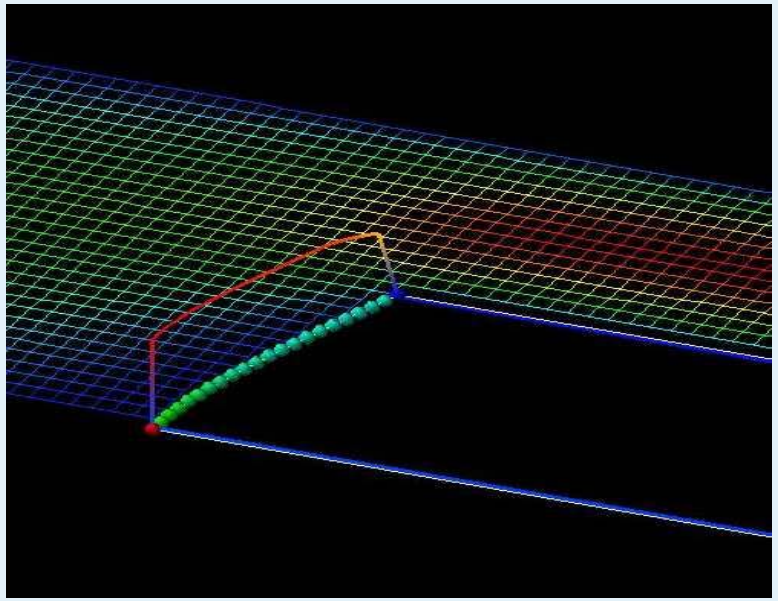

Force evaluation

momentum exchange

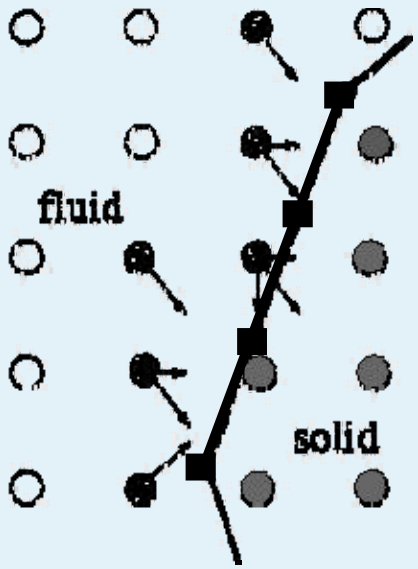

- weighted nodal forces

→ integration along the whole obstacle

→ for lines of subnodal length not appropriate

Conversion LB-System – ‚real world‘

Force:

$$\frac{F_{real}}{H_{real}} = \frac{F_{LB}}{H_{LB}} \frac{\rho_{real} u_{real}^{2}}{\rho_{LB} u_{LB}^{2}}$$

Time:

$$T_{real} = T_{LB} \frac{\upsilon_{LB} H_{real}^{2}}{\upsilon_{real} H_{LB}^{2}}$$

Fluid-Structure interaction

Ferrybridge, England 1965

Fluid-Structure interaction

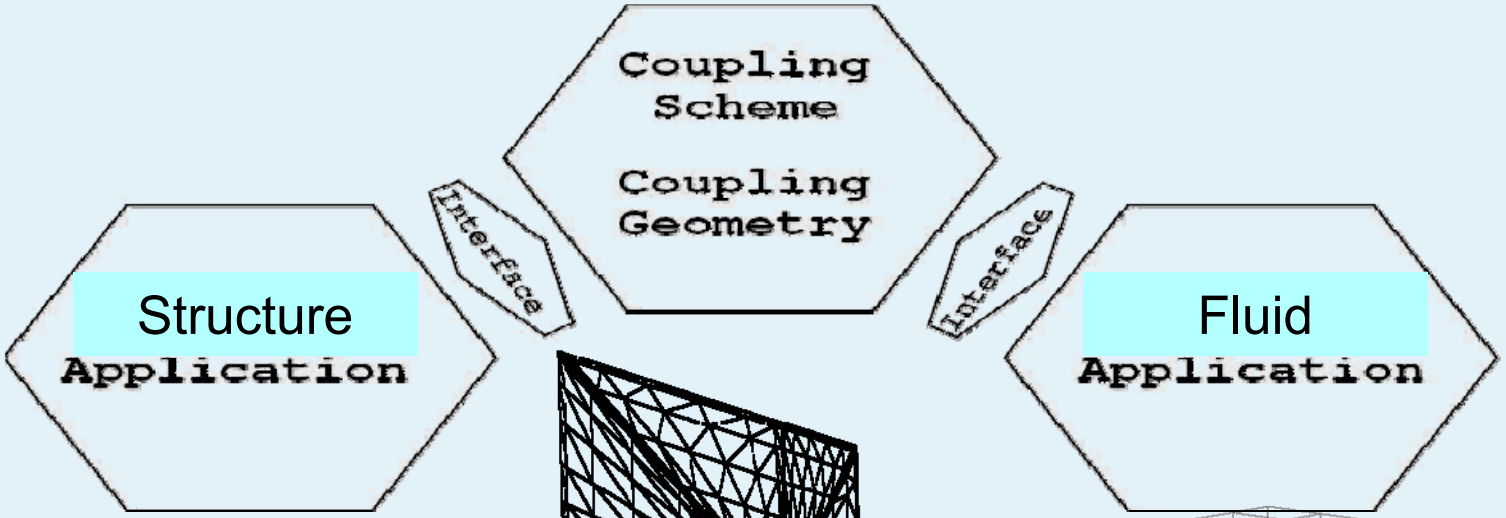

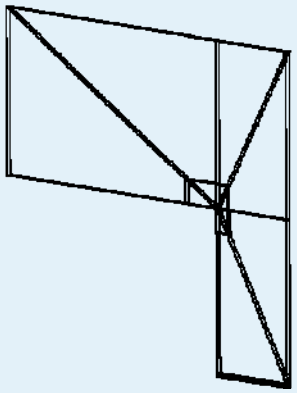

p-FEM solver “AdhoC”

(TU München)

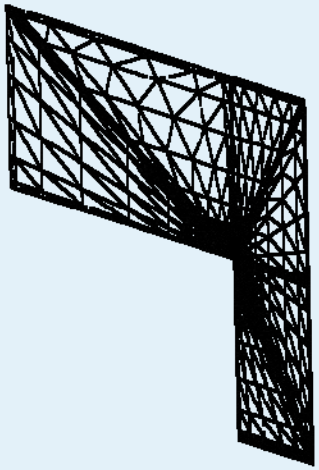

Surface mesh

on Gaussian points

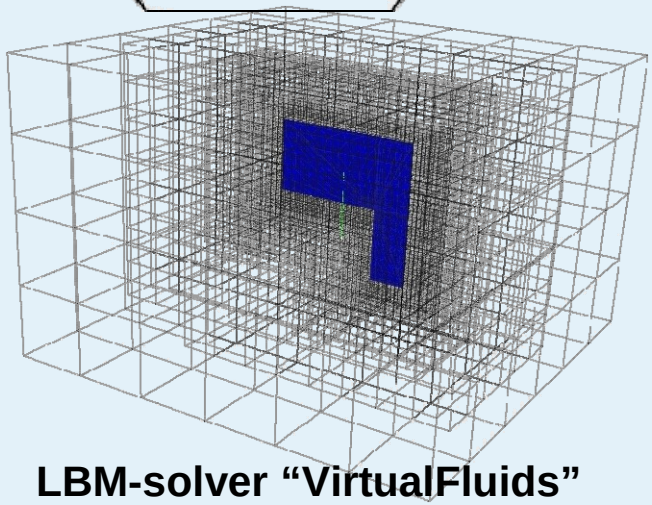

LBM-solver “VirtualFluids”

(TU Braunschweig)

Coupling algorithm (explicit)

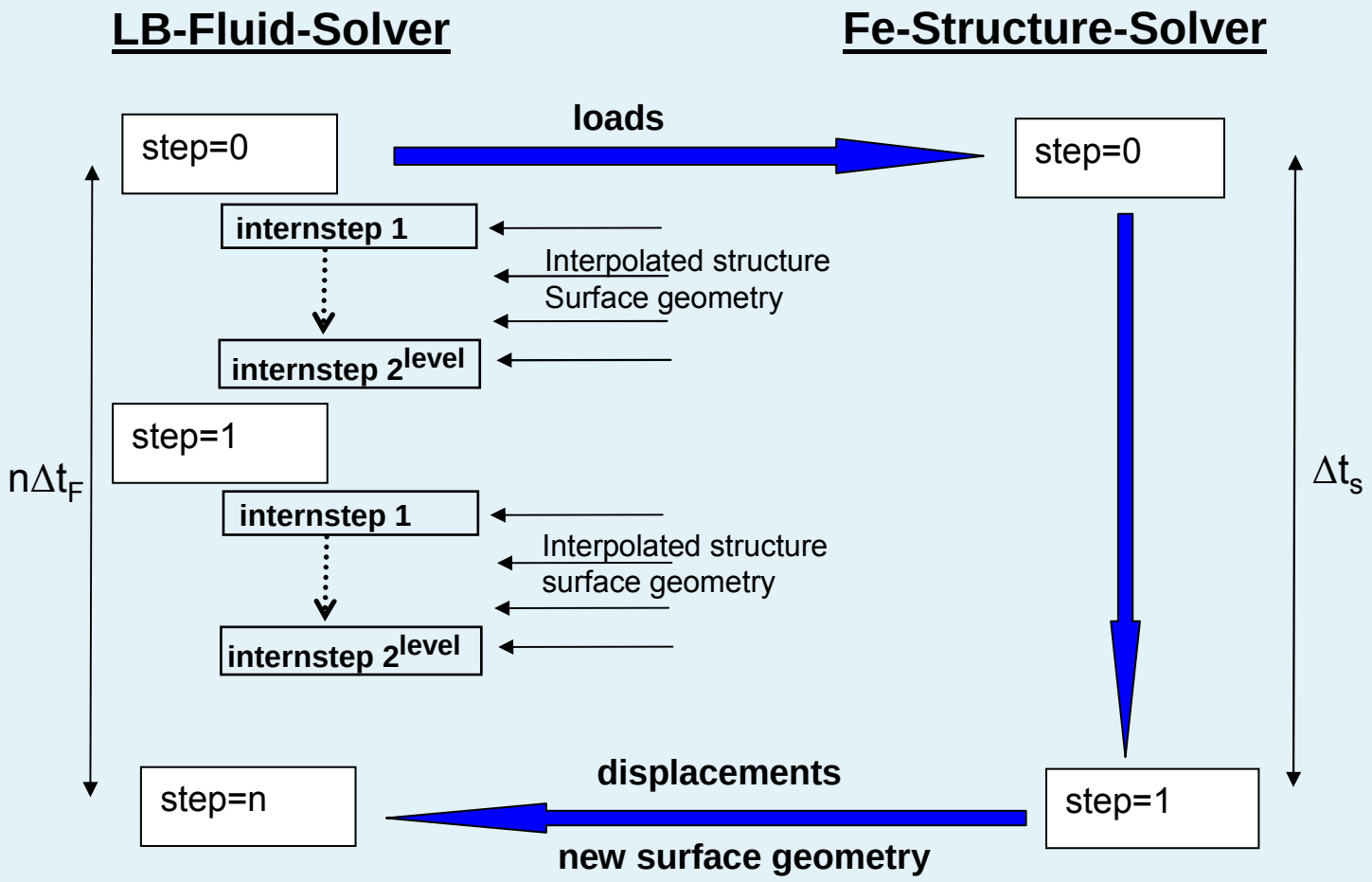

Lattice-Boltzmann Method on quadtree type Grids for Fluid-Structure-Interaction
S. Geller, J. Tölke, M. Krafczyk in H.-J. Bungartz and M. Schäfer, editors, Fluid-Structure Interaction: Modelling, Simulation, Optimisation, Springer Verlag, 2007, preprint available.

Coupling algorithm (implicit)

LB-Fluid-Solver

$$F(t+1) = h(U(t), U(t+1))$$

Fe-Structure-Solver

$$U(t+1) = g(F(t), F(t+1))$$

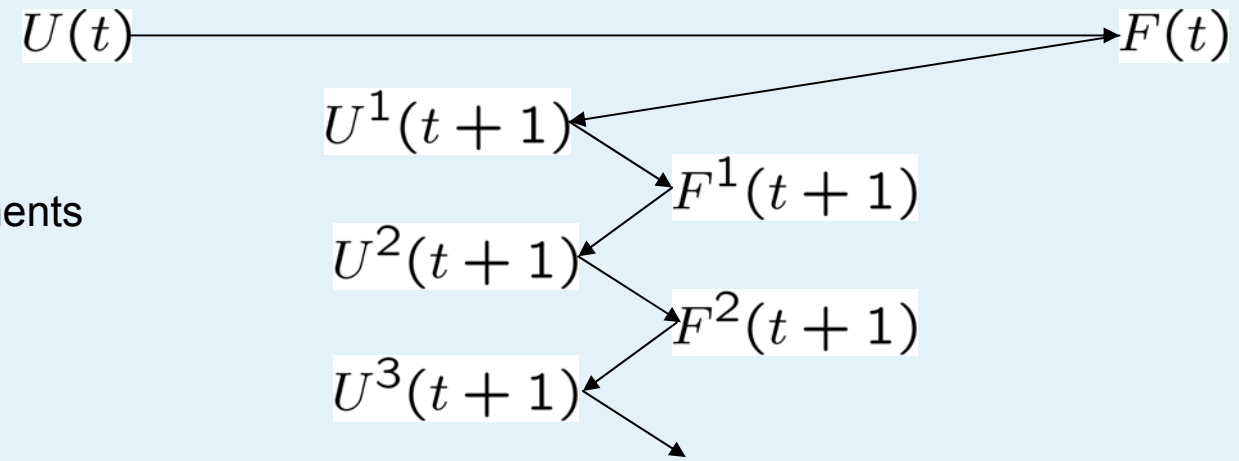

U displacements

F loads

Iterate until convergence

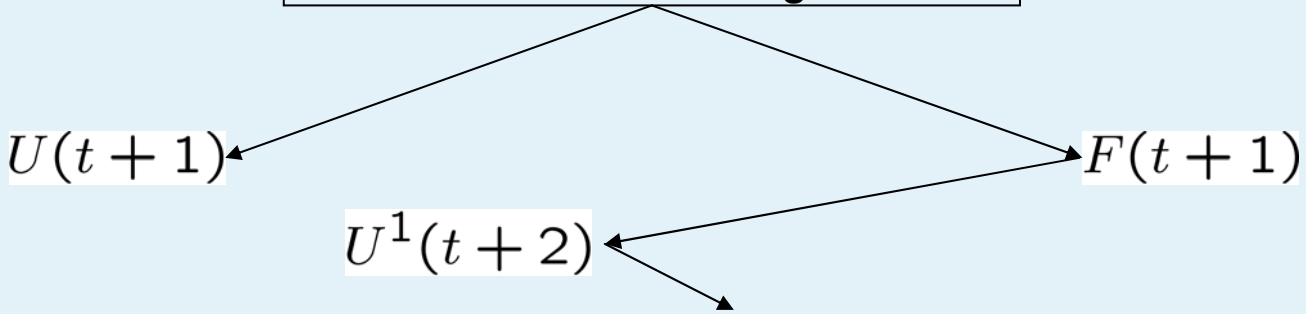

Coupling algorithm (implicit)

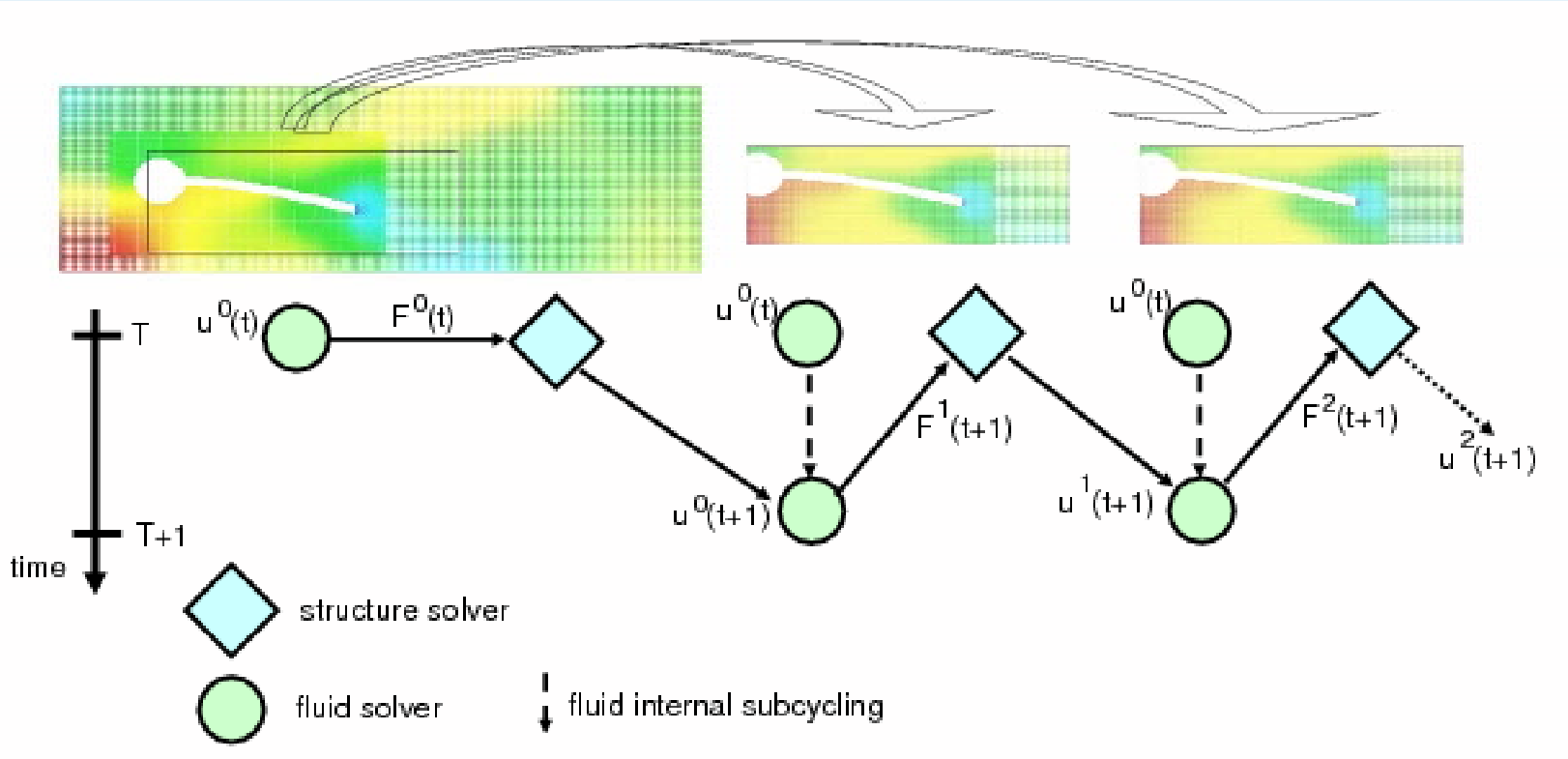

Benchmark FSI 1/3

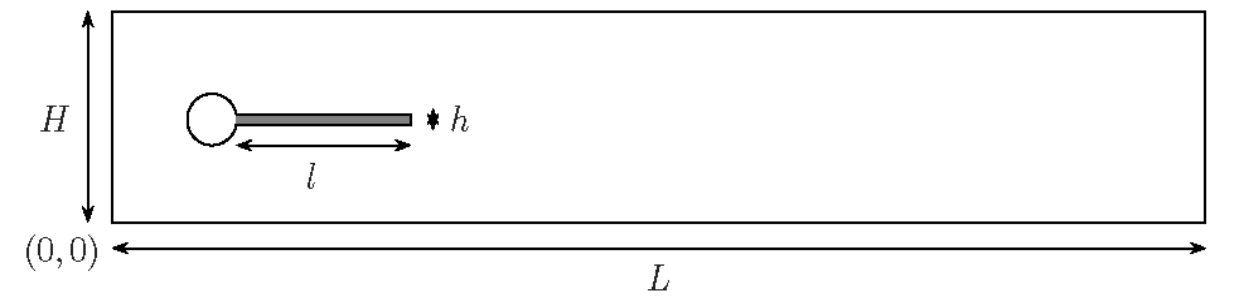

$$\rho_f = 1000[\mathrm{kg\,m^{-3}}]$$
$$\rho_s = 1000[\mathrm{kg\,m^{-3}}]$$
$$\nu_f = 1/1000[\mathrm{m^2 s^{-1}}]$$
$$\nu_s = 0.4[-]$$

1D-beam-elements
- ca. 50 DOF
- Newmark

FE-Solver Adhoc
- ca. 1000 DOF
- Newmark

FSI 1 (Re=20):

$$E = 1.4E6[\mathrm{Pa}]$$
$$\bar{U} = 0.2[\mathrm{m\,s^{-1}}]$$

	VF+1D-Beam	VF+AdhoC	VF+AdhoC
#dof	972054	972054	773334
Ma	0.1	0.1	0.02
Rel. Fehler	**243.9** %	**7.3** %	**1.2** %

FSI 3 (Re=200):

$$E = 5.6E6[\mathrm{Pa}]$$
$$\bar{U} = 2.0[\mathrm{m\,s^{-1}}]$$

Ma=0.1: **1h/Periode**
Ma=0.02: **5h/Periode**

	VF+1D-Beam	VF+AdhoC	VF+AdhoC
#dof	2318904	1835863	1836495
Ma	0.1	0.1	0.02
Rel. F., Mittel	**21.7 %**	**14.0 %**	**3.1 %**
Rel. F., Ampl.	**14.2 %**	**16.0 %**	**1.2 %**
Rel. F., Frequ.	**7.8 %**	**0.2 %**	**1.5 %**

Numerical Methods for the discrete Boltzmann equation

Manfred Krafczyk

contributors:
B. Ahrenholz, S. Freudiger, S. Geller, B. Nachtwey, M. Stiebler, J. Tölke

kraft@cab.bau.tu-bs.de

http://www.cab.bau.tu-bs.de

Overview

- **Reminder: the discrete Boltzmann equation**
- **explicit FD approach**
  - **grid refinement**
  - **adaptivity**
- **implicit FD approach**
- **geometric Multigrid for the stationary problem**
- **FV**
- **p-FEM**

from Boltzmann to Navier Stokes and LBGK

small Knudsen number

Boltzmann equation

$$\frac{\partial f}{\partial t} + \vec{\xi}\frac{\partial f}{\partial \vec{x}} = \Omega(f, f)$$

Chapman-Enskog-Expansion

BGK-Approximation (Bhatnagar, Gross, Krook)

Navier Stokes equations

$$\frac{\partial \vec{v}}{\partial t} + (\vec{v}\nabla)\vec{v} = -\frac{1}{\rho}\nabla p + \frac{\eta}{\rho}\Delta\vec{v}$$

continuity equation

$$\frac{\partial \rho}{\partial t} + \nabla(\rho\vec{u}) = 0$$

$$\frac{\partial f}{\partial t} + \vec{\xi}\frac{\partial f}{\partial \vec{x}} = -\frac{1}{\tau}\left(f - f^{(0)}\right)$$

discretization in space and time

Lattice Boltzmann equation (LBGK)

$$f_i(t+\Delta t, \vec{x}+\xi_i\Delta t) = f_i(t,\vec{x}) - \frac{\Delta t}{\tau}\left(f_i(t,\vec{x}), f_i^{(0)}(t,\vec{x})\right)$$

small Knudsen number
small Mach number

Chapman-Enskog-Expansion

LB or „conventional“ approach ?
→ direct discretization of the Navier-Stokes equations

- Second-order symmetric Finite Difference in space, explicit first order in time
  - → unconditionally unstable for the advection equation
  - → max. cell Reynolds number <2 (Navier-Stokes)
- Finite Volume second order in space, explicit in time
- Finite Differences implicit in space and time
- Spectral methods
- Finite Elements (h-, p-, hp-version, discontinuous Galerkin)
- meshless methods (SPH, X-FEM, ...)
- …

A general statement concerning the efficiency of LB-methods in comparison to all of the above methods in general is inappropriate and very probably misleading !

From the discrete BE to LBGK:

explicit Finite Difference discretization

$$\frac{f_i(\vec{x},t+\Delta t)-f_i(\vec{x},t)}{\Delta t}+c\frac{f_i(\vec{x}+\vec{e}_i\Delta t,t+\Delta t)-f_i(\vec{x},t+\Delta t)}{\Delta x}=-\frac{1}{\tau}\left(f_i(\vec{x},t)-f_i^{eq}(\vec{x},t)\right)$$

$$\Downarrow$$

$$\Delta t = c\Delta x$$

$$\Downarrow$$

$$f_i(\vec{x}+\vec{e}_i\Delta t,t+\Delta t)-f_i(\vec{x},t+\Delta t)=-\frac{\Delta t}{\tau}\left(f_i(\vec{x},t)-f_i^{eq}(\vec{x},t)\right)$$

Taylor expansion + Chapman-Enskog analysis:

viscosity: $$\mu = c_s^2\rho\left(\tau-\frac{\Delta t}{2}\right)$$

grid refinement (Filippova 1998, Krafczyk 1998, Yu, 2002, Crouse, 2002)

LBGK for grid level l:

$$f_{i,l}(\vec{x}+\vec{e}_i\cdot\Delta t_l, t+\Delta t_l) - f_{i,l}(\vec{x},t) = -\frac{\Delta t_l}{3\frac{\nu}{c^2}+\frac{1}{2}\Delta t_l}\left(f_{i,l}(\vec{x},t) - f_{i,l}{}^{(0)}(\vec{x},t)\right)$$

continuity of density/pressure and momentum requires for two grids of level l={c, f }:

$$f_{i,c}{}^{(0)}(\vec{x},t) = f_{i,f}{}^{(0)}(\vec{x},t) = f_i^{(0)}(\vec{x},t)$$

Additionally stresses have to be continuous:

$$S_{\alpha\beta} = \left(\frac{\Delta t_l}{2\tau_l} - 1\right)\Pi_{\alpha\beta}{}^{(neq)} \propto \sum_i e_{i\alpha}e_{i\beta}f_i^{(neq)}$$

Taylor-expansion delivers equivalent PDE:

$$\frac{\partial f_i(\vec{x},t)}{\partial t} + \vec{e}_i \nabla f(\vec{x},t) + O(\Delta t) = \frac{Df_i}{Dt} = -\frac{1}{3\nu + \frac{1}{2}\delta t_l}\left(f_i(\vec{x},t) - f_i^{(eq)}(\vec{x},t)\right)$$

Linear approximation:

$$\frac{\partial f_i^{(eq)}(\vec{x},t)}{\partial t} + \vec{e}_i \nabla f_i^{(eq)}(\vec{x},t) + O(\Delta t) = \frac{Df_i^{(eq)}}{Dt} = -\frac{1}{3\nu + \frac{1}{2}\delta t_l}\left(f_i^{(1)}(\vec{x},t)\right)$$

Identity of total derivatives implies for non-equilibrium distributions:

$$\frac{f_{i,c}^{(1)}}{f_{i,f}^{(1)}} = -\frac{3\nu + \frac{1}{2}\delta t_c}{3\nu + \frac{1}{2}\delta t_f}$$

nested timestepping on non uniform grids

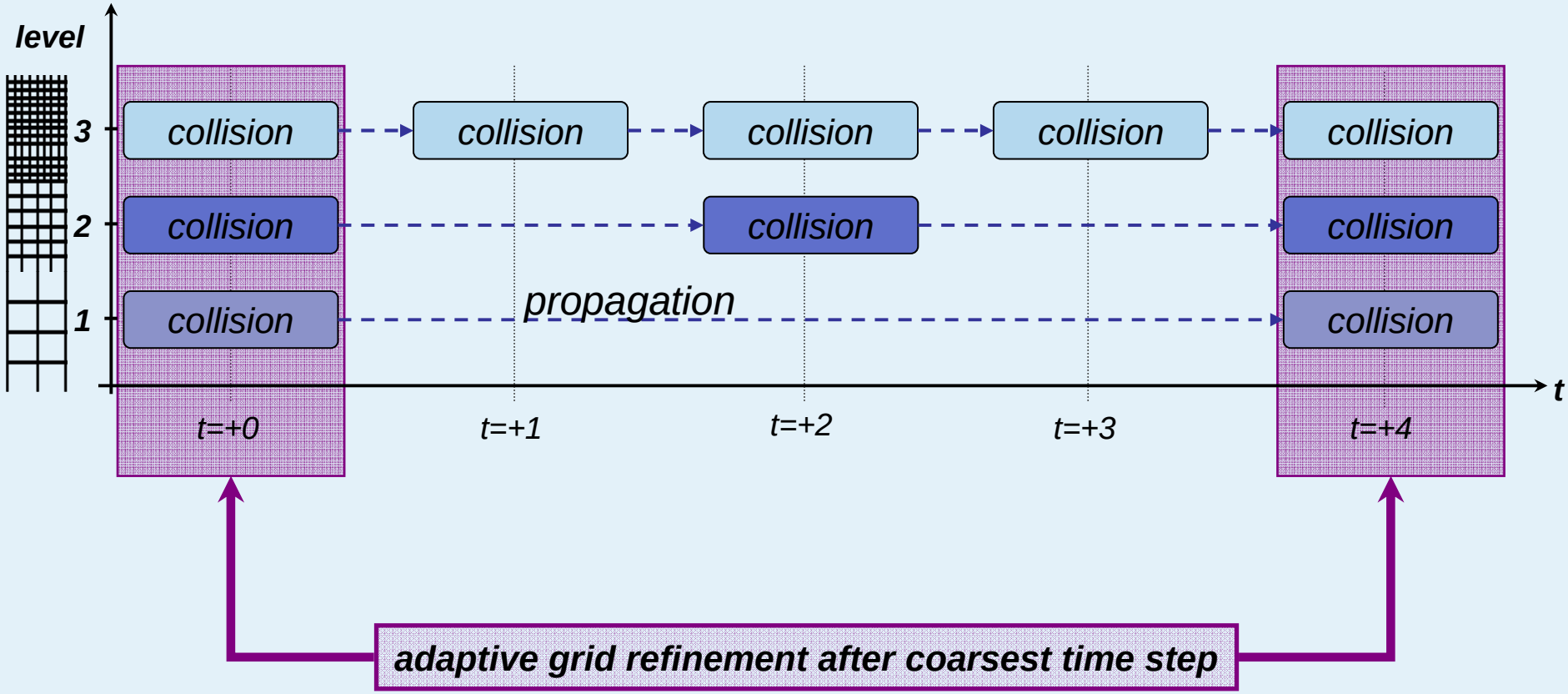

adaptivity (Crouse et al. 2002, Tölke et al. 2006)

motivation:

1. less expert knowledge required
2. much more flexible in terms of complicated geometries
3. maximum efficiency for given resources

requirements:

1. unstructured grids for local refining / coarsening
2. error indicator / estimator
3. semi-automatic generation of interface configurations
   e.g. with respect to interpolation
4. implementation optimization to maximize data locality

error indicator / estimator

estimator: residual measure for upper and lower error bound,
for LBE not yet available !

indicator: heuristic measure without guaranteed lower/upper error limit
(often based on physical properties instead of residua)

Indicator examples:

- curl magnitude
- divergence magnitude
- velocity difference between nodes
- magnitude of mixed derivatives, e.g. $\sqrt{\left(\frac{\partial u_1}{\partial x_2}\right)^2 + \left(\frac{\partial u_2}{\partial x_1}\right)^2}$
- .....

adaptive cycle:

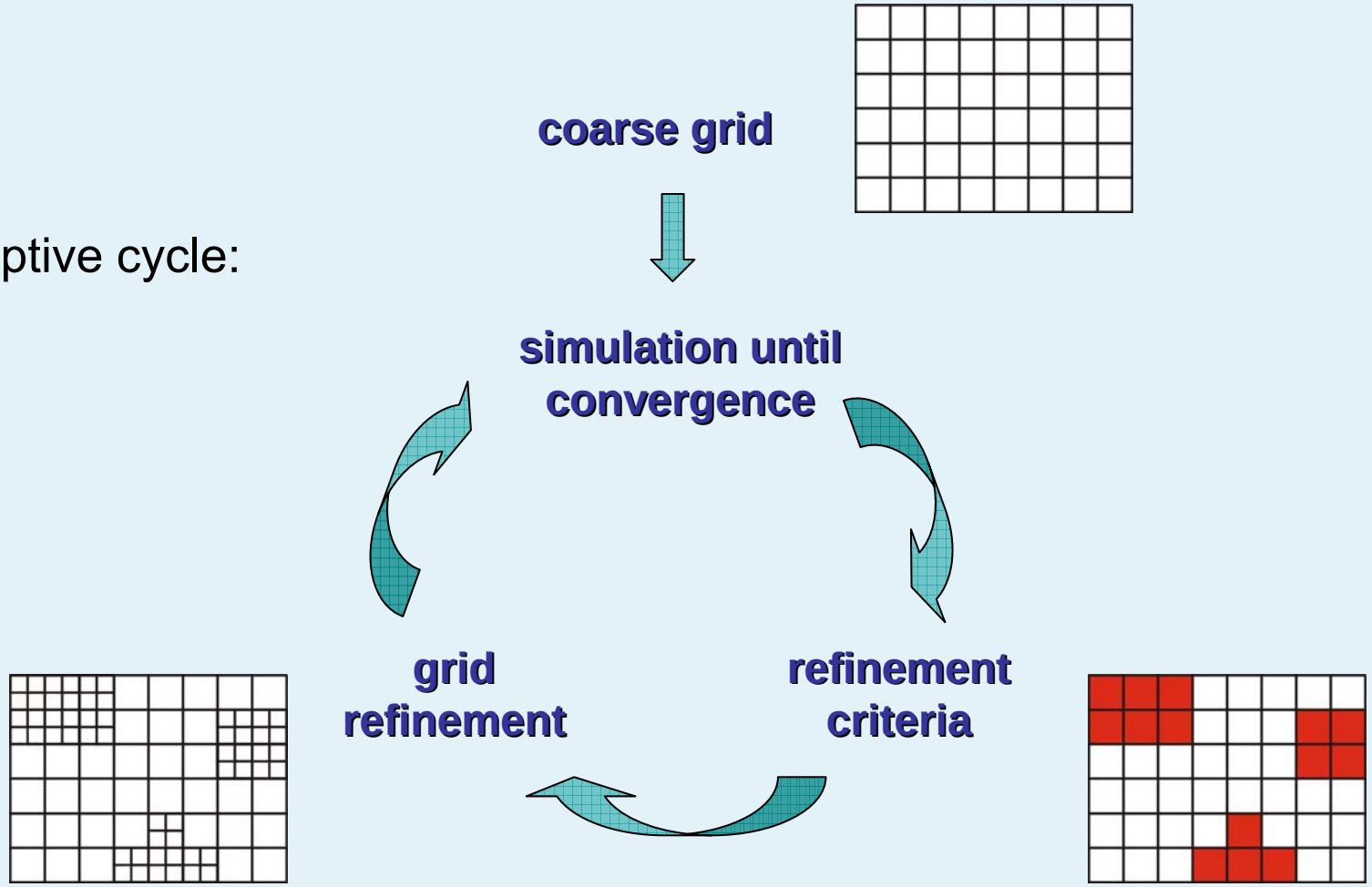

LOCAL refinement: recursive space tiling using tree data structures

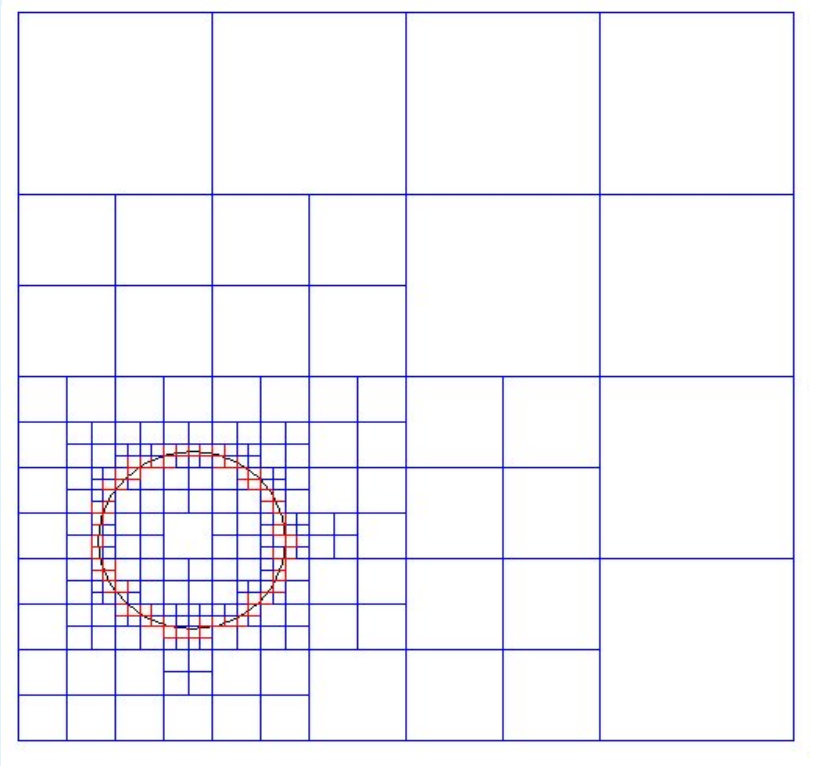

level 0 (root level)

level 1

level 2

level 3

level 4

level 5

level 6

level 6 (smoothed)

(Crouse, Rank, Krafczyk, Tölke, 2002)

Stokes flow
(Re = 1):

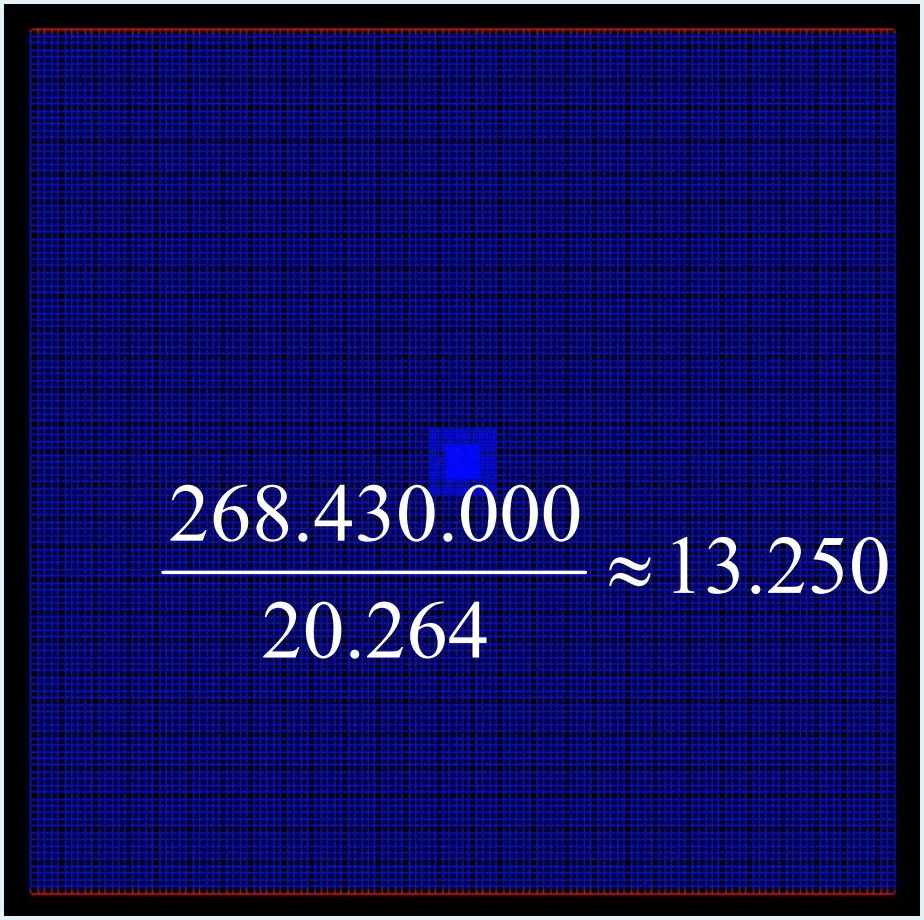

nonuniform:
20.264
grid points

uniform:
~ 268.430.000
grid points

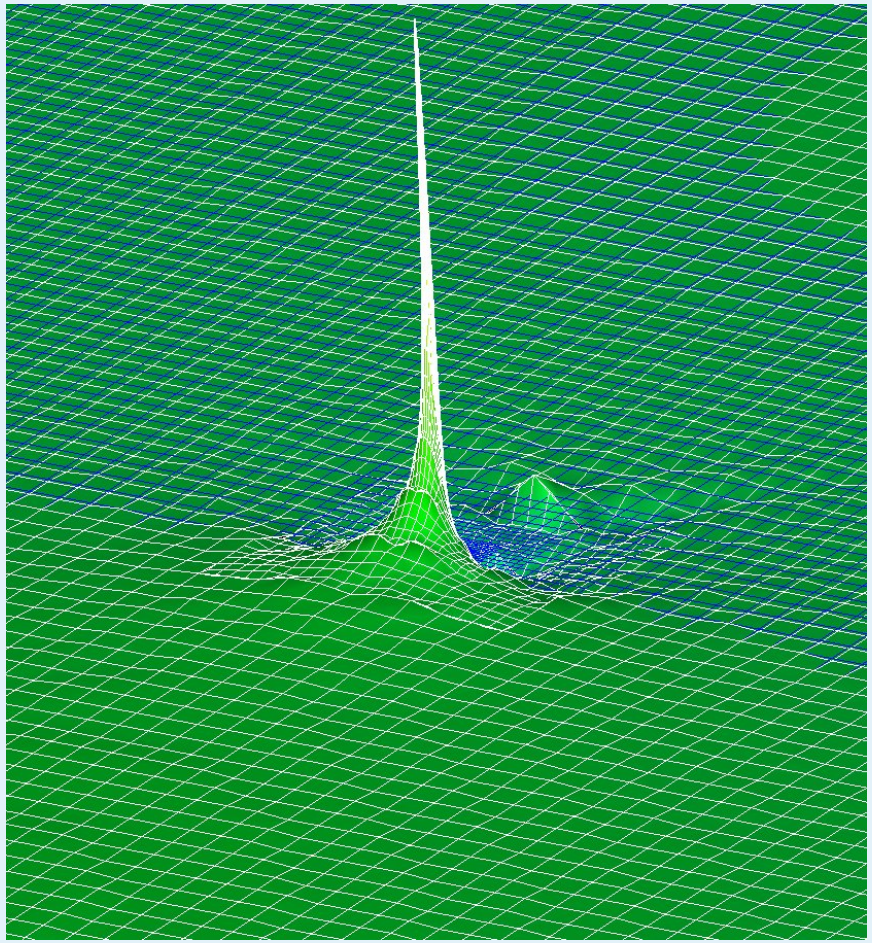

´a priori´ refinement:

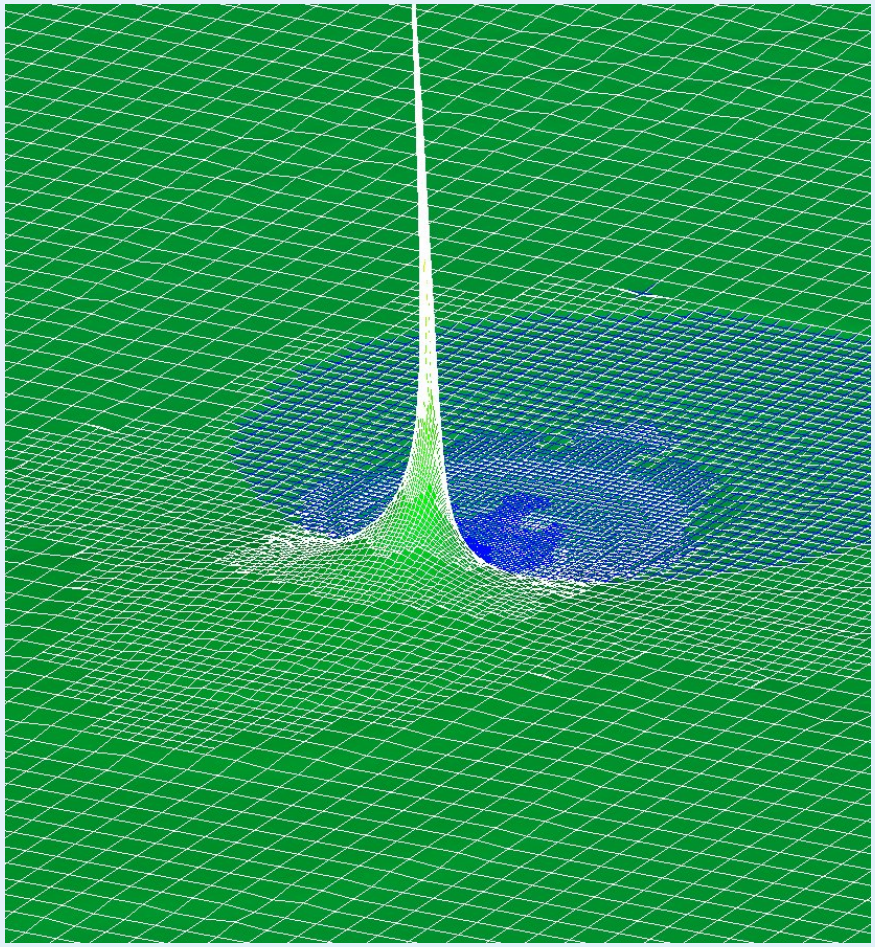

adaptive refinement:

- refinement criterion:
  divergence magnitude
- ´a priori refinement´:
  - 20135 grid nodes
  - c_D = 10,01 (error: 3,8%)
- adaptive simulation:
  - 25658 grid nodes (+ 27,4 %)
  - c_D = 10,42
    (error: 0,115%, i.e. reduction by a factor of 33)

Multi-Grid-acceleration for the stationary discrete BE:

PDE:

$$\vec{e}_i \nabla f_i(\vec{x},t) = -\frac{1}{\tau}\left(f_i(\vec{x},t) - f_i^{eq}(\vec{x},t)\right)$$

Discretization of the spatial derivatives with 2nd order upwind results in a non-linear system of equations

$$\vec{G}_l(\vec{f}_1,\vec{f}_2,\vec{f}_3,\ldots,\vec{f}_n) = 0 \qquad l = 1,\ldots,n$$

smoothing: collective Gauss-Seidel leads to local Newton-Raphson for $\vec{f}_k$

$$L_k(\vec{f}_1,\vec{f}_2,\ldots,\vec{f}_k,\ldots,\vec{f}_n) = 0$$

prolongation and restriction:

$$\frac{1}{16}\begin{bmatrix} 1 & 2 & 1 \\ 2 & 4 & 2 \\ 1 & 2 & 1 \end{bmatrix} \qquad \frac{1}{8}\begin{bmatrix} 0 & 1 & 0 \\ 1 & 4 & 1 \\ 0 & 1 & 0 \end{bmatrix}$$

+bilinear interpolation

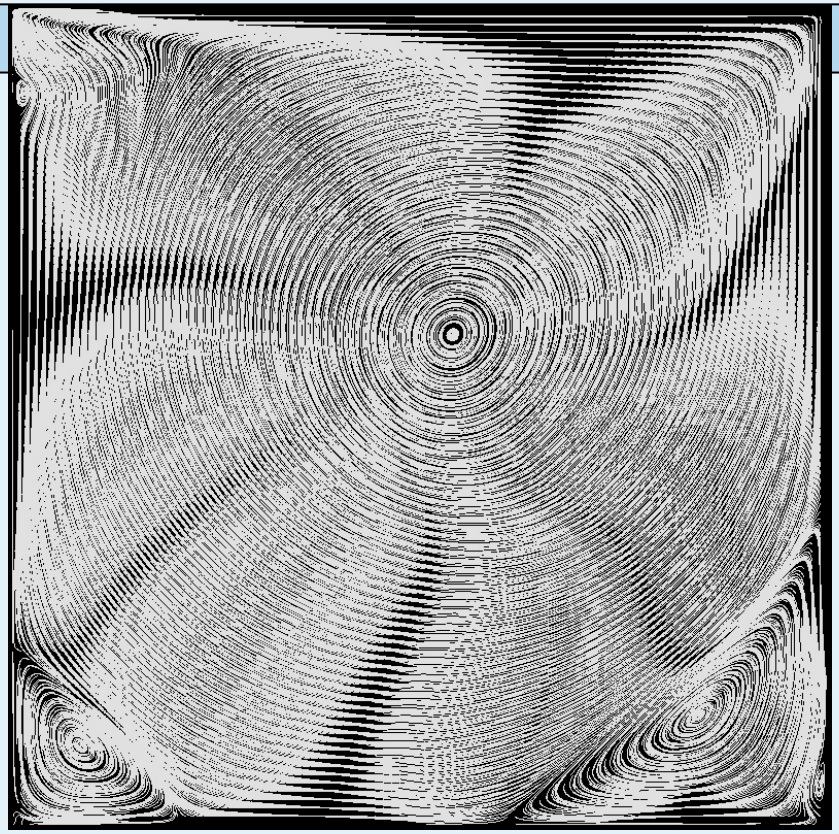

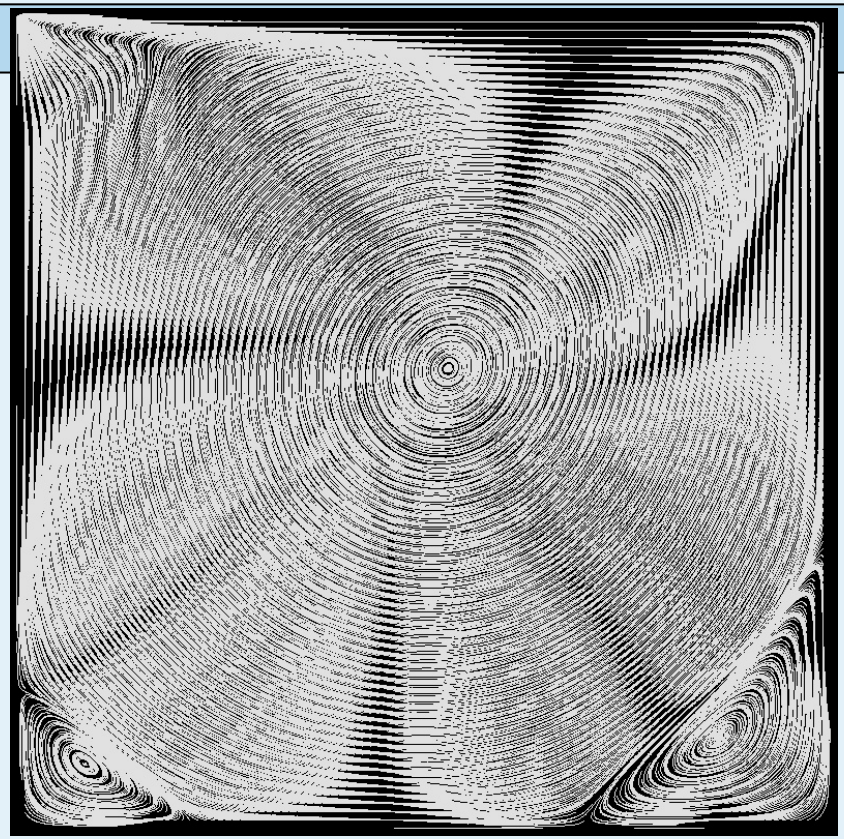

LBGK

FLASH MG prototype

Driven Cavity

Re = 1000

512 x 512 nodes

CPU-ratio ~ 1:100

LBGK Code

FLASH

FV-discretization of the discrete BE

$$\frac{\partial f_a(t,\mathbf{x})}{\partial t} + \boldsymbol{\xi}_a \cdot \frac{\partial f_a(t,\mathbf{x})}{\partial \mathbf{x}} = -\frac{1}{\tau}\left(f_a(t,\mathbf{x}) - f_a^{(0)}(\rho(t,\mathbf{x}),\mathbf{u}(t,\mathbf{x}))\right) \qquad a = 0,\ldots,8$$

$$\rho = \sum_{a=0}^{8} f_a \qquad \rho\mathbf{u} = \sum_{a=0}^{8} \boldsymbol{\xi}_a f_a$$

$$f_a^{(0)} = w_a \rho \left[1 + 3(\boldsymbol{\xi}_a \cdot \mathbf{u}) + \frac{9}{2}(\boldsymbol{\xi}_a \cdot \mathbf{u})^2 - \frac{3}{2}\mathbf{u}\cdot\mathbf{u}\right]$$

$$w_a = \frac{1}{36}\begin{cases} 16, a = 0 \\ 4, a = 1..4 \\ 1, a = 5..8 \end{cases}$$

(resting partikel)

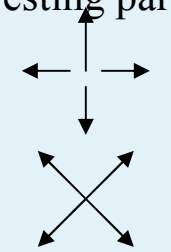

motivation for FV Discretization:

engineering flows are often anisotropic, thus anisotropic elements may be advantageous

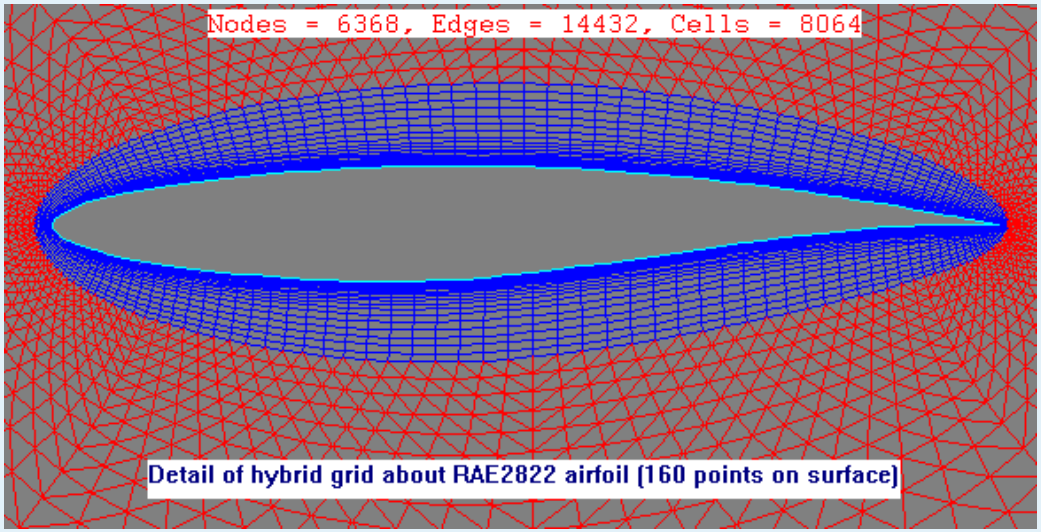

unstructured / anisotropic FV meshes

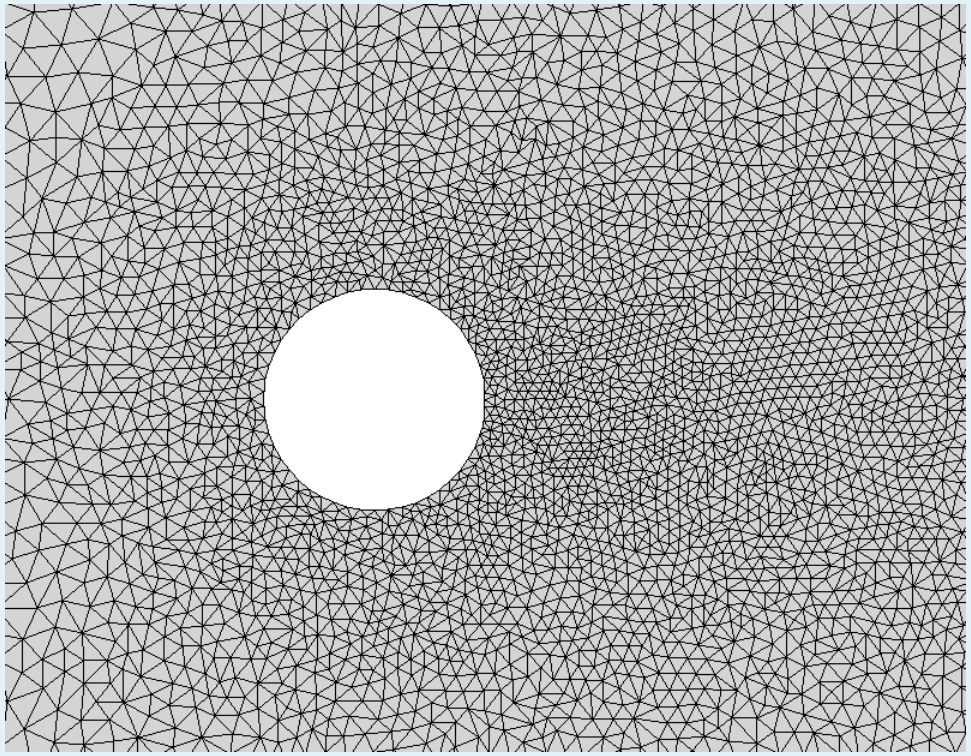

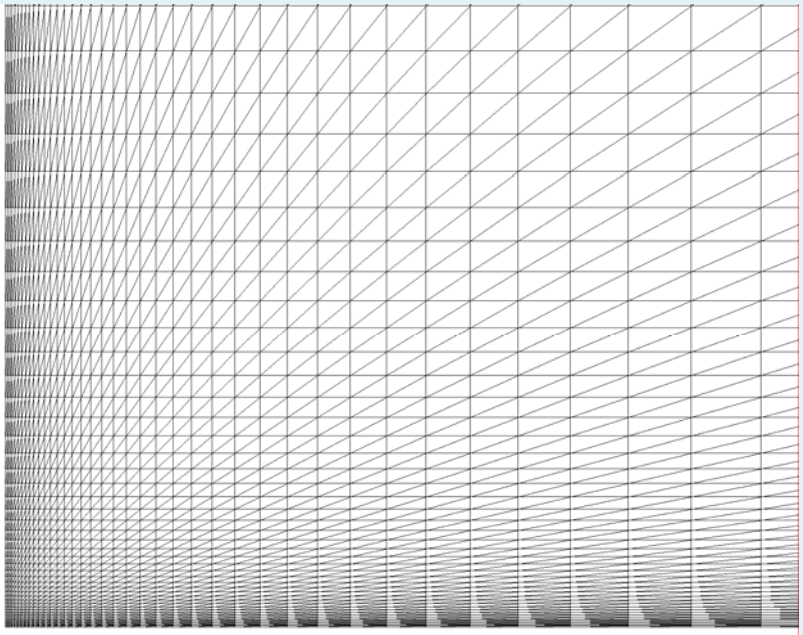

Finite-Volume-approach (Xi et al. 1999)

discrete Boltzmann equation:

$$\frac{\partial f_a(t,\mathbf{x})}{\partial t} + \boldsymbol{\xi}_a \cdot \frac{\partial f_a(t,\mathbf{x})}{\partial \mathbf{x}} = -\frac{1}{\tau}\left(f_a(t,\mathbf{x}) - f_a^{(0)}(t,\mathbf{x})\right)$$

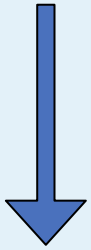

Integration over control volume containing node P

$$A_{CV}\frac{\partial f_a(t,P)}{\partial t} + \boldsymbol{\xi}_a \cdot \oint_{\Gamma_{CV}} \mathbf{n}_\Gamma f_a(t,\mathbf{x})\, d\Gamma = -\frac{1}{\tau}\int_{\Omega_{CV}} f_a(t,\mathbf{x}) - f_a^{(0)}(t,\mathbf{x})\, d\Omega$$

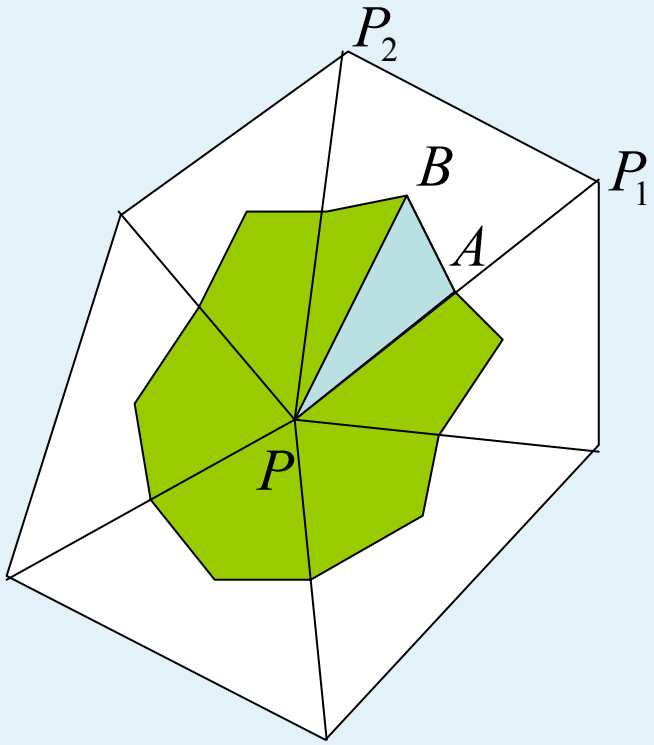

$$\vec{A} = \frac{1}{2}(\vec{P} + \vec{P}_1)$$

$$\vec{B} = \frac{1}{3}(\vec{P} + \vec{P}_1 + \vec{P}_2)$$

Discrete form of the collision operator:

$$\frac{1}{\tau}\int_{PAB}(f(t,\mathbf{x}) - f^{(0)}(t,\mathbf{x}))d\Omega = A_{PAB}\frac{\sum_{\mathbf{x}=\vec{P},\vec{A},\vec{B}}[f(t,\mathbf{x}) - f^{(0)}(t,\mathbf{x})]}{3}$$

where

$$f(A) = \frac{1}{2}[f(P) + f(P_1)]$$

$$f(B) = \frac{1}{3}[f(P) + f(P_1) + f(P_2)]$$

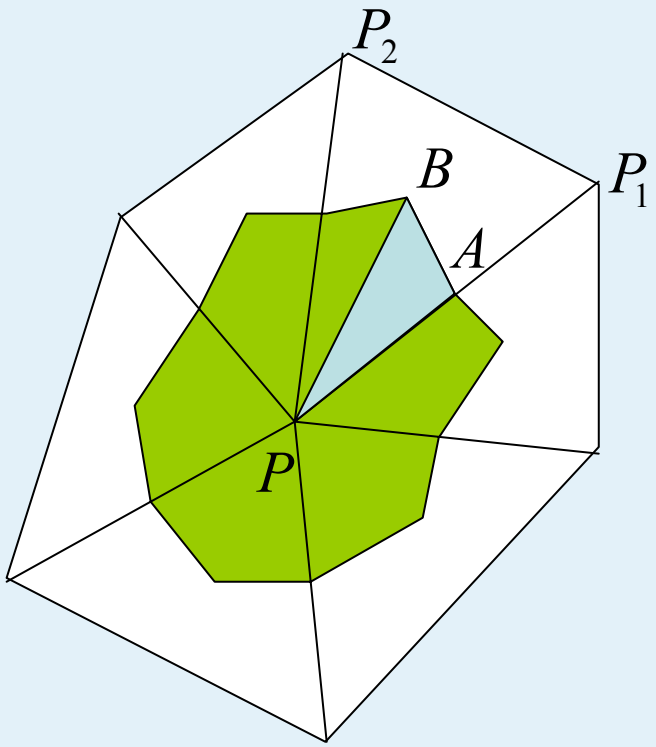

$$\vec{A} = \frac{1}{2}(\vec{P} + \vec{P}_1)$$

$$\vec{B} = \frac{1}{3}(\vec{P} + \vec{P}_1 + \vec{P}_2)$$

Discrete form of the propagation operator:

$$\xi \cdot \oint_{AB} \mathbf{n}_{AB} f(t, \mathbf{x}) d\Gamma = (\xi \cdot \mathbf{n}_{AB}) l_{AB} f_{flux}$$

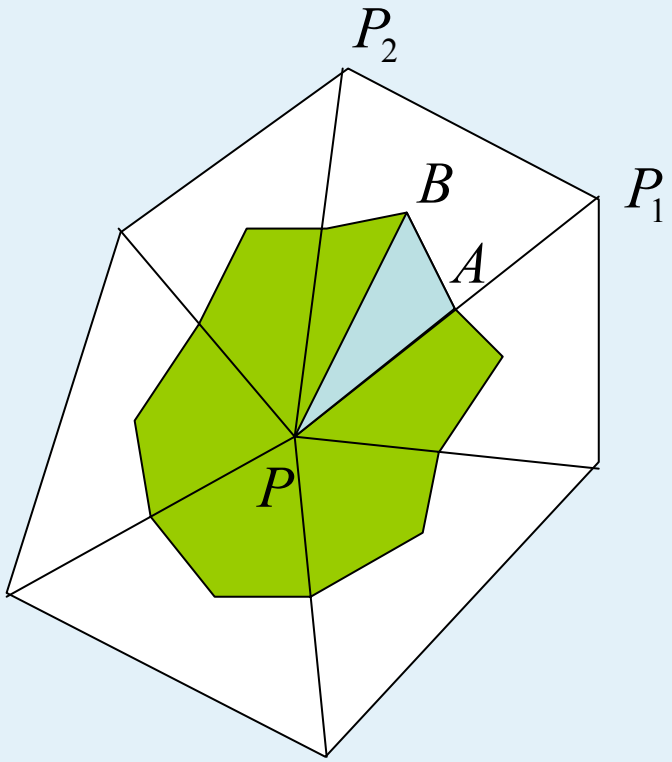

$$\vec{A} = \frac{1}{2}(\vec{P} + \vec{P}_1)$$

$$\vec{B} = \frac{1}{3}(\vec{P} + \vec{P}_1 + \vec{P}_2)$$

computation of flux density:

- central scheme:

$$f_{flux} = \frac{f(t,A) + f(t,B)}{2}$$

$$f(A) = \frac{1}{2}[f(P) + f(P_1)]$$

$$f(B) = \frac{1}{3}[f(P) + f(P_1) + f(P_2)]$$

Finite-Volume-Method

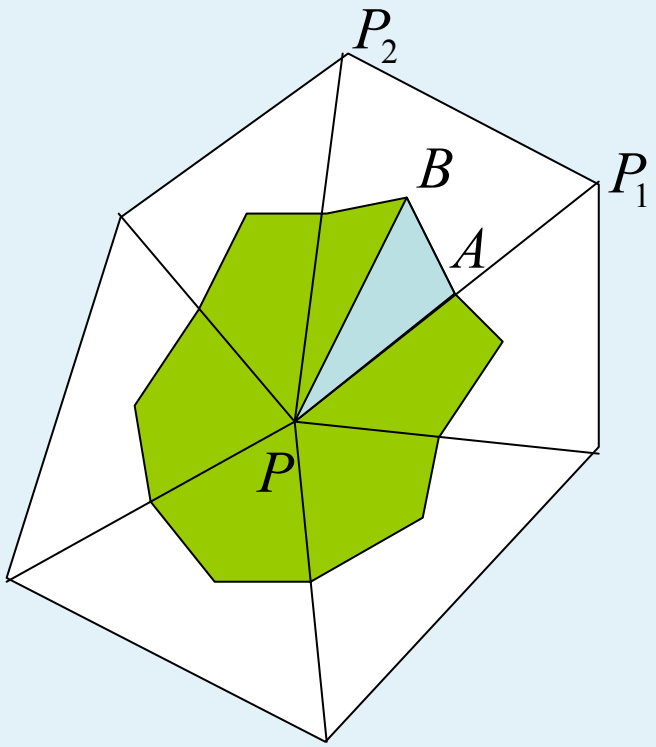

$$\vec{A} = \frac{1}{2}(\vec{P} + \vec{P}_1)$$

$$\vec{B} = \frac{1}{3}(\vec{P} + \vec{P}_1 + \vec{P}_2)$$

computation of flux density:

- first order upwind:

$$f_{a,AB,flux} = \begin{cases} f_{a,P}; \boldsymbol{\xi}_a \cdot \mathbf{n}_{AB} > 0 \\ f_{a,P_1}; \boldsymbol{\xi}_a \cdot \mathbf{n}_{AB} \leq 0 \end{cases}$$

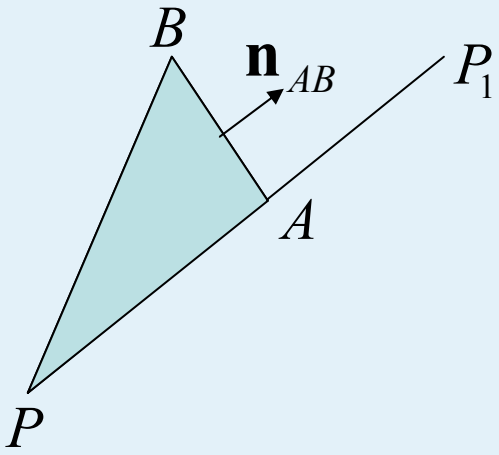

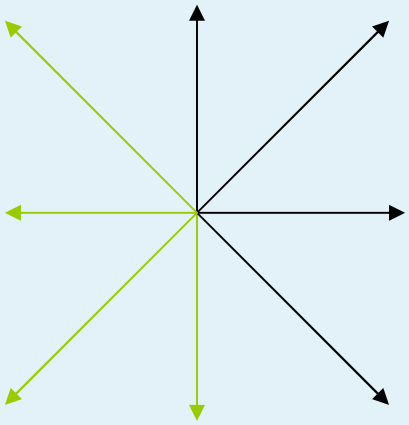

first order upwind

problem: introduces substantial numerical dissipation

→ may work as a simple limiter in areas with large gradients

shear rate criterion:

$$\left\| S_{ij} \right\| = \left\| \sum_a \xi_{ai} \xi_{aj} f_a^{(neq)} \right\| > S_{thresh}$$

cell Re-criterion:

$$Re_{\text{cell}} = \frac{|\mathbf{u}| \Delta x}{\nu} > Re_{thresh}$$

alternative: Least-Squares-Linear-Reconstruction

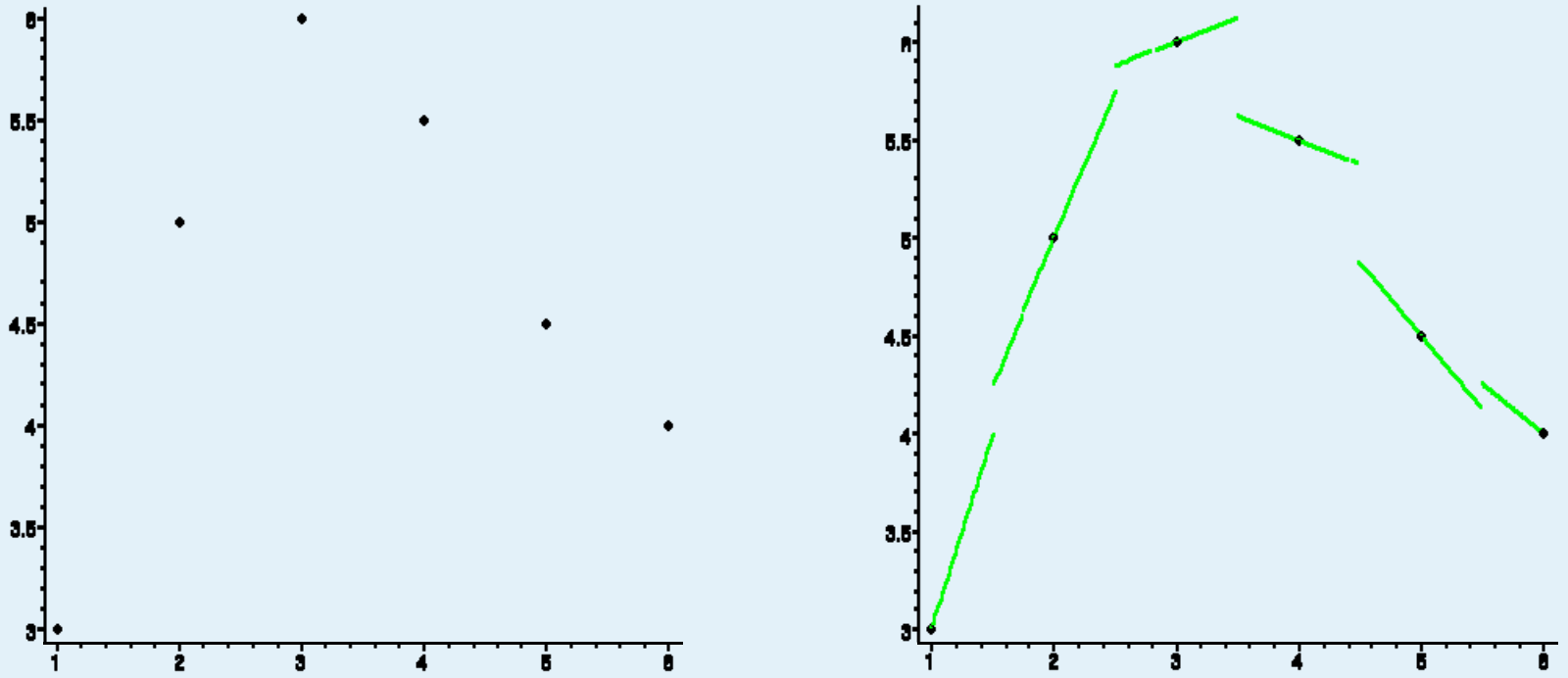

Idea: The assumed distribution gradients in each cell are chosen such that the resulting linear functions optimally extrapolate to the values of f at the neighboring nodes in a least squares sense.

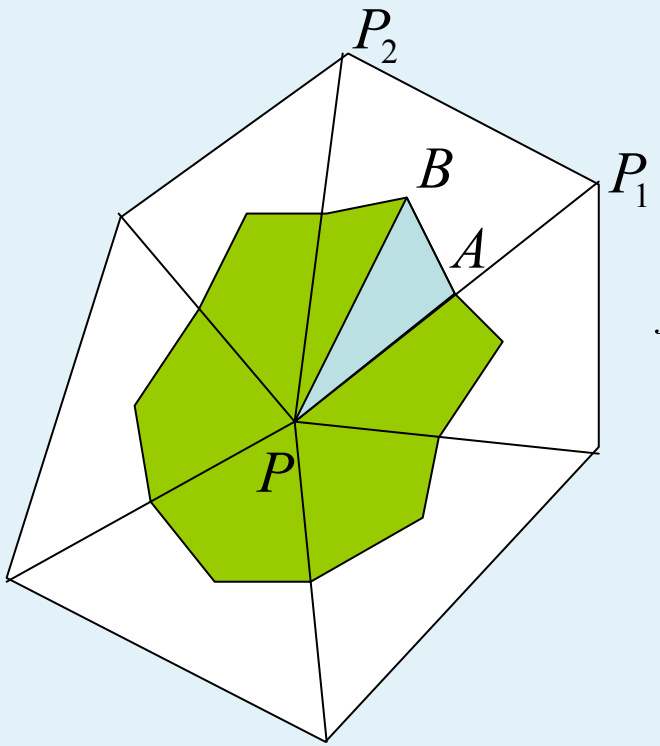

$$\vec{A} = \frac{1}{2}(\vec{P} + \vec{P}_1)$$

$$\vec{B} = \frac{1}{3}(\vec{P} + \vec{P}_1 + \vec{P}_2)$$

Stiebler et al., Comp. & Fluids, 2006

computation of flux density:

- upwind based on LSLR:

$$f_{a,AB,\text{flux}} = \begin{cases} f_{a,P} + \vec{\tilde{\nabla}} f_{a,P} \cdot \left[\{\mathbf{x}_A + \mathbf{x}_B\}/2 - \mathbf{x}_P(P) \right]; & \xi_a \cdot \mathbf{n}_{AB} > 0 \\ f_{a,P_1} + \vec{\tilde{\nabla}} f_{a,P_1} \cdot \left[\{\mathbf{x}_A + \mathbf{x}_B\}/2 - \mathbf{x}_{P_1}(P_1) \right]; & \xi_a \cdot \mathbf{n}_{AB} \le 0 \end{cases}$$

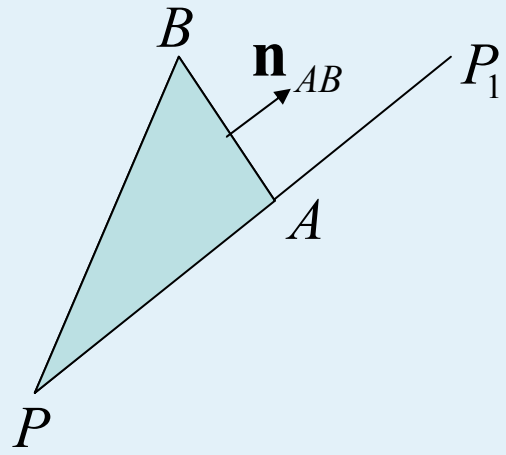

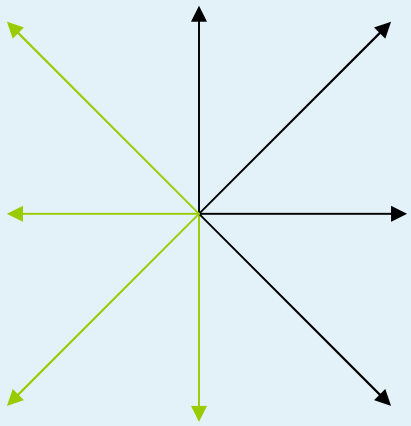

least squares – linear reconstruction (LSLR)-scheme

- increase in stability compared to central scheme
- comparable accuracy to central scheme
- additional computational cost to determine the gradient ~50 %

testcase: flow arround cylinder

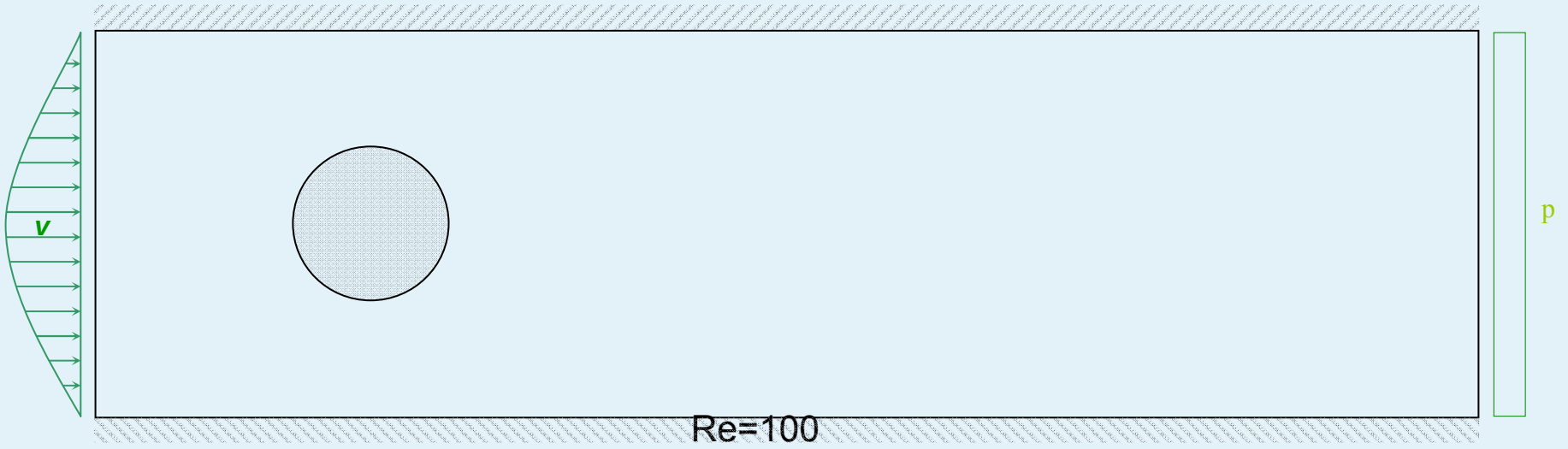

central scheme:

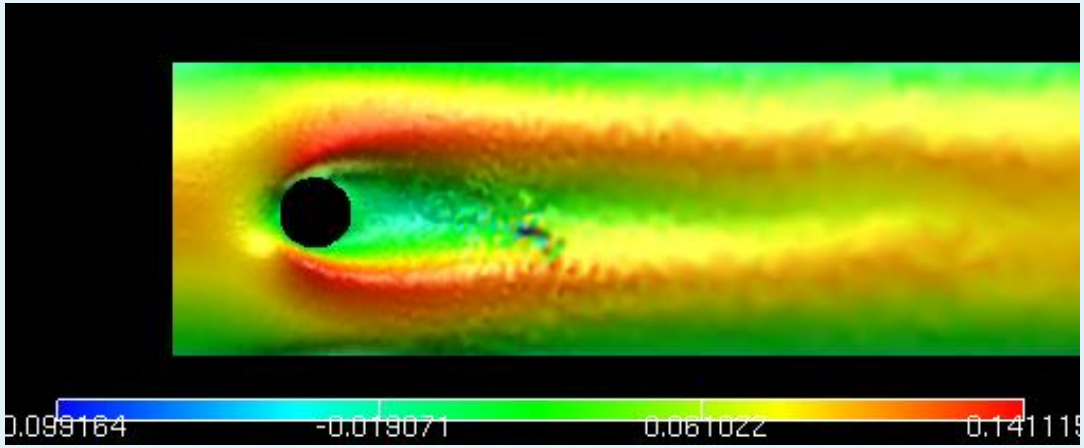

first order upwind-scheme:

$S_{thresh} = 0.5$

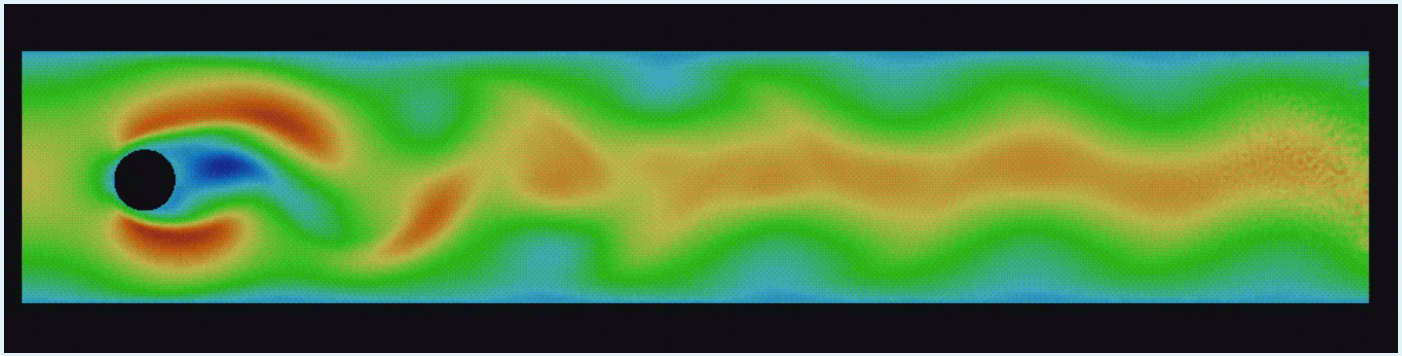

drag coefficient

S_{Thresh}	c_D
0,8	3,92
1,0	3,67
1,2	3,26
LSLR:	3,17
reference:	3,23

testcase: Poiseuille flow

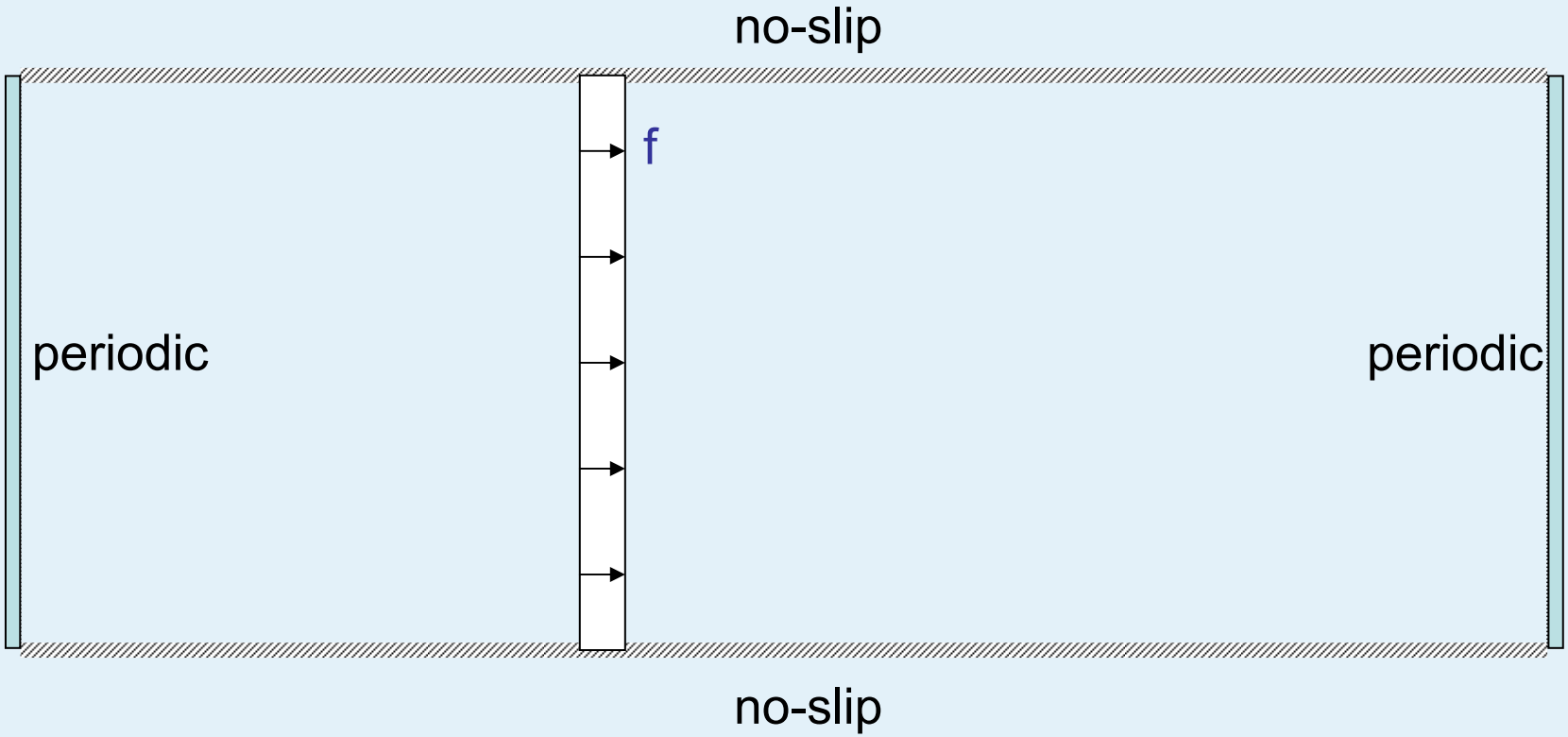

numerical viscosity in channel flow

τ	ν_{centr}	ν_{upw}	$\nu_{upw}-\nu_{centr}$	rel. err.	Re-#
0.075	0,025	0,544	0,520	20,960	320
0.150	0,049	0,560	0,511	10,484	160
0.300	0,096	0,602	0,505	5,239	80
0.600	0,201	0,729	0,528	2,629	40

$$\Delta x \approx 1.00 = \frac{H}{80}$$

τ	ν_{centr}	ν_{upw}	$\nu_{upw}-\nu_{centr}$	rel. err.	Re-#
0.075	0,026	0,719	0,694	27,182	320
0.150	0,051	0,746	0,695	13,573	160
0.300	0,104	0,797	0,693	6,664	80
0.600	0,203	0,904	0,701	3,449	40

$$\Delta x \approx 1.33 = \frac{H}{60}$$

τ	ν_{centr}	ν_{upw}	$\nu_{upw}-\nu_{centr}$	rel. err.	Re-#
0.075	0,027	1,072	1,046	39,279	320
0.150	0,054	1,099	1,046	19,504	160
0.300	0,118	1,261	1,143	9,698	80
0.600	0,228	1,323	1,096	4,814	40

$$\Delta x \approx 2.00 = \frac{H}{40}$$

drag coefficient for Re=20

	# Nodes	cD	CPU-time
Ma=0.173:			
LBM Grid #1	10200	5,63	16
LBM Grid #2	40800	5,595	120
LBM Grid #3	163000	5,580	900
FVM central #1	7564	5,51	240
FVM central #2	11736	5,48	360
FVM central #3	17293	5,48	480
FVM LSLR #1	7564	5,62	300
FVM LSLR #2	11736	5,6	400
FVM LSLR #3	17293	5,6	690
Ma=0.086:			
LBM Grid #1	10200	5,67	30
LBM Grid #2	40800	5,61	200
LBM Grid #3	163000	5,596	1850
FVM central #1	7564	5,4	830
FVM LSLR #1	7564	6,0	16500
reference solution		5.57-5.59	

Poiseuille flow

		Re=230	Re=450	Re=900	Re=2300
grid #1	central	---	---	---	---
(7 nodes)	LSLR	0,248	0,377	0,537	0,739
grid #2	central	---	---	---	---
(11 nodes)	LSLR	0,123	0,201	0,323	0,538
grid #3	central	---	---	---	---
(21 nodes)	LSLR	0,0608	0,124	0,253	0,387
grid #4	central	0,00627	---	---	---
(41 nodes)	LSLR	0,01028	0,0318	0,05	0,203

numbers represent $$e_{L_2} = \left[\frac{\sum (u_{x,theory} - u_{x,sim})^2}{\sum u_{x,theory}}\right]^{\frac{1}{2}}$$

unstructured FVM vs. hierarchichal LBM

Leading error $O(\Delta x^2)$

Meshing Flexibility

Only Cartesian grids (but subgrid corrections possible)

Anisotropic elements for e.g. boundary layers

Local refinement / coarsening only in powers of two

Computational effort substantially higher

Automatic and fast grid generation in 3D

conclusion for present FV Lattice-Boltzmann approaches

- upwind scheme can be used to stabilize a computation in critical regions of the flow
- to reduce the amount of numerical viscosity, higher order upwind schemes will have to be introduced
- a locally implicit time stepping scheme can improve the stability of the method at a considerable computational cost
- least square variants improve stability while maintaining accuracy
- present FV LB implementations are not competitive CFD solvers

Finite Element Discretization of the discrete Boltzmann equation

motivation:

- weak formulation facilitates development of *a posteriori* error estimators
- allows anisotropic elements
- allows unstructured meshes
- allows curved element boundaries (blending method)
- allows anisotropic ansatz spaces (p-version)

The following slides describing a high-order FEM discretization of the discrete Boltzmann equation are a summary of work recently published by Dr. Alexander Düster in IJNME 2006 (***www.inf.bv.tum.de/~duester***).

Discontinuous Galerkin method

$$\frac{\partial f_i}{\partial t} + \mathbf{e}_i \cdot \nabla f_i = C_i \quad \text{in } \Omega \subset \mathbb{R}^2,\ i = 0, 1, 2, ..., 8$$

$$\int_{\Omega_e} \phi \frac{\partial f_i}{\partial t} d\Omega = -\int_{\Omega_e} \phi \mathbf{e}_i \cdot \nabla f_i \, d\Omega + \int_{\Gamma_{in}(\Omega_e)} \phi [f_i] \mathbf{e}_i \cdot \mathbf{n} d\Gamma + \int_{\Omega_e} \phi \, C_i \, d\Omega$$
$$i = 0, 1, 2, ..., 8, \ \forall \phi$$

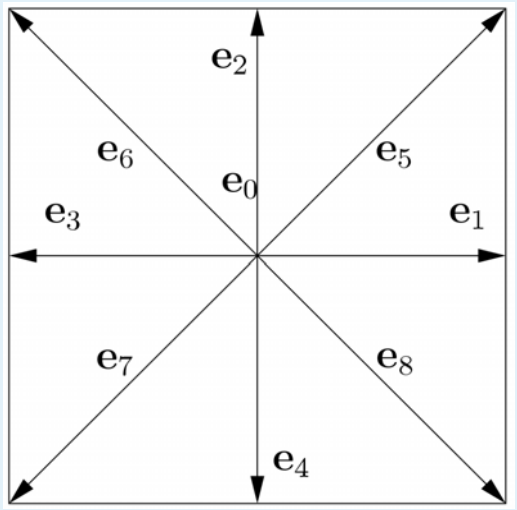

$$[f_i] = f_i^+ - f_i^-$$

$$f_i^{\pm} = \lim_{\varepsilon \to 0} f_i(\mathbf{x} \pm \varepsilon \mathbf{e}_i)$$

$$f_i^-(\mathbf{x}) = f_i^*(\mathbf{x}) \quad \text{if } \mathbf{x} \in \Gamma_{in}(\Omega)$$

$$\mathbf{e}_i \cdot \mathbf{n} \geq 0 \quad \text{on } \Gamma_{out}(\Omega_e)$$

$$\mathbf{e}_i \cdot \mathbf{n} < 0 \quad \text{on } \Gamma_{in}(\Omega_e)$$

Spatial discretization:

$$\hat{\phi} = \sum_{k=1}^{k_{modes}} N_k \hat{\phi}_k = \mathbf{N}\hat{\boldsymbol{\phi}} \qquad \hat{f}_i = \sum_{k=1}^{k_{modes}} N_k \hat{f}_{i,k} = \mathbf{N}\hat{\mathbf{f}}_i$$

$$\nabla\hat{\phi} = \sum_{k=1}^{k_{modes}} \nabla N_k \hat{\phi}_k = \mathbf{B}\hat{\boldsymbol{\phi}} \qquad \nabla\hat{f}_i = \sum_{k=1}^{k_{modes}} \nabla N_k \hat{f}_{i,k} = \mathbf{B}\hat{\mathbf{f}}_i$$

$$\mathbf{N} = \begin{bmatrix} N_1 & N_2 & N_3 & \cdots & N_{k_{modes}} \end{bmatrix} \qquad \mathbf{B} = \begin{bmatrix} \frac{\partial N_1}{\partial x} & \frac{\partial N_2}{\partial x} & \frac{\partial N_3}{\partial x} & \cdots & \frac{\partial N_{k_{modes}}}{\partial x} \\ \frac{\partial N_1}{\partial y} & \frac{\partial N_2}{\partial y} & \frac{\partial N_3}{\partial y} & \cdots & \frac{\partial N_{k_{modes}}}{\partial y} \end{bmatrix}$$

$$\int_{\Omega_e} \phi \frac{\partial f_i}{\partial t} d\Omega = -\int_{\Omega_e} \phi \mathbf{e}_i \cdot \nabla f_i \, d\Omega + \int_{\Gamma_{in}(\Omega_e)} \phi [f_i] \mathbf{e}_i \cdot \mathbf{n} d\Gamma + \int_{\Omega_e} \phi \, C_i \, d\Omega$$
$$i = 0, 1, 2, ..., 8, \; \forall \phi$$

$$\int_{\Omega_e} \mathbf{N}^T \mathbf{N} \, d\Omega \frac{d\hat{\mathbf{f}}_i}{dt} = -\int_{\Omega_e} \mathbf{N}^T \mathbf{e}_i \cdot \nabla \hat{f}_i \, d\Omega + \\ + \int_{\Gamma_{in}(\Omega_e)} \mathbf{N}^T \mathbf{n} \cdot \mathbf{e}_i \, [\hat{f}_i] \, d\Gamma + \int_{\Omega_e} \mathbf{N}^T C_i \, d\Omega$$

$$\mathbf{M} \frac{d\hat{\mathbf{f}}_i}{dt} = \mathbf{L}(\hat{\mathbf{f}}_i)$$

Temporal discretization: forward Euler:

$$\mathbf{M}\frac{d\hat{\mathbf{f}}_i}{dt} = \mathbf{L}(\hat{\mathbf{f}}_i)$$

$$\mathbf{M}\frac{\hat{\mathbf{f}}_i^{n+1} - \hat{\mathbf{f}}_i^{n}}{\Delta t} = \mathbf{L}(\hat{\mathbf{f}}_i^{n})$$

$$\begin{aligned} \mathbf{M}\Delta\hat{\mathbf{f}}_i^{n+1} &= \Delta t\,\mathbf{L}(\hat{\mathbf{f}}_i^{n}), \quad i = 0,1,2,...,8 \\ \hat{\mathbf{f}}_i^{n+1} &= \hat{\mathbf{f}}_i^{n} + \Delta\hat{\mathbf{f}}_i^{n+1} \end{aligned}$$

Hierarchic shape functions of high order finite elements in 1D (Szabó, Babuška 1991)

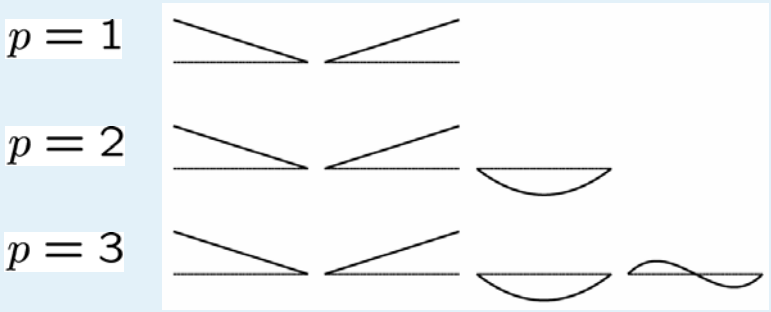

$$\left.\begin{aligned} N_1(\xi) &= \frac{1}{2}(1-\xi) \\ N_2(\xi) &= \frac{1}{2}(1+\xi) \end{aligned}\right\} \; p = 1$$

$$N_i(\xi) = \phi_{i-1}(\xi), \quad i = 3, 4, \ldots, p+1$$

Integrated Legendre Polynomials

$$\phi_j(\xi) = \sqrt{\frac{2j-1}{2}} \int_{-1}^{\xi} L_{j-1}(x)\, dx = \frac{1}{\sqrt{4j-2}} \left(L_j(\xi) - L_{j-2}(\xi)\right), \quad j = 2, 3, \ldots$$

Orthogonality property

$$\int_{-1}^{1} \frac{d\,N_i}{d\,\xi} \frac{d\,N_j}{d\,\xi}\, d\,\xi = \delta_{ij}, \; i \geq 3 \text{ and } j \geq 1 \text{ or } i \geq 1 \text{ and } j \geq 3$$

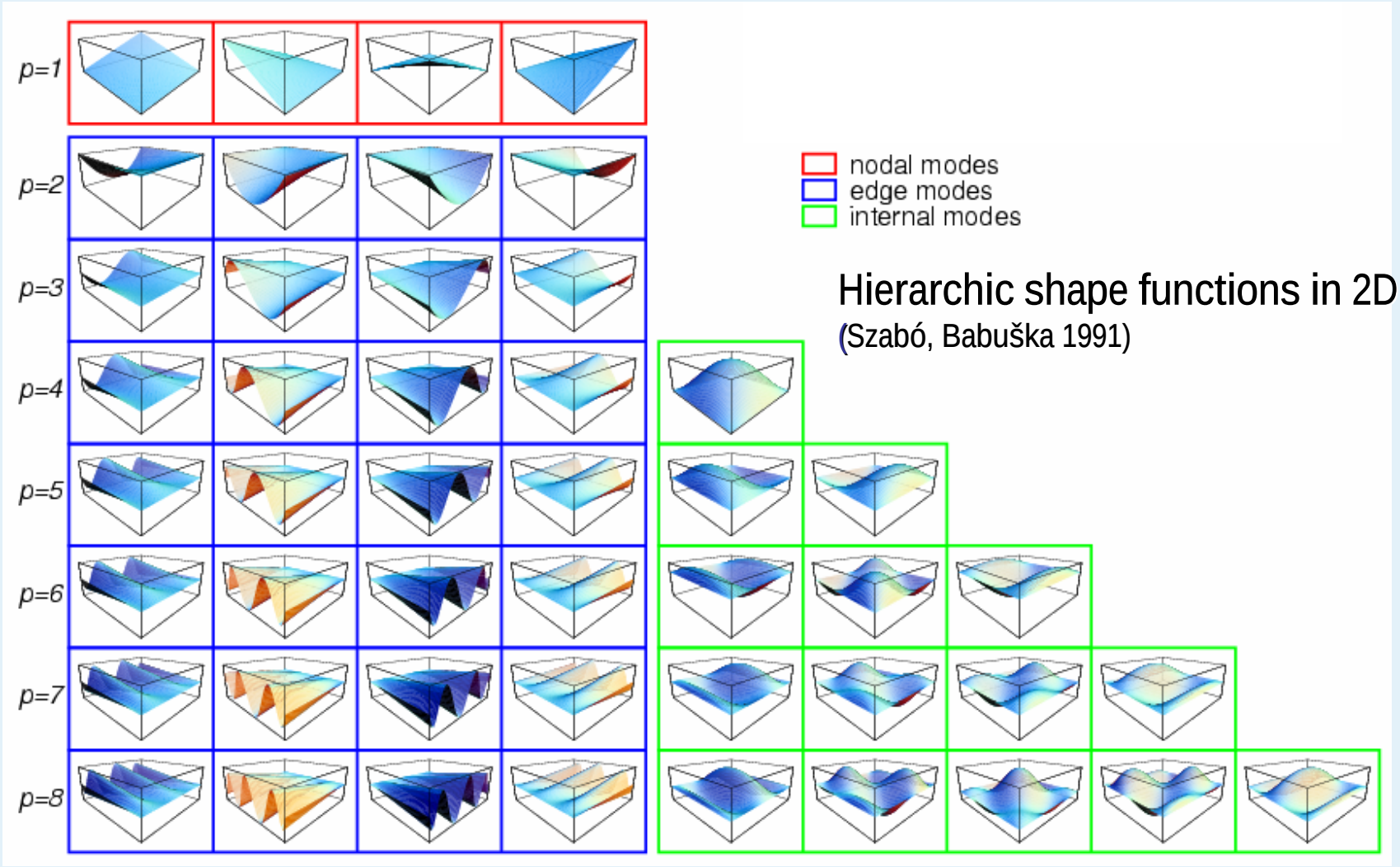

Hierarchic shape functions in 2D

(Szabó, Babuška 1991)

Blending function method (Gordon, Hall 1973)

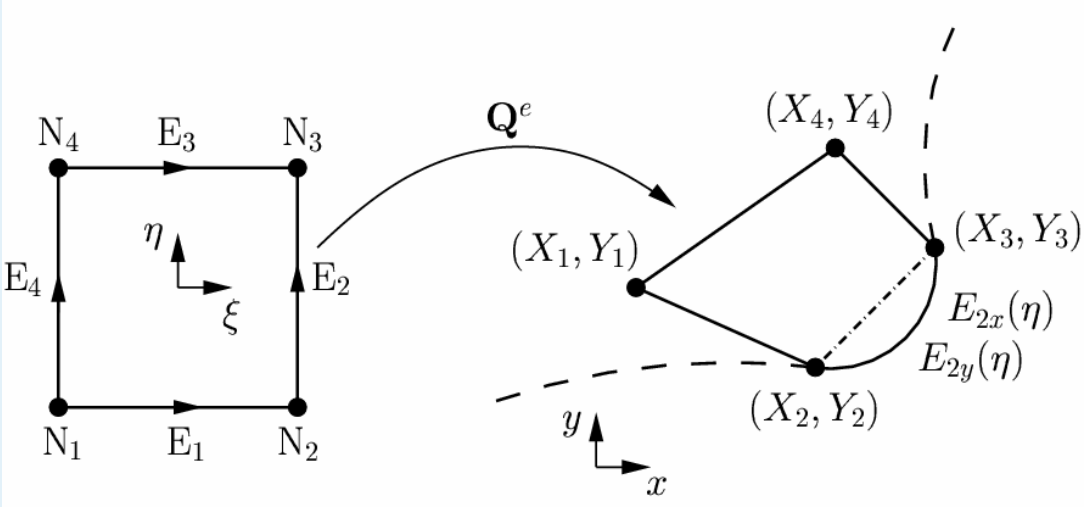

$$x = Q_x^e(\xi,\eta) = \sum_{i=1}^{4} N_{1,1}^{\mathsf{N}_i}(\xi,\eta)\, X_i + \left[E_{2x}(\eta) - \left(\frac{1-\eta}{2} X_2 + \frac{1+\eta}{2} X_3 \right) \right] \frac{1+\xi}{2}$$

$$y = Q_y^e(\xi,\eta) = \sum_{i=1}^{4} N_{1,1}^{\mathsf{N}_i}(\xi,\eta)\, Y_i + \left[E_{2y}(\eta) - \left(\frac{1-\eta}{2} Y_2 + \frac{1+\eta}{2} Y_3 \right) \right] \frac{1+\xi}{2}$$

$$N_{1,1}^{\mathsf{N}_i}(\xi,\eta) = \frac{1}{4}(1+\xi_i\xi)(1+\eta_i\eta), i = 1,2,3,4$$

Poiseuille flow

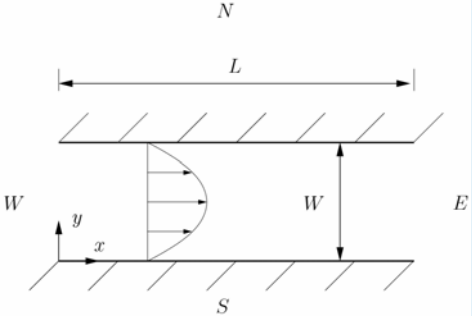

Navier-Stokes solution

$$u_x = \frac{F_x W^2}{8\rho\nu}\left(1-(\frac{2y}{W}-1)^2\right)$$
$$u_y = 0$$

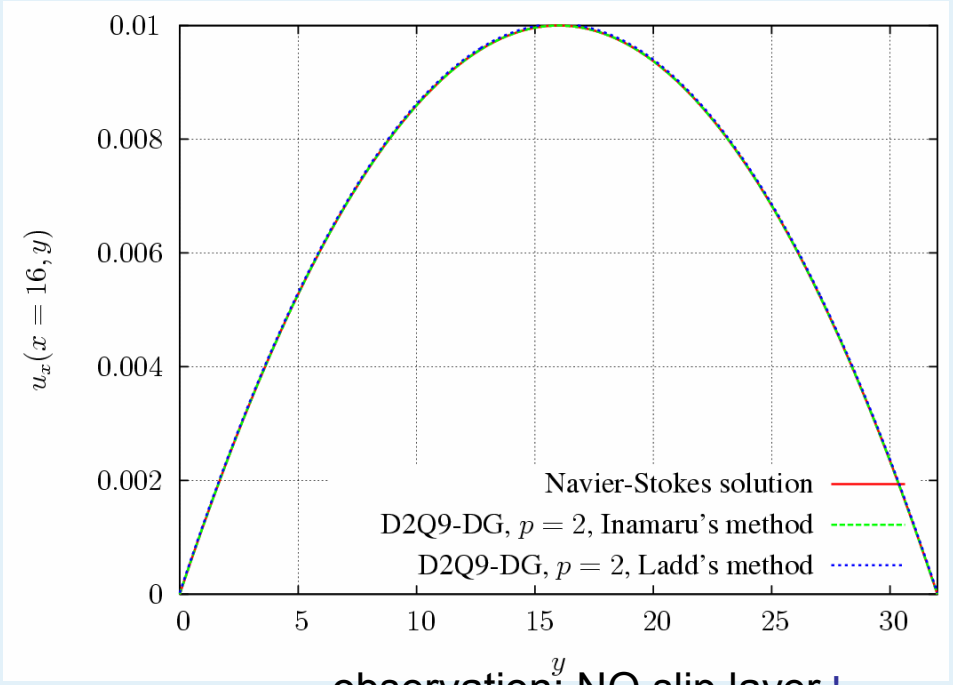

observation: NO slip layer !

convergence to stationary solution with $p = 2$:
Inamaru's method: after 9000 time steps:
error in L_2 norm $\approx 1.1 \times 10^{-13}$
Ladd's method: after 11000 time steps:
error in L_2 norm $\approx 8.3 \times 10^{-4}$

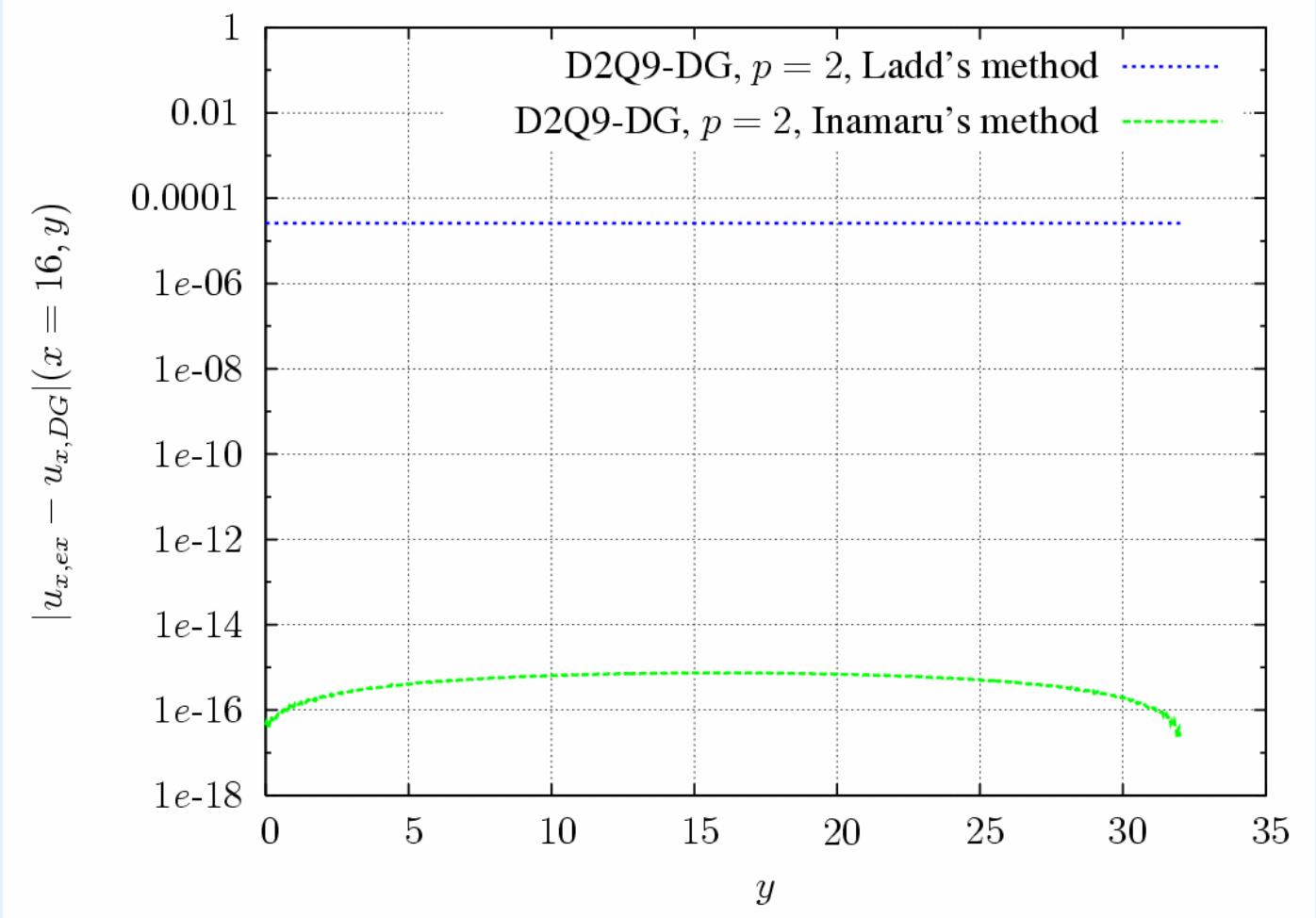
D2Q9-DG, $p = 2$, Ladd's method
D2Q9-DG, $p = 2$, Inamaru's method
$|u_{x,ex} - u_{x,DG}|(x = 16, y)$
y
1
0.01
0.0001
1e-06
1e-08
1e-10
1e-12
1e-14
1e-16
1e-18
0
5
10
15
20
25
30
35

Rotating Couette flow

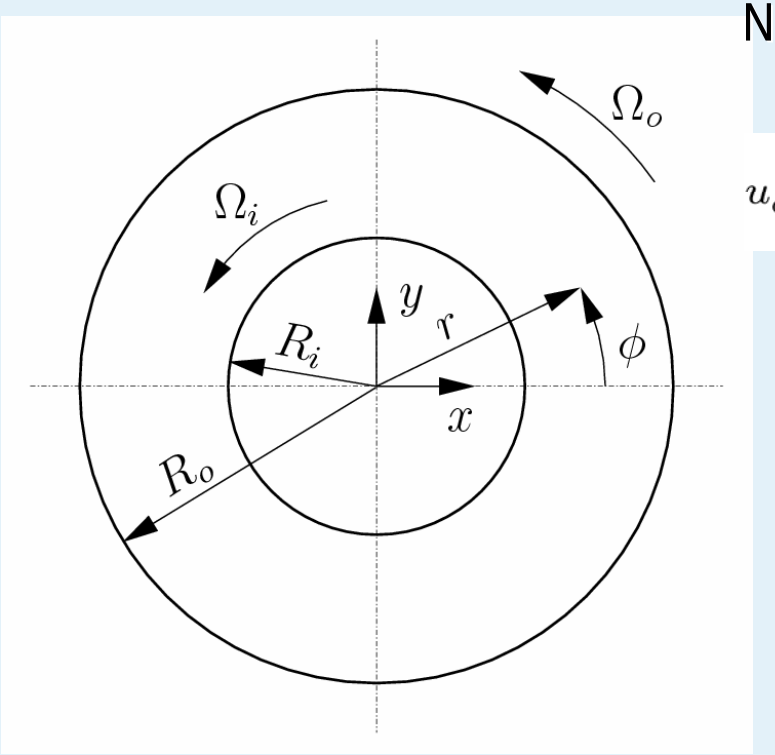

Navier-Stokes solution

$$u_\phi(r) = \frac{1}{R_o^2 - R_i^2}\left((\Omega_o R_o^2 - \Omega_i R_i^2)r + (\Omega_i - \Omega_o)\frac{R_i^2 R_o^2}{r}\right)$$

Comparison Navier-Stokes / D2Q9-DG, p=8, τ=2.0

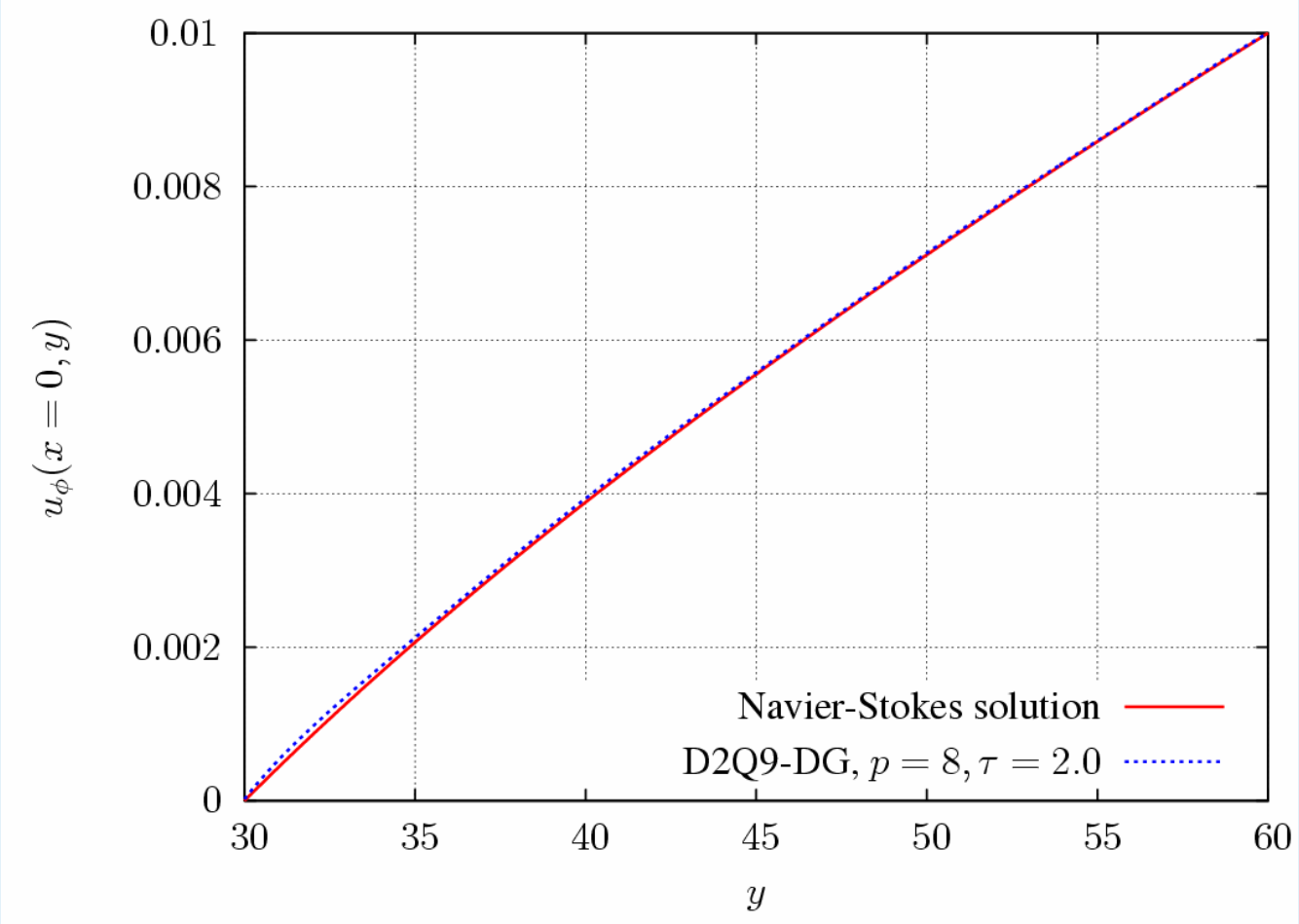

Comparison Navier-Stokes / D2Q9-DG, p=8, τ=0.5

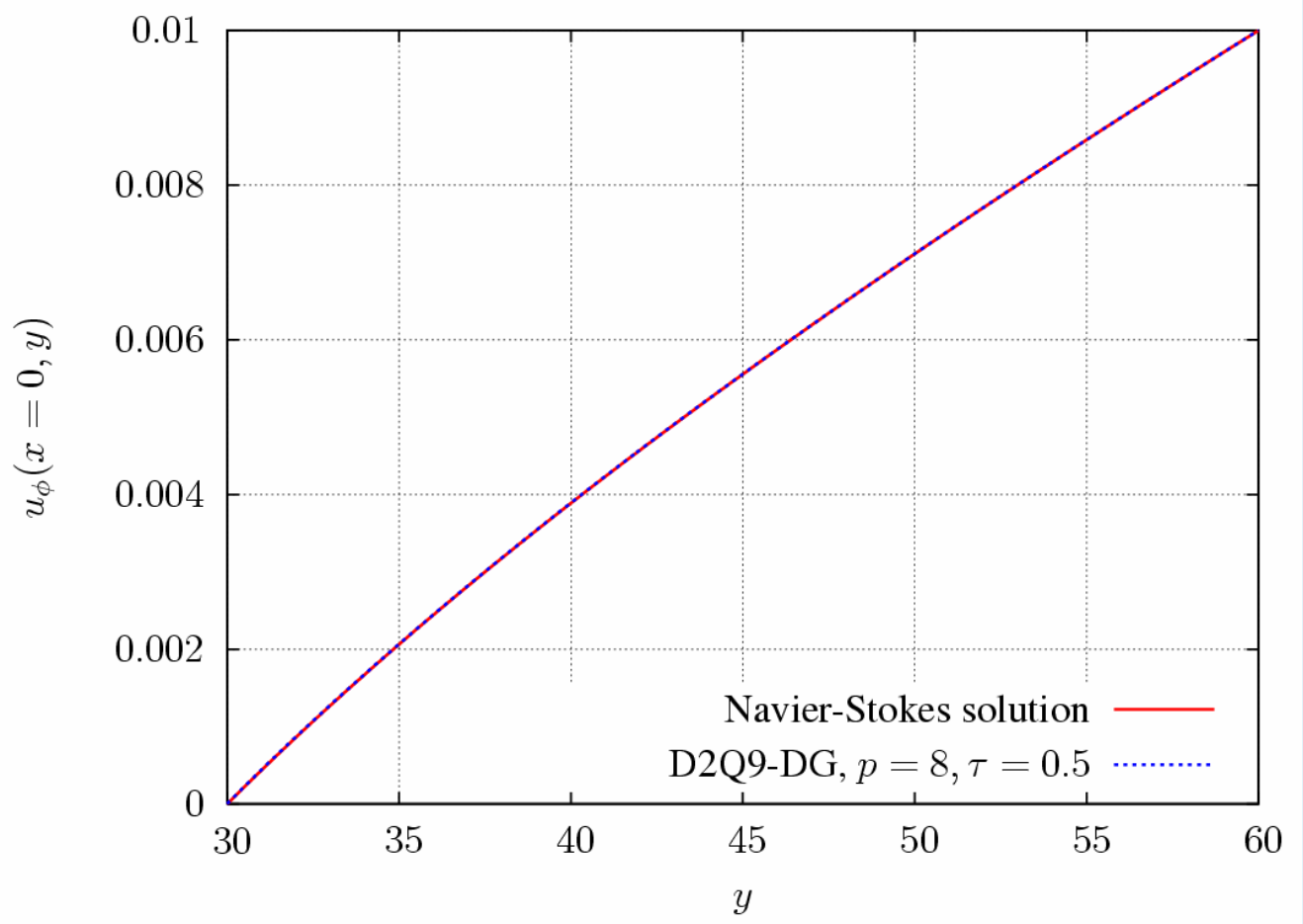

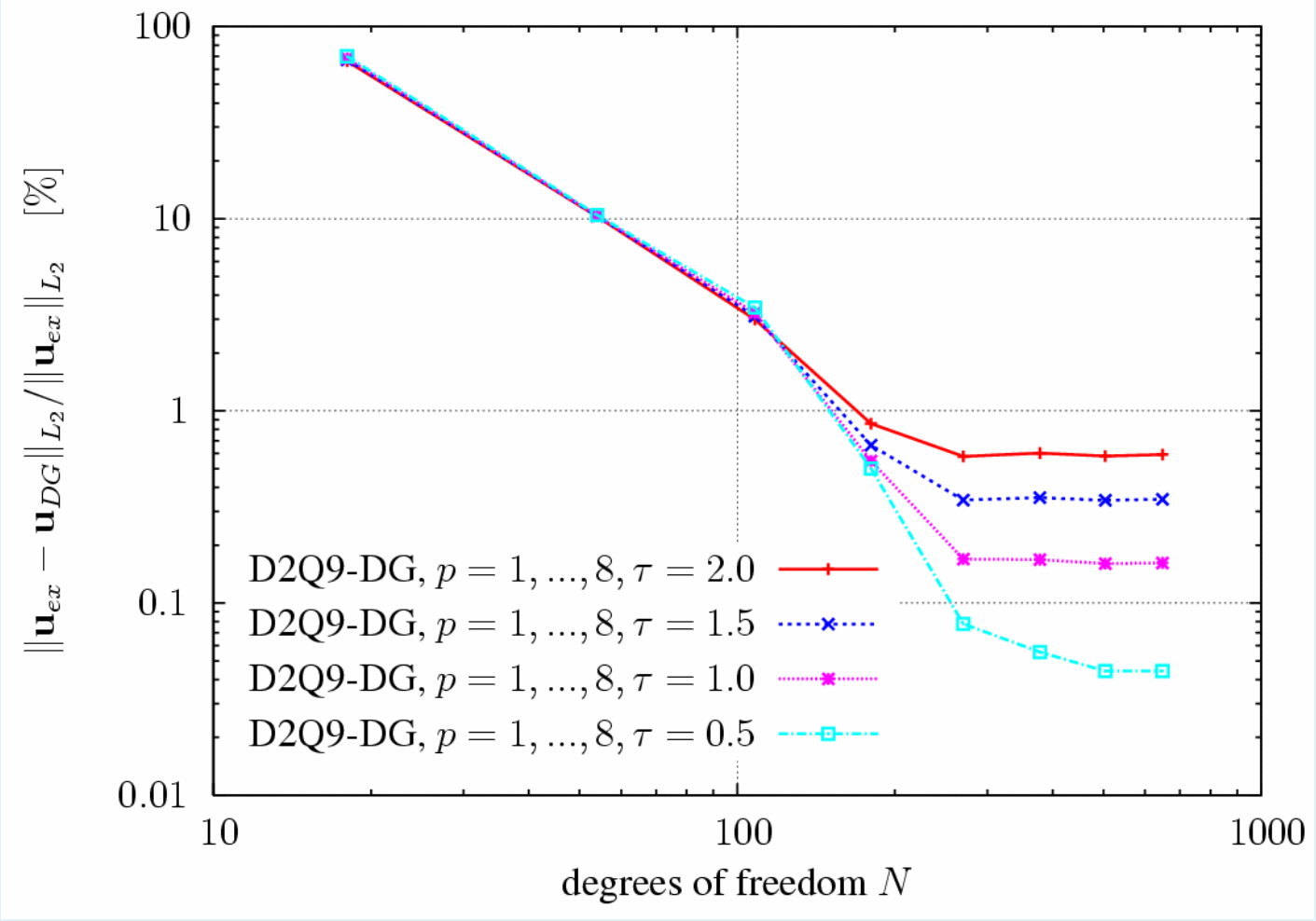

observation:
model deviation
with respect to
Navier-Stokes
dynamics due
to finite Kn number

Taylor vortex flow

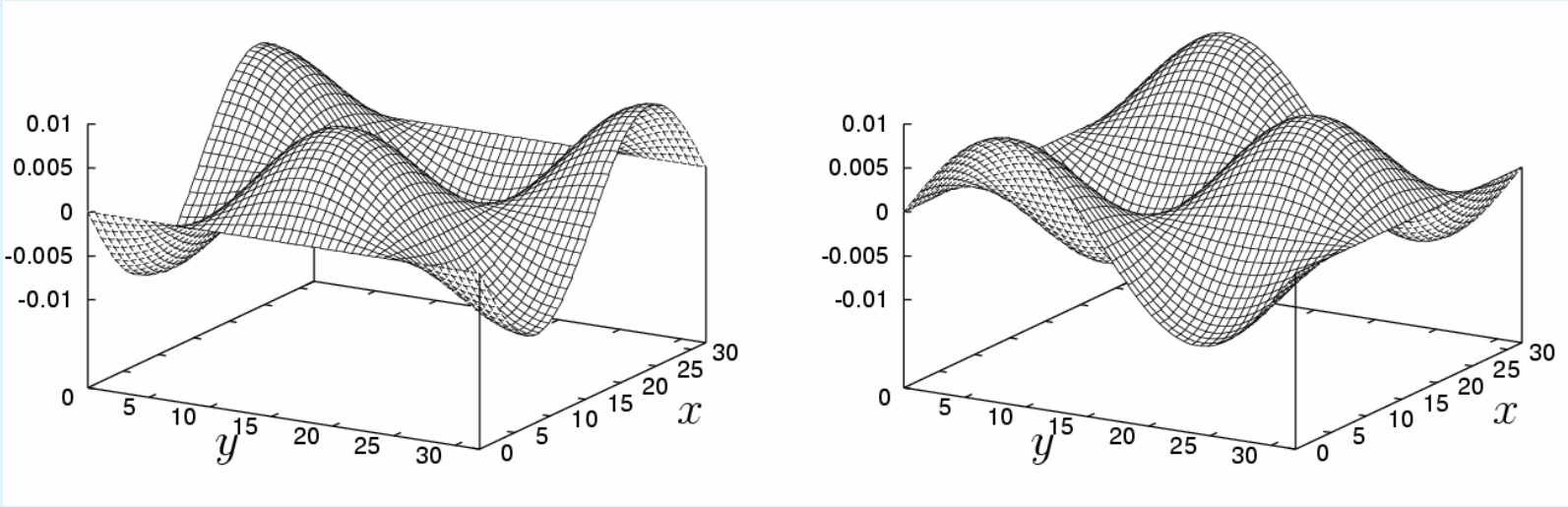

Navier-Stokes solution

$$u_x(x,y,t) = -u_0 \exp\left(-\nu t(k_1^2+k_2^2)\right)\cos(k_1 x)\sin(k_2 y)$$
$$u_y(x,y,t) = u_0\, k_1/k_2 \exp\left(-\nu t(k_1^2+k_2^2)\right)\sin(k_1 x)\cos(k_2 y)$$

Comparison Navier-Stokes / D2Q9-DG, p=4

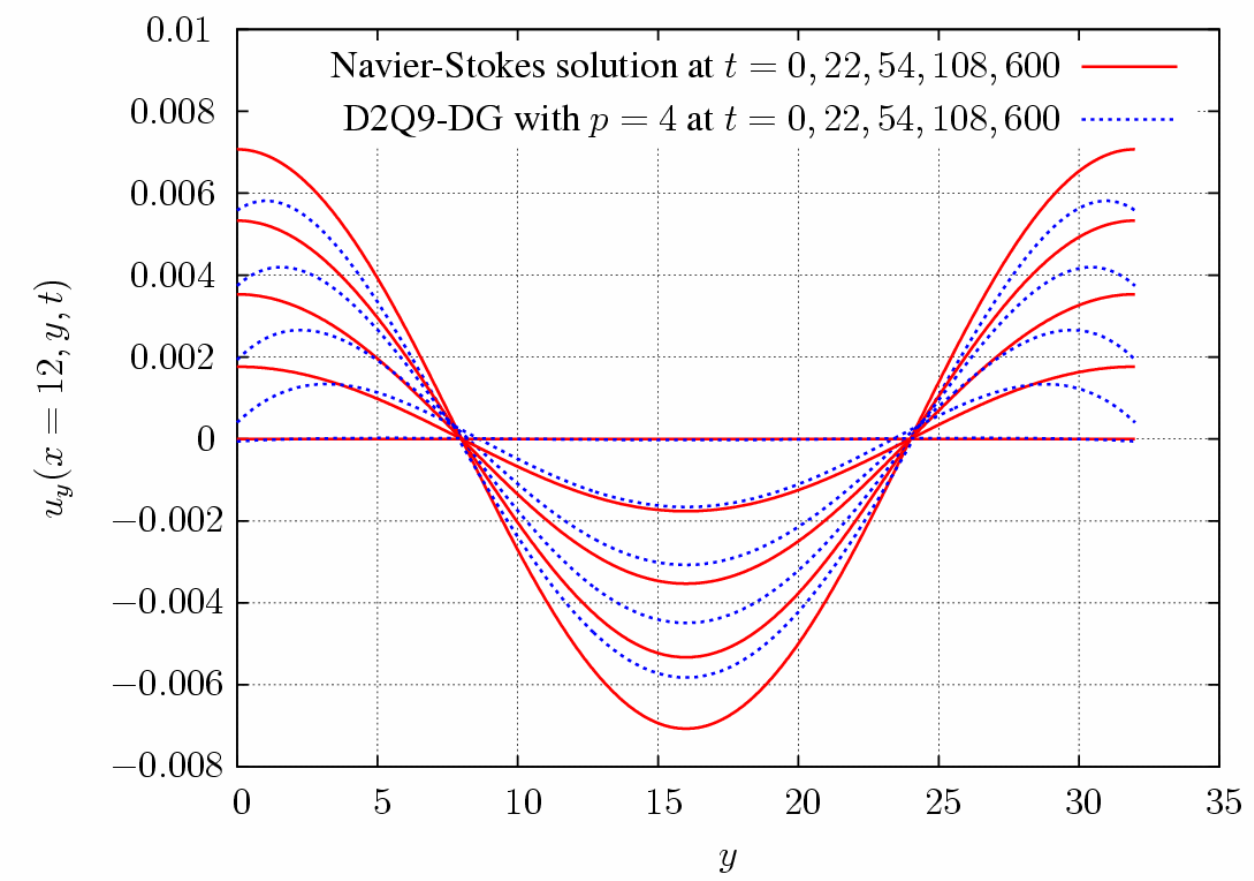

Comparison Navier-Stokes / D2Q9-DG, p=8

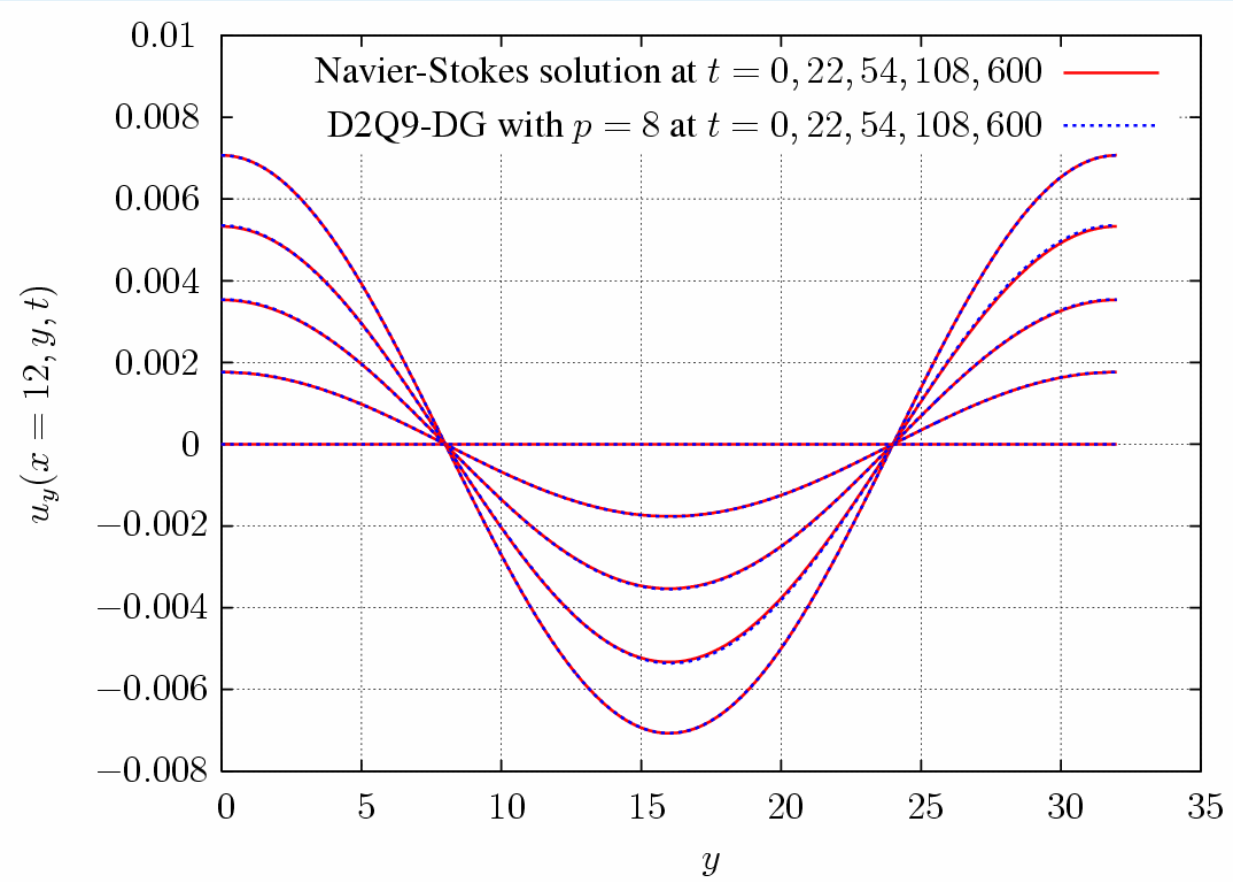

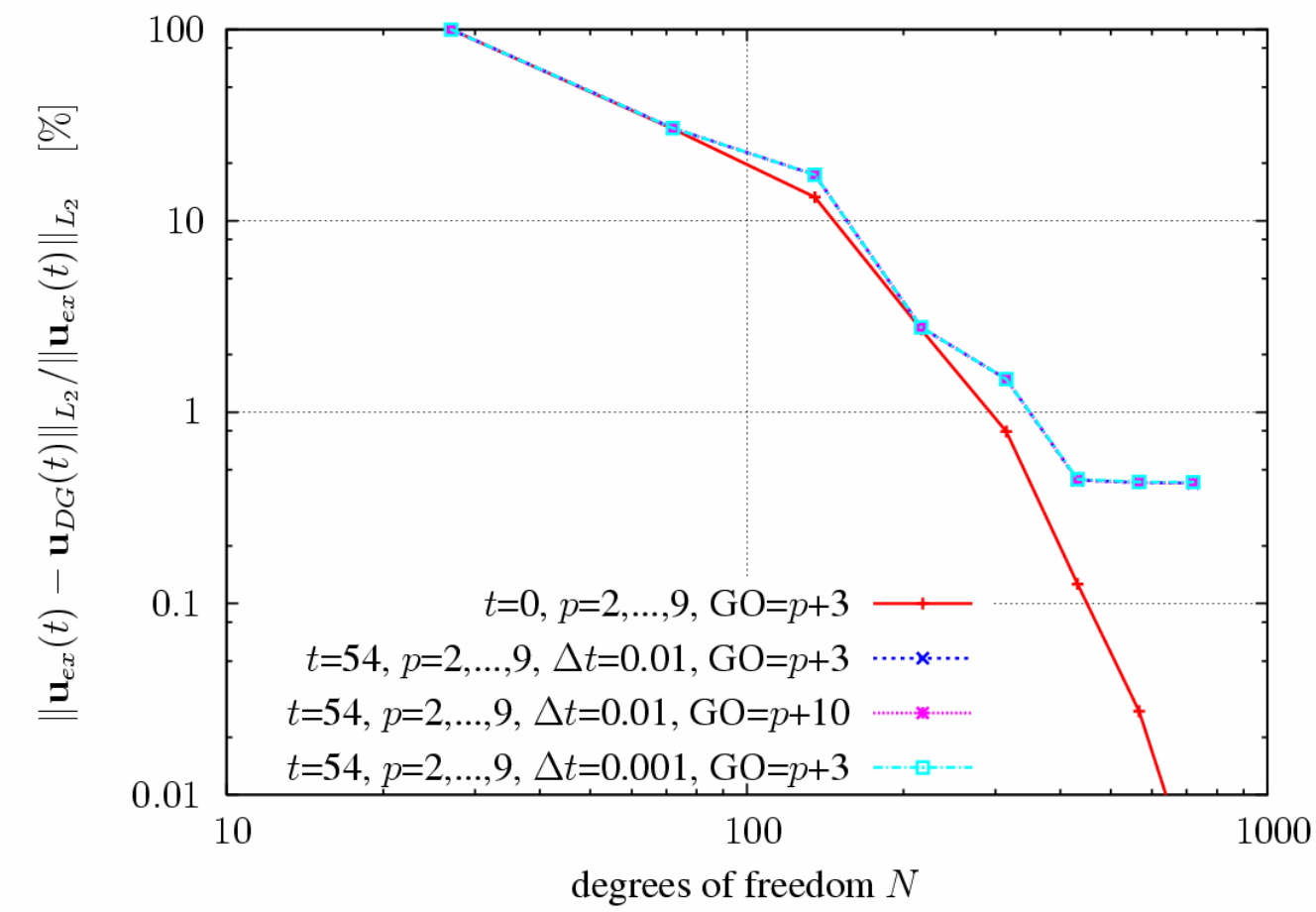
100
10
1
0.1
0.01
10
100
1000
$\|\mathbf{u}_{ex}(t) - \mathbf{u}_{DG}(t)\|_{L_2} / \|\mathbf{u}_{ex}(t)\|_{L_2}$ [%]
degrees of freedom N
t=0, p=2,...,9, GO=p+3
t=54, p=2,...,9, Δt=0.01, GO=p+3
t=54, p=2,...,9, Δt=0.01, GO=p+10
t=54, p=2,...,9, Δt=0.001, GO=p+3

conclusions and outlook p-FEM for LB

- exact / accurate representation of curved boundaries
- boundary conditions are defined *on* the boundary
- exponential convergence
- model error (discrete Boltzmann vs Navier-Stokes) can be analyzed (asymptotic behaviour)
- suitable for unstructured grids

- to do: higher order time stepping schemes (Runge-Kutta)

LB-Methods for multicomponent / multiphase, thermal and turbulent flows

Manfred Krafczyk

contributors:
B. Ahrenholz, S. Freudiger, S. Geller, B. Nachtwey, M. Stiebler, J. Tölke

kraft@cab.bau.tu-bs.de

http://www.cab.bau.tu-bs.de

Overview

- advection-diffusion problems
  - grid refinement
  - thermal flows
- multiphase models
  - grid refinement
- turbulent flows
  - LES
  - RANS
  - entropic and cascaded LB models

A LB extension for advection-diffusion on hierarchical grids

$$\frac{\partial C}{\partial t} + u_j \frac{\partial C}{\partial x_j} = \alpha \frac{\partial^2 C}{\partial x_i \partial x_i}$$

Goal: To develop a numerical scheme for advection-diffusion that works on the same grid as the flow field simulation

$\Rightarrow$LB methods for advection-diffusion
(e.g. Flekkoy 1993, van der Smaan 1999, Ginzburg 2004)

-efficient (cell Peclet number up to 100)

-inherently mass conservative

-can naturally be extended to hierarchical grids (Stiebler et al. 2006)

advection-diffusion LB method (Ginzburg 2004)

$$\frac{\partial C}{\partial t} + u_j \frac{\partial C}{\partial x_j} = \alpha \frac{\partial^2 C}{\partial x_i \partial x_i}$$

$$C = \sum_i g_i = \sum_i g_i^{(eq)}, \quad i = 0,\ldots,4$$

LB equation: $$g_i(t+\Delta t, \mathbf{x}+\boldsymbol{\xi}_i \Delta t) = g_i(t,\mathbf{x}) + \lambda\left(g_i(t,\mathbf{x}) - g_i^{(eq)}(t,\mathbf{x})\right)$$

with $\lambda = -3+\sqrt{3}$ and equilibrium distributions

$$g_0^{(eq)}(C(\mathbf{x},t),u(\mathbf{x},t),a_e(\mathbf{x},t)) = \frac{C}{3}\left(1-2a_e-3\frac{\mathbf{u}^2}{c^2}\right), \quad a_e = \frac{6\sqrt{3}\alpha}{c^2\Delta t} - 1$$

$$i \neq 0: \quad g_i^{(eq)}(C(\mathbf{x},t),u(\mathbf{x},t),a_e(\mathbf{x},t)) = \frac{C}{6}\left(1+a_e+3\frac{(\mathbf{u}\cdot\boldsymbol{\xi}_i)^2}{c^4}+3\frac{\mathbf{u}\cdot\boldsymbol{\xi}_i}{c^2}\right)$$

Taylor-Aris-dispersion

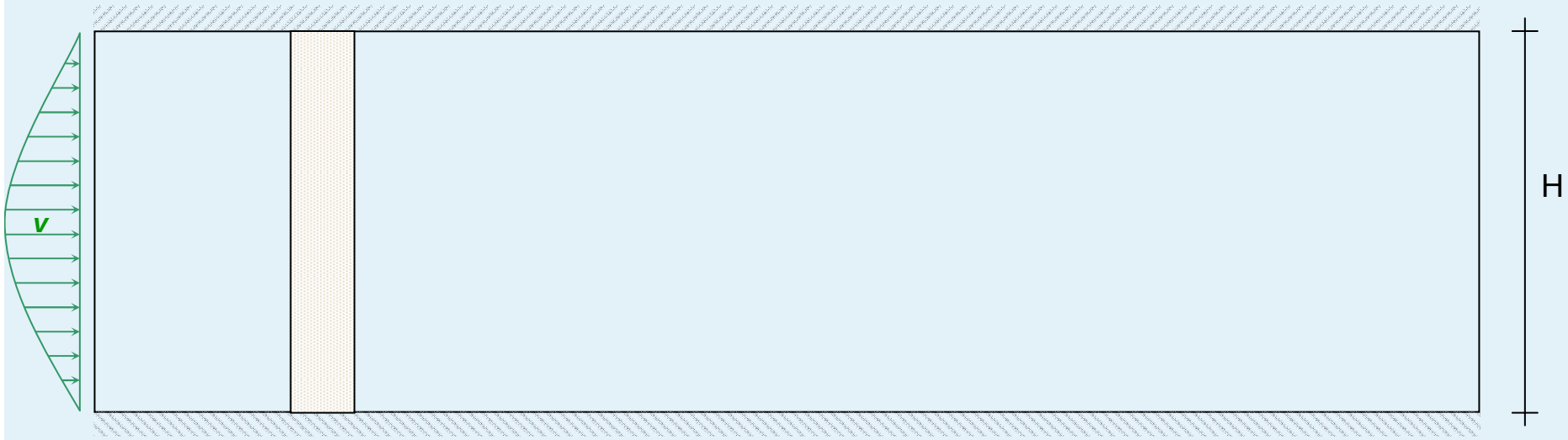

$$\sigma^2$$

concentration averaged over channel height goes towards a Gaussian density distribution with variance

$$\alpha^* = \frac{1}{2}\frac{d(\sigma^2)}{dt} = \alpha(1 + \mathrm{Pe}^2 / 210), \quad \mathrm{Pe} = \bar{v}H / \alpha$$

Taylor-Aris-Dispersion

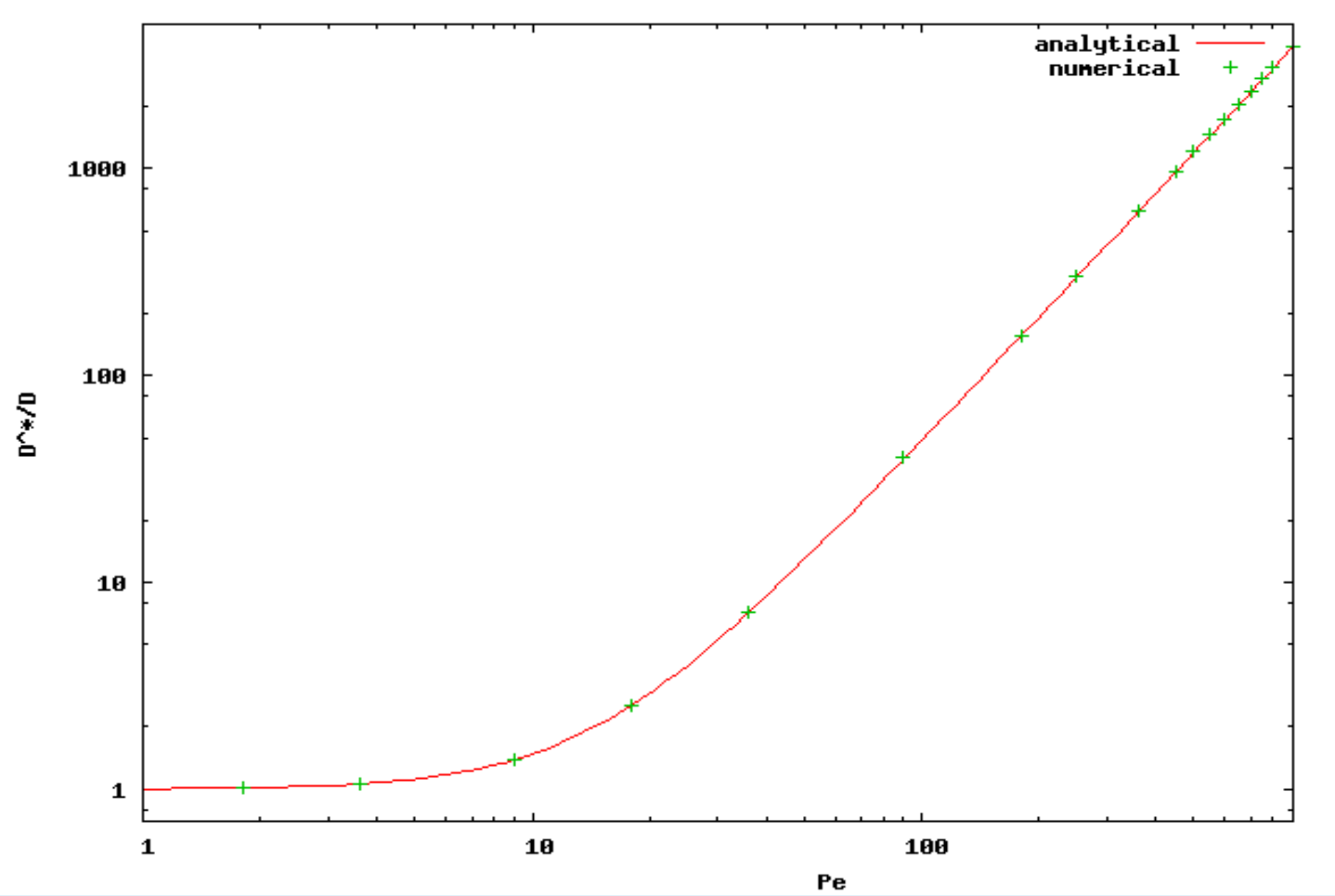

Taylor-Aris-Dispersion

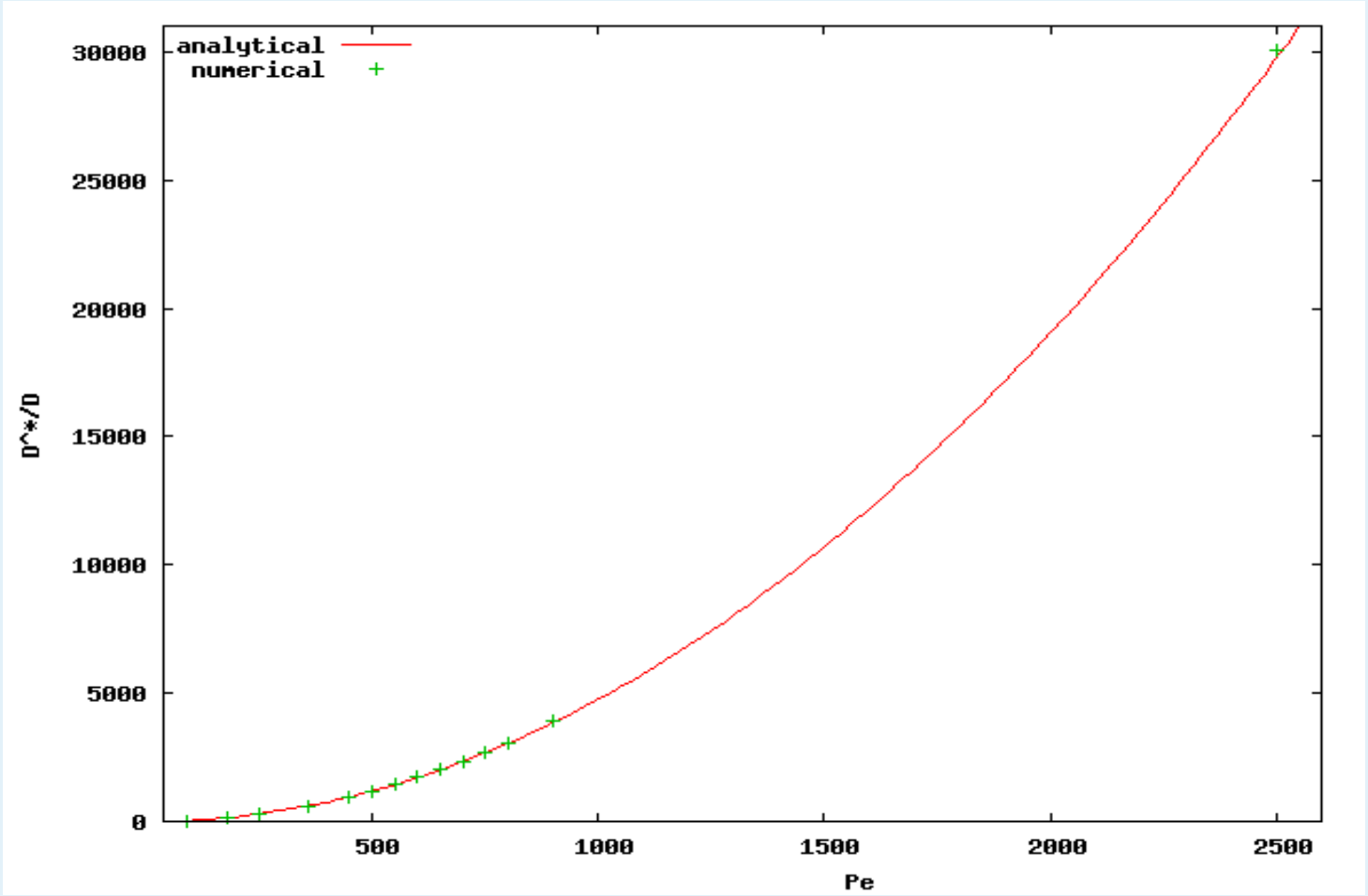

advection diffusion LB method on hierarchical grids

$$g_i(t+\Delta t, \mathbf{x}+\boldsymbol{\xi}_i\Delta t) - g_i(t,\mathbf{x}) = \lambda\left(g_i(t,\mathbf{x}) - g_i^{(eq)}(t,\mathbf{x})\right)$$

Taylor series and summation $\sum_i$:

$$\frac{DC}{Dt} = -\left(\frac{\lambda}{2}+1\right)\sum_i\left(\boldsymbol{\xi}_i \cdot \frac{\partial g_i^{(neq)}}{\partial \mathbf{x}}\right) + O(\Delta t)$$

grid invariance of total derivative of transported scalar

↓

no scaling of non-equilibrium parts of distributions

Scaling from fine grid to coarse:

$$g_{c,i} = g_i^{(eq)}(C,\mathbf{u},a_{e,c}) + [g_{f,i} - g_i^{(eq)}(C,\mathbf{u},a_{e,f})]$$

Test case

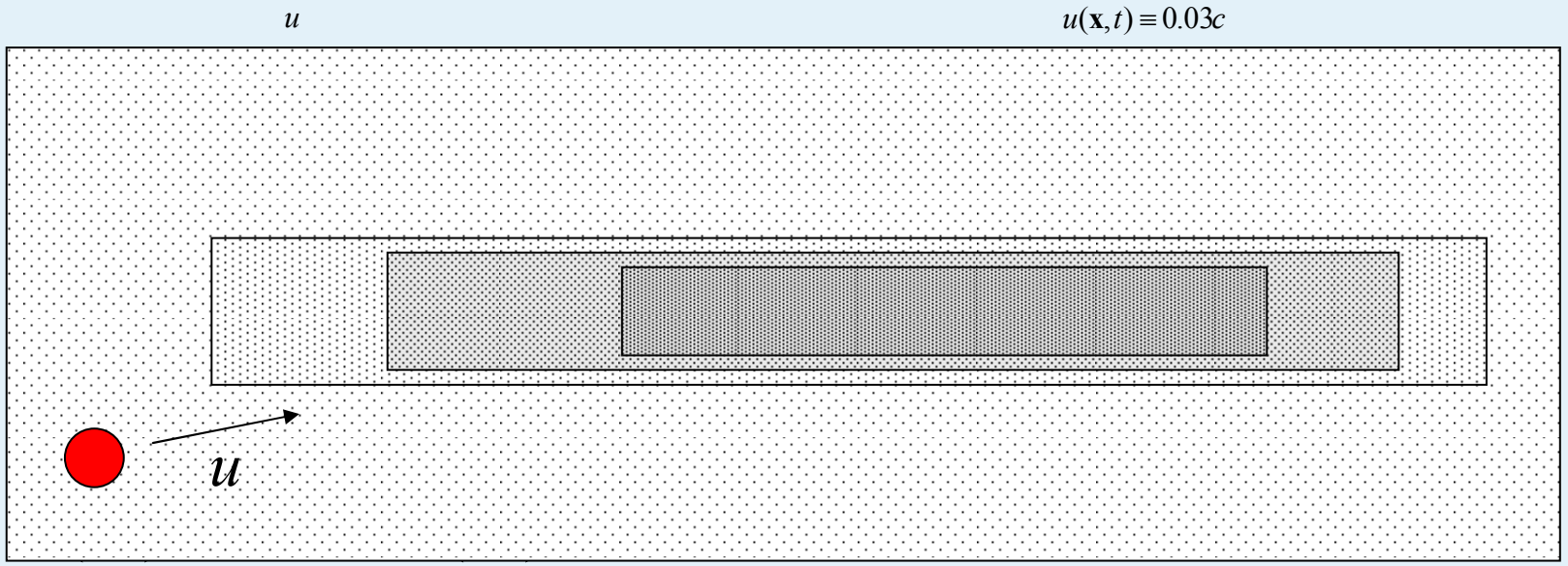

$$\alpha(\mathbf{x},t) \equiv \frac{u\Delta x_c}{50}$$

Test case

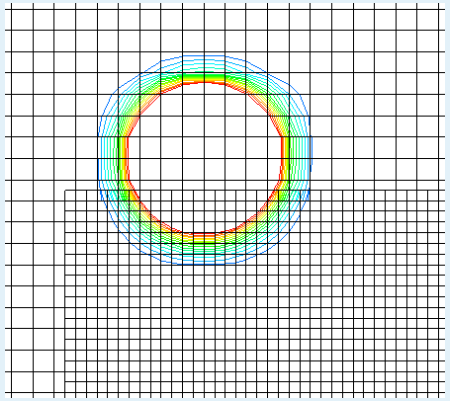

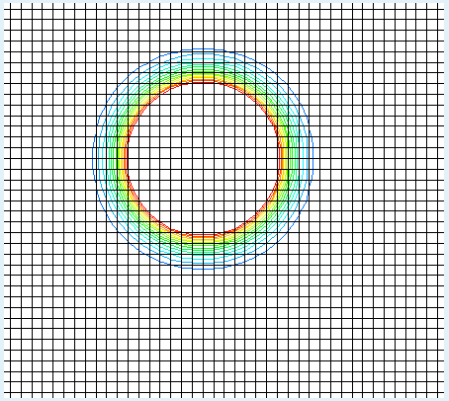

after 30000 time steps

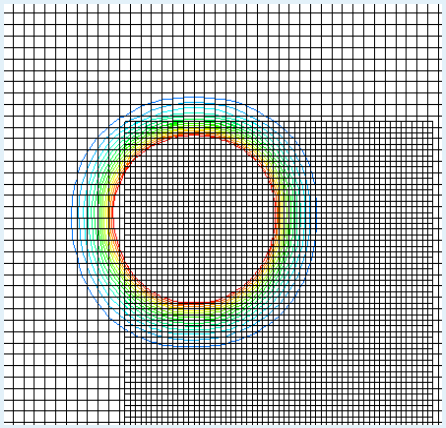

after 60000 time steps

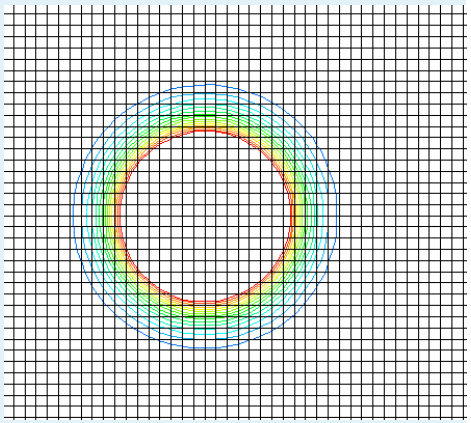

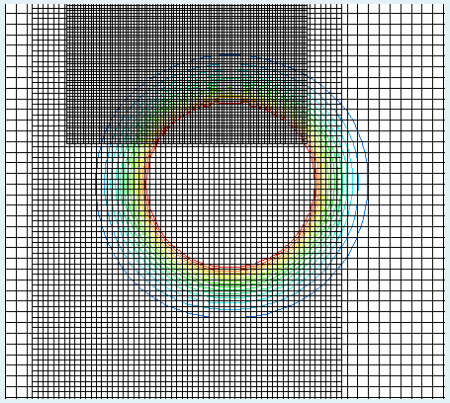

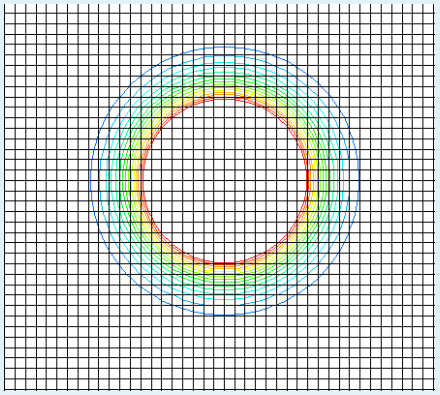

after 90000 time steps

Test case

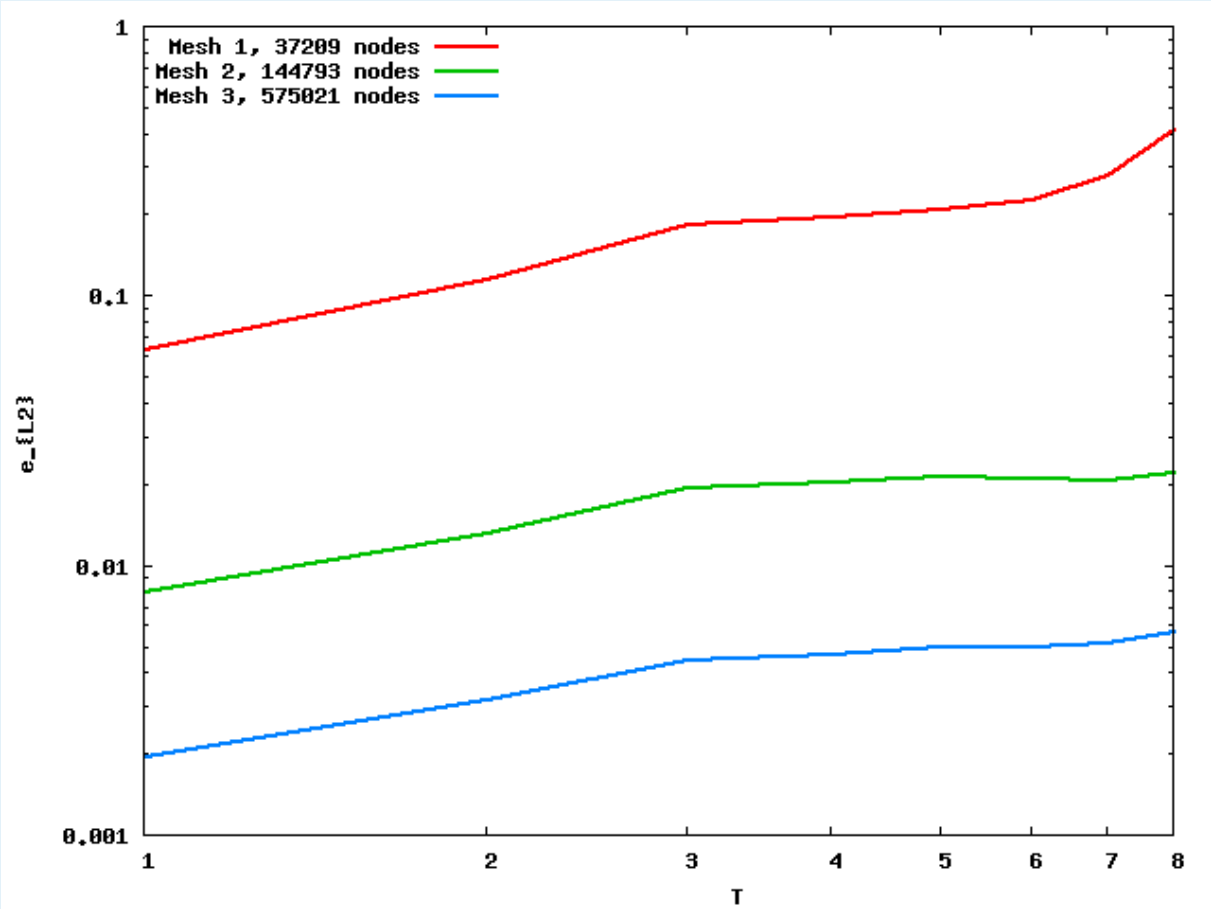

L2 error over time for non-uniform meshes of different resolutions

Test case: Diffusion without advection

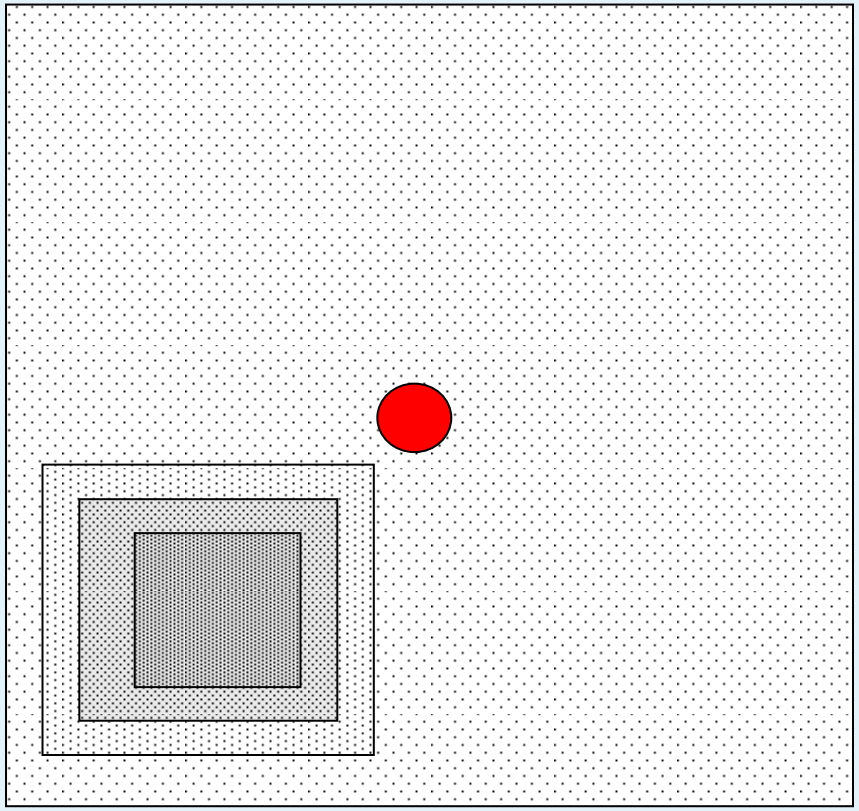

$$\alpha(\mathbf{x},t) \equiv 0.0064 c \Delta x_c$$

Test case diffusion without advection

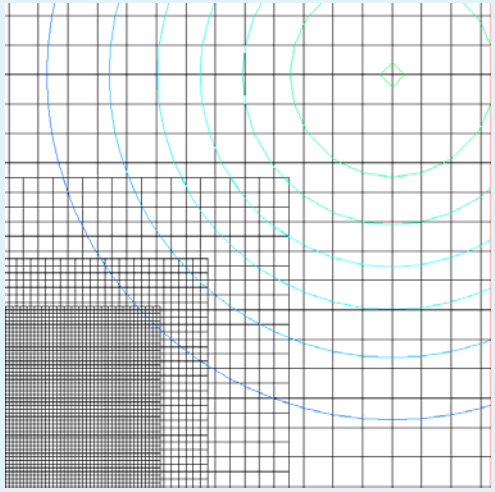

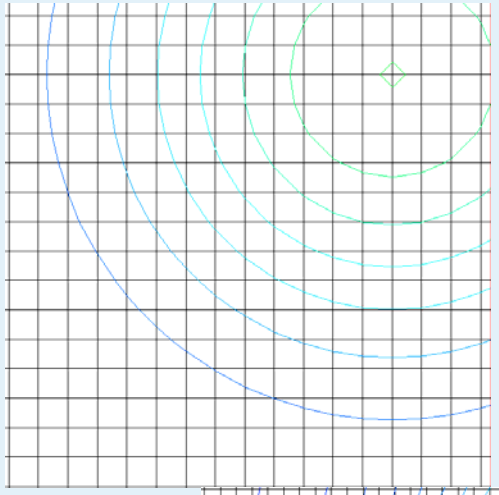

after 6000 time steps

after 12000 time steps

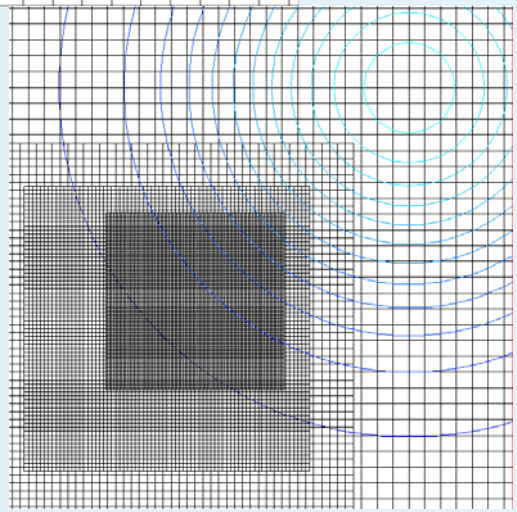

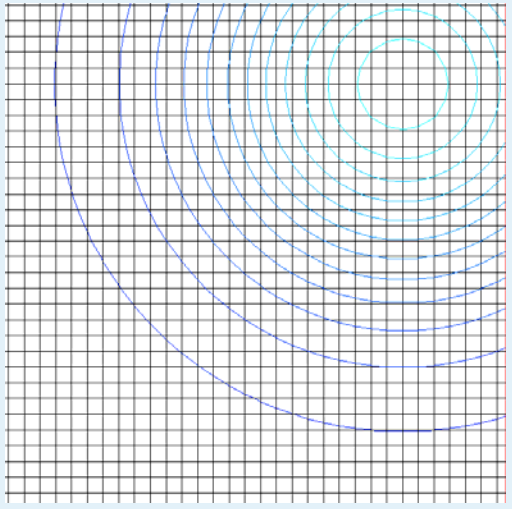

Thermal flows

One can find four distinct classes of thermal models in the literature:

1. fully compressible models with extended sets of lattice vectors resulting in non-local propagation and difficult boundary conditions (ray tracing, interpolation), e.g. C. Sun, Phys. Rev. E, 61, 2645, 2000
2. Low Ma number models with a large set of discrete velocities
3. Energy dependent discrete velocities
4. hybrid models which solve an additional energy transport equation which is coupled to LB equations in different ways resulting in low Ma number Boussinesq type models usually only valid for small temperature ratios.

$$\frac{c_{\min}^2}{D} < T < \frac{c_{\max}^2}{D}$$

a compressible thermal low Ma model

Hybrid model (Tölke 2006)

- Couple speed of sound and temperature
- Correct wrong stresses by additional terms in equilibrium moments (MRT)
- Finite Difference scheme for advection diffusion equation
- non-local collision (next neighbour)

basic idea:

$$c_s^2(\vec{x},t)\rho(\vec{x},t) = \frac{\partial P}{\partial \rho} RT(\vec{x},t)\rho(\vec{x},t) = T^*(\vec{x},t)\rho(\vec{x},t)$$

$$p = p_{therm} + p_{hydro} = \underbrace{\rho_1(\vec{x},t)T^*(\vec{x},t)}_{\cong const.} + \underbrace{\Delta\rho(\vec{x},t)T^*(\vec{x},t)}_{\text{fluctuation}}$$

- Validation for several analytical compressible low Ma problems successful
- density ratios up to 50 achievable
- stability comparable to athermal MRT when energy equation FD stability is provided

numerical example (301x201 nodes):

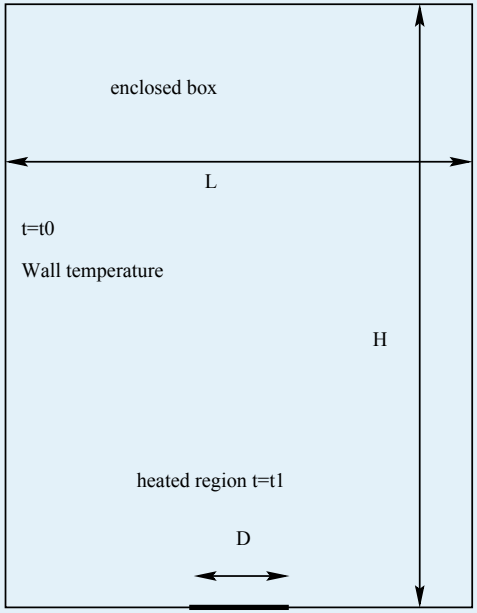

$$\mathrm{Re} \cong 2000$$

$$Ra = \frac{gD^3 \Delta t}{\alpha_0 \upsilon t_0} \cong 300.000$$

$$\mathrm{Pr} = \frac{\upsilon}{\alpha_0} = 1$$

$$\frac{t_1}{t_0} = 4$$

Low-Mach number Approximation (LMNA):

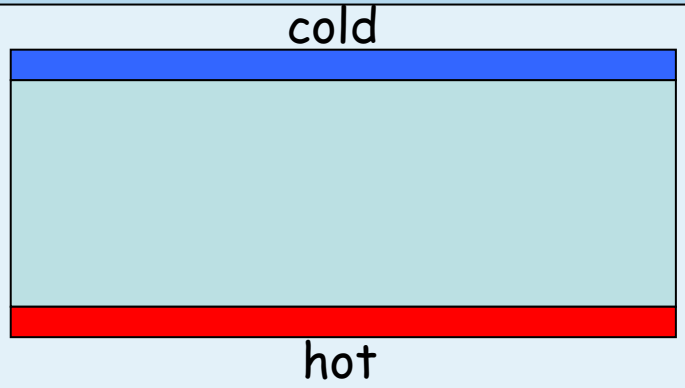

energy transport equation

$$\frac{\partial T}{\partial t} + \frac{T\rho\vec{u}}{T_0\rho_0}\vec{\nabla}T = \frac{T}{T_0\rho_0}\vec{\nabla}\chi\rho\vec{\nabla}T$$

extension of LBGK-equilibrium distributions
f = f(p,u,T) (Filippova 2000)
allows to simulate thermal flows.

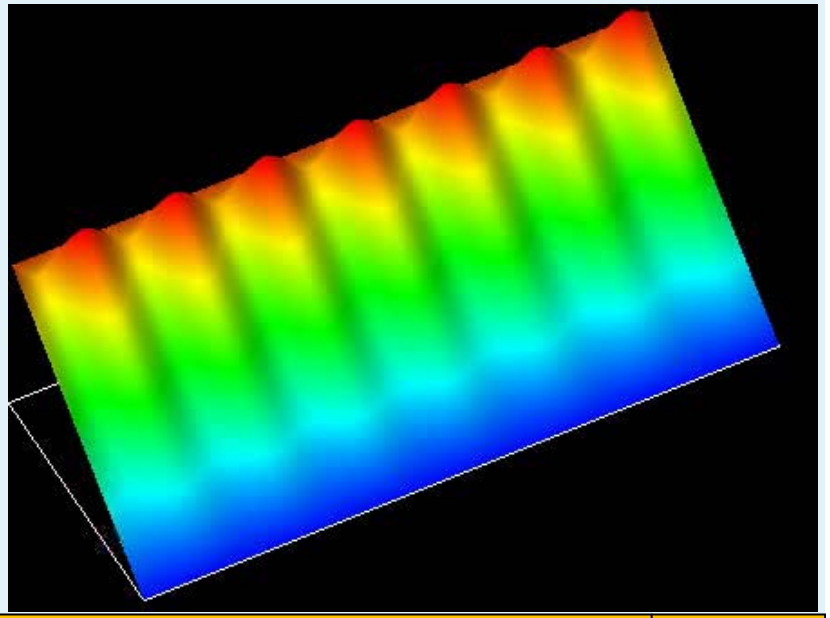

Rayleigh-Benard instability
(Ra=1.000.000, 400x200 nodes)

Multi-phase LB models

Numerical simulations of multiphase flows are either based on the surface tracking method, where the interface is modeled explicitly or on a surface capturing method, where the interface is handled implicitly by using a phase field or an index function.

Surface capturing methods are very convenient for handling topological changes. Two examples are the volume of fluid method [10,29] and the level set method. In addition, a coupled version of the volume of fluid and level set method have been developed.

All published LB multiphase models belong to the class of interface capturing schemes. The most prominent models are the Shan-Chen model (1994), Swift‘s free energy model (1995/96) and the Rothman-Keller LG-approach (1988) and its LB-variant (Gunstensen 1991).

Extension to multiphase flows (Gunstensen '92)

- use two sets of distributions f_i^{air} and f_i^{water}
- The collision operator of each phase consists of two parts

$$\Omega = \Omega^{(1)} + \Omega^{(2)}$$

$$\Omega^{(2)} = \frac{A_k}{2}\left|\vec{F}\right|\left[\frac{\left(\vec{e}_i\vec{F}\right)^2}{\left|\vec{F}\right|^2} - \frac{1}{2}\right]$$

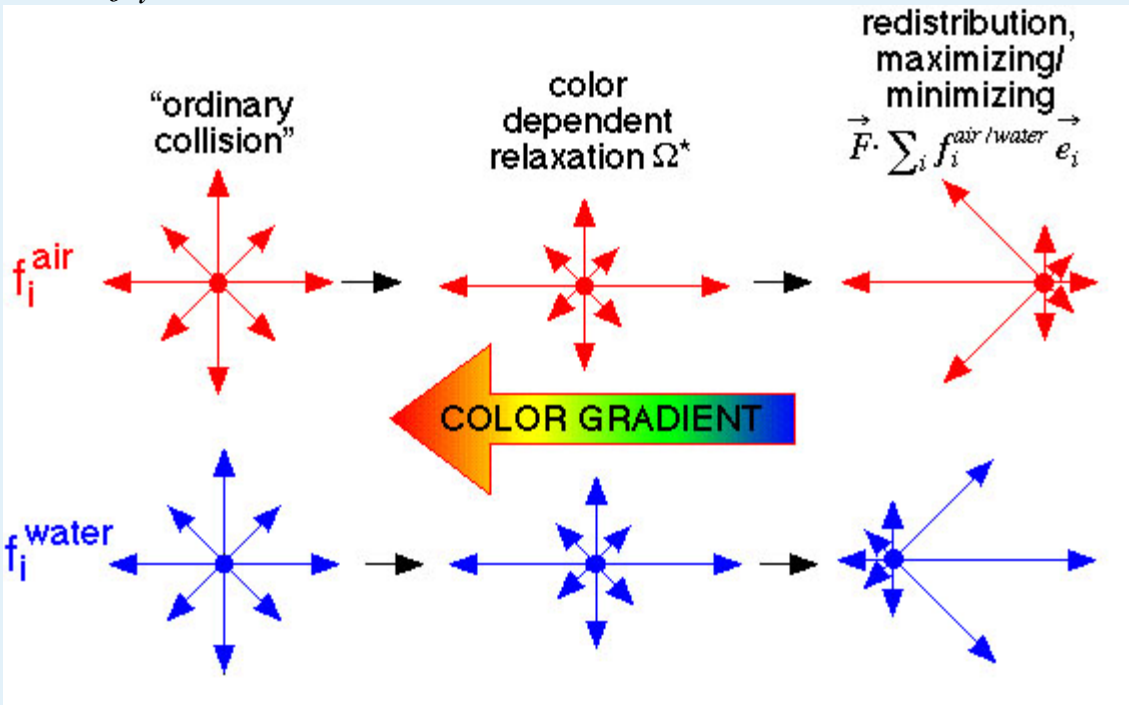

and a ‚color' gradient

$$\vec{F}(\vec{x}) = \sum_i \vec{e}_i\left[\rho^{air}\left(\vec{x}+\vec{e}_i\right) - \rho^{water}\left(\vec{x}+\vec{e}_i\right)\right]$$

Model validation:

- Laplace law (surface tension)
- contact angle (wetting)
- capillary tube (wetting)
- bubble flows (dynamics)

Surface tension can be approximately computed (D3Q19):

$$\sigma_{a,b} \cong 120 A \tau (\rho_a + \rho_b)$$

Laplace law: $\sigma = \frac{\Delta p}{\kappa} = \frac{\Delta p R}{2}$ for a sphere

sphere resolution: 18 nodes

ρ_a	ρ_b	A	σ_{theory}	σ_{test}	rel. error
1.0	1.0	1E-4	0.024	0.024	0.00
1.0	1.0	4E-4	0.096	0.097	0.01
1.0	1.0	1E-3	0.240	0.277	0.15
10.0	1.0	1E-4	0.132	0.131	0.01
0.125	8.0	1E-5	0.01	0.009	0.1

Contact angle:

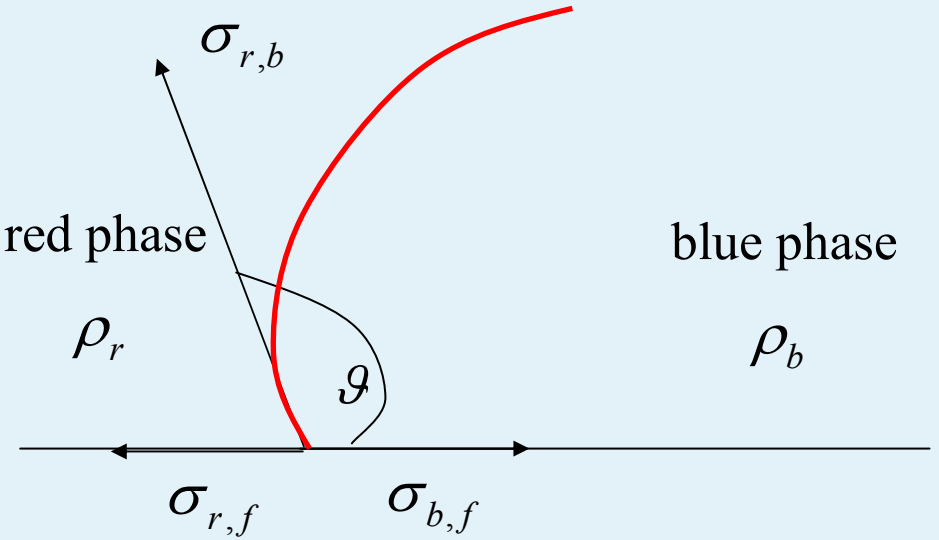

Youngs equation: $\sigma_{r,f} - \sigma_{b,f} - \sigma_{r,b} \cos\vartheta = 0$

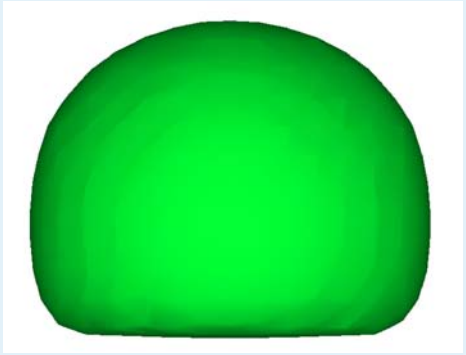

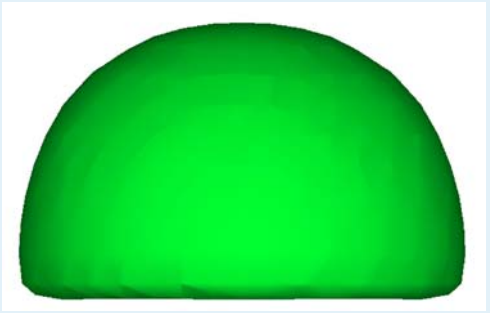

varying contact angles

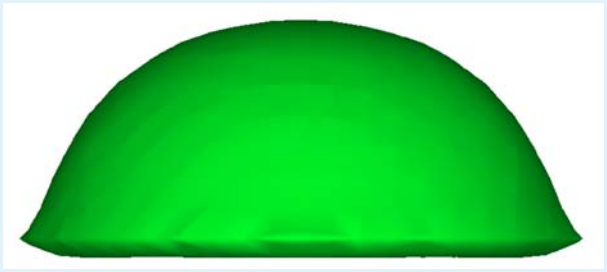

channel test
(11 nodes vertical)

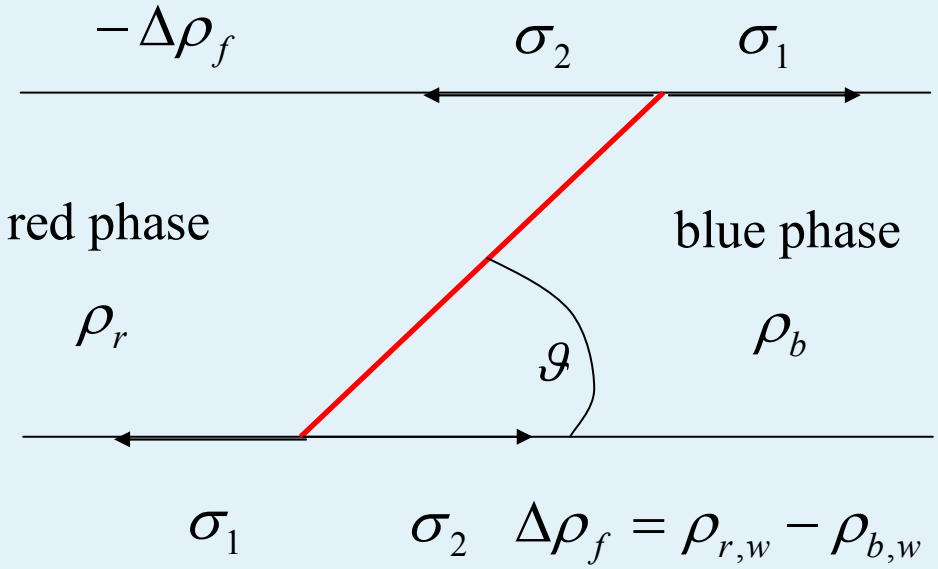

$\rho_{r,w}$	$\rho_{b,w}$	$\Delta\rho_f$	ϑ_{theory}	ϑ_{num}
1.1	0.9	0.2	78°	73°
1.2	0.8	0.4	66°	62°
1.3	0.7	0.6	53°	50°
1.4	0.6	0.8	37°	33°

capillary tube test

equilibrium between surface tension and gravity forces implies

$$h = \frac{2\sigma\cos(\gamma)}{r\rho g}$$

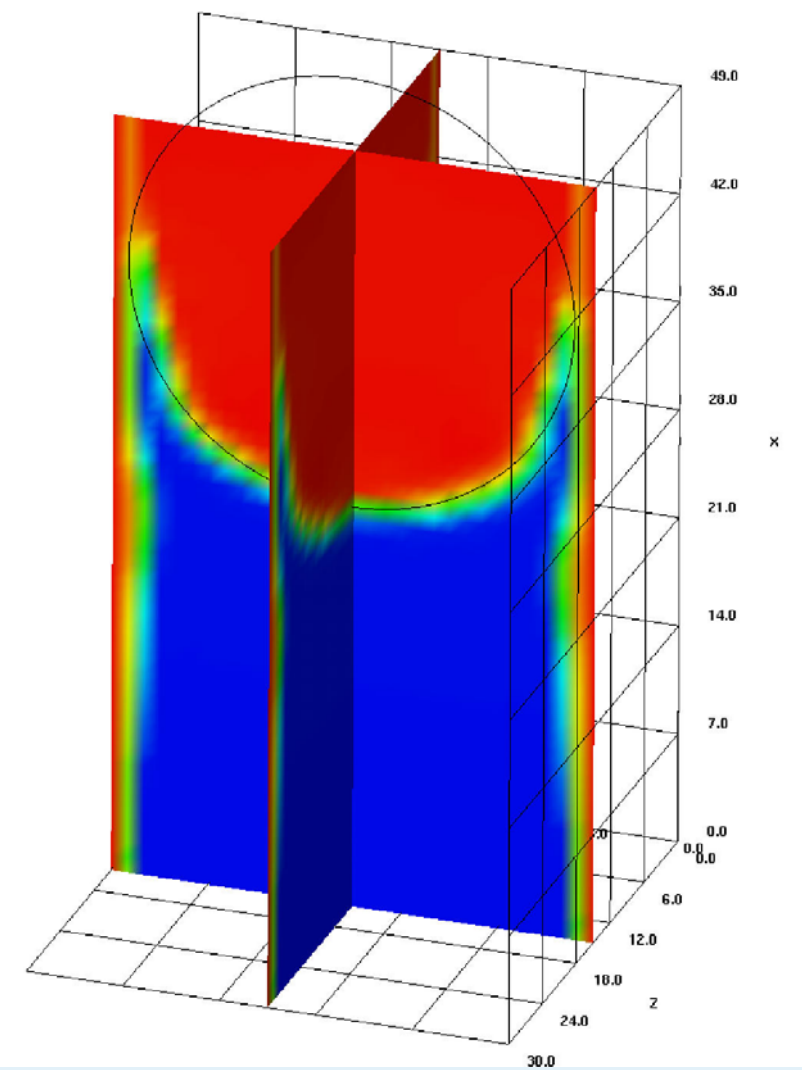

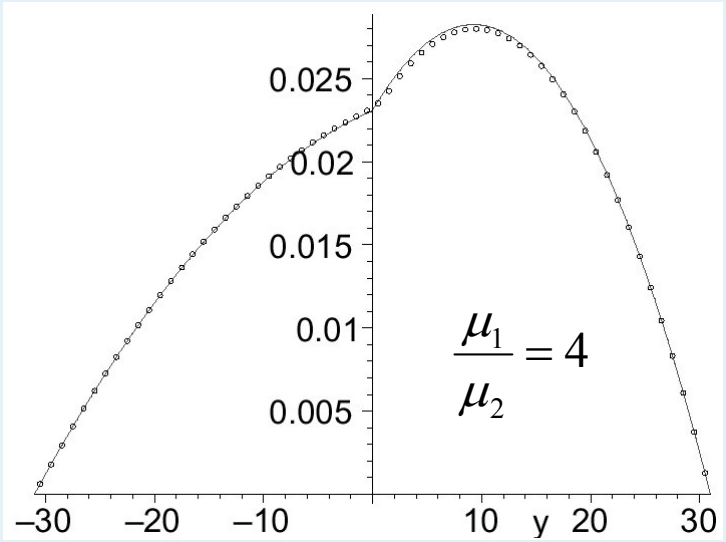

channel test
(two-phase
Poiseuelle flow)

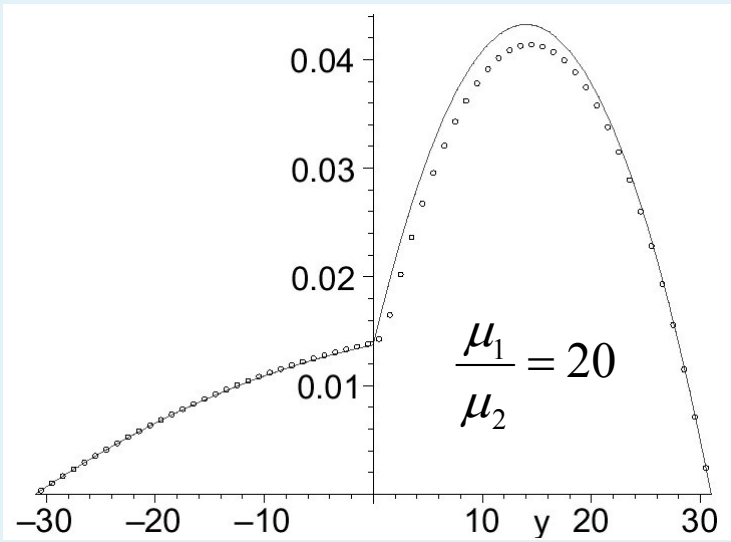

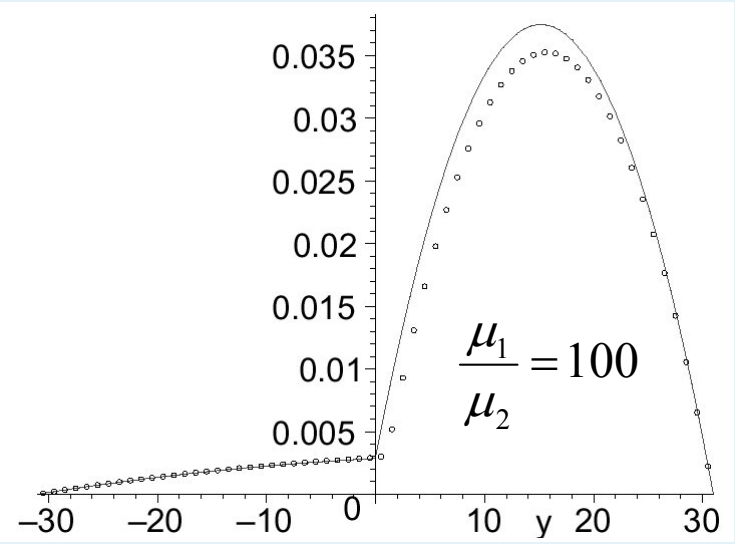

implementation of a new extension of the Rothmann-Keller[1] model

[1] (Gunstensen (Rothmann-Keller), 1991)

differences compared to one phase models:

- *two phases (red/blue)*
- *generation of surface tension (!capillary forces!)*
- *separation of phases (!immiscible!)*

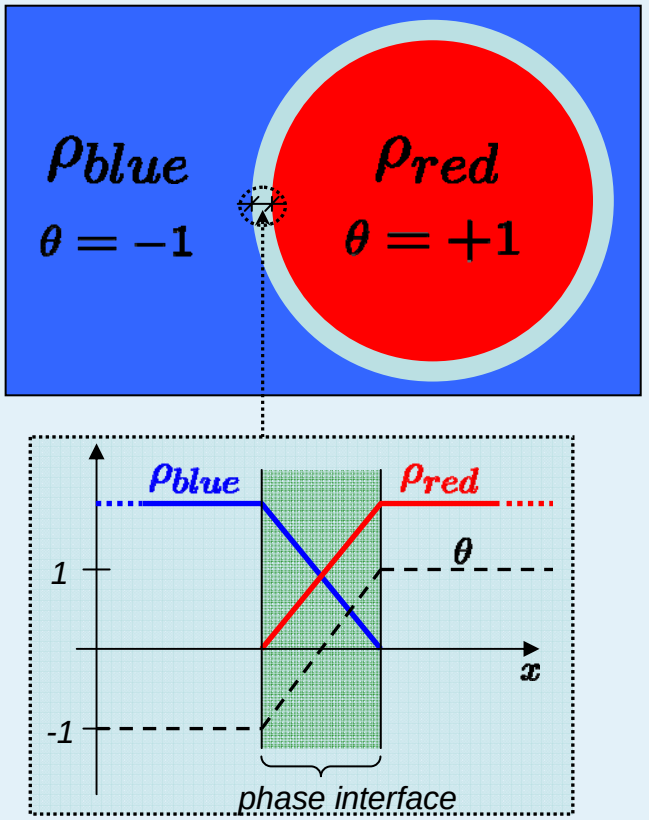

multi phase extensions:

Lattice Boltzmann nodal information:

- ***one** set of distributions*
- *phase parameter* $\theta = \underbrace{\frac{\rho_{red} - \rho_{blue}}{\rho_{red} + \rho_{blue}}}_{\rho_\theta} \in [-1;+1]$

implementation of a new extension of the Rothmann-Keller model

surface tension: (Kehrwald, 2004 PhD, Tölke et. al., 2005)

$$m_i^{eq,l} = m_i^{eq,l} + m_i^{ST,l}$$

$$\begin{aligned}
m_1^{ST,l} &= -2\,\sigma\,|\vec{C}_l|\,(n_{l,x}{}^2 + n_{l,y}{}^2 + n_{l,z}{}^2) \\
m_9^{ST,l} &= \quad -\sigma\,|\vec{C}_l|\,(2\,n_{l,x}{}^2 - n_{l,y}{}^2 - n_{l,z}{}^2) \\
m_{11}^{ST,l} &= \quad -\sigma\,|\vec{C}_l|\,(n_{l,y}{}^2 - n_{l,z}{}^2) \\
m_{13}^{ST,l} &= \quad -\sigma\,|\vec{C}_l|\,(n_{l,x}\,n_{l,y}) \\
m_{14}^{ST,l} &= \quad -\sigma\,|\vec{C}_l|\,(n_{l,y}\,n_{l,z}) \\
m_{15}^{ST,l} &= \quad -\sigma\,|\vec{C}_l|\,(n_{l,x}\,n_{l,z})
\end{aligned}$$

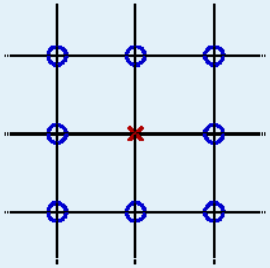

σ : surface tension

$\vec{C}_l$: gradient of phase field $\quad \vec{C}_l(t,\vec{x}) = \dfrac{3}{2\,c\,\Delta t}\sum_i w_i \dfrac{\vec{e}_i}{c}\,\theta(t,\vec{x}+\vec{e}_i\Delta t_l)$

$n_{l,\alpha}$: vector normal to phase interface $\quad n_{l,\alpha} = \dfrac{C_{l,\alpha}}{|\vec{C}_l|}$

implementation of a new extension of the Rothmann Keller model

separation: (algorithm of Toelke et. al., 2001)

$$max\ \vec{C}\cdot\vec{j}^{p}(after\ separation) = max\ \vec{C}\cdot\sum_i \vec{e}_i f_i^{p}(after\ separation)$$

maximum separation of phases by recoloring (optimization problem!)

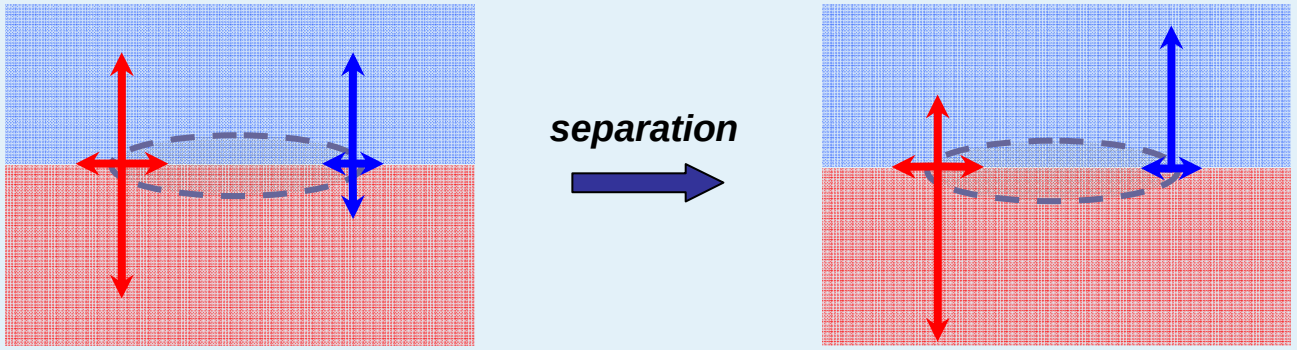

after collision ***after separation***

advection of phase field information (additional to the flow field advection):

$$g_{i,l,p}(t+\Delta t_l, \vec{x}+\vec{e}_i\Delta t_l) = g_{i,p}^{eq}\left(\rho_p(t,\vec{x}), \vec{u}(t,\vec{x})\right)$$

with $$g_{i,p}^{eq}\left(\rho_p(t,\vec{x}), \vec{u}(t,\vec{x})\right) = w_i\,\rho_p(t,\vec{x})\left(1+\frac{3}{c^2}\vec{e}_i\cdot\vec{u}(t,\vec{x})\right)$$

$$p = red,\ blue$$

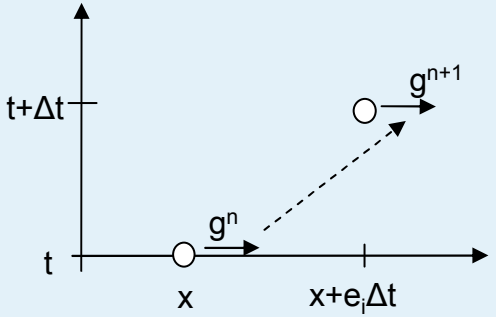

comparison of refinement types for one and multi phase flow simulations

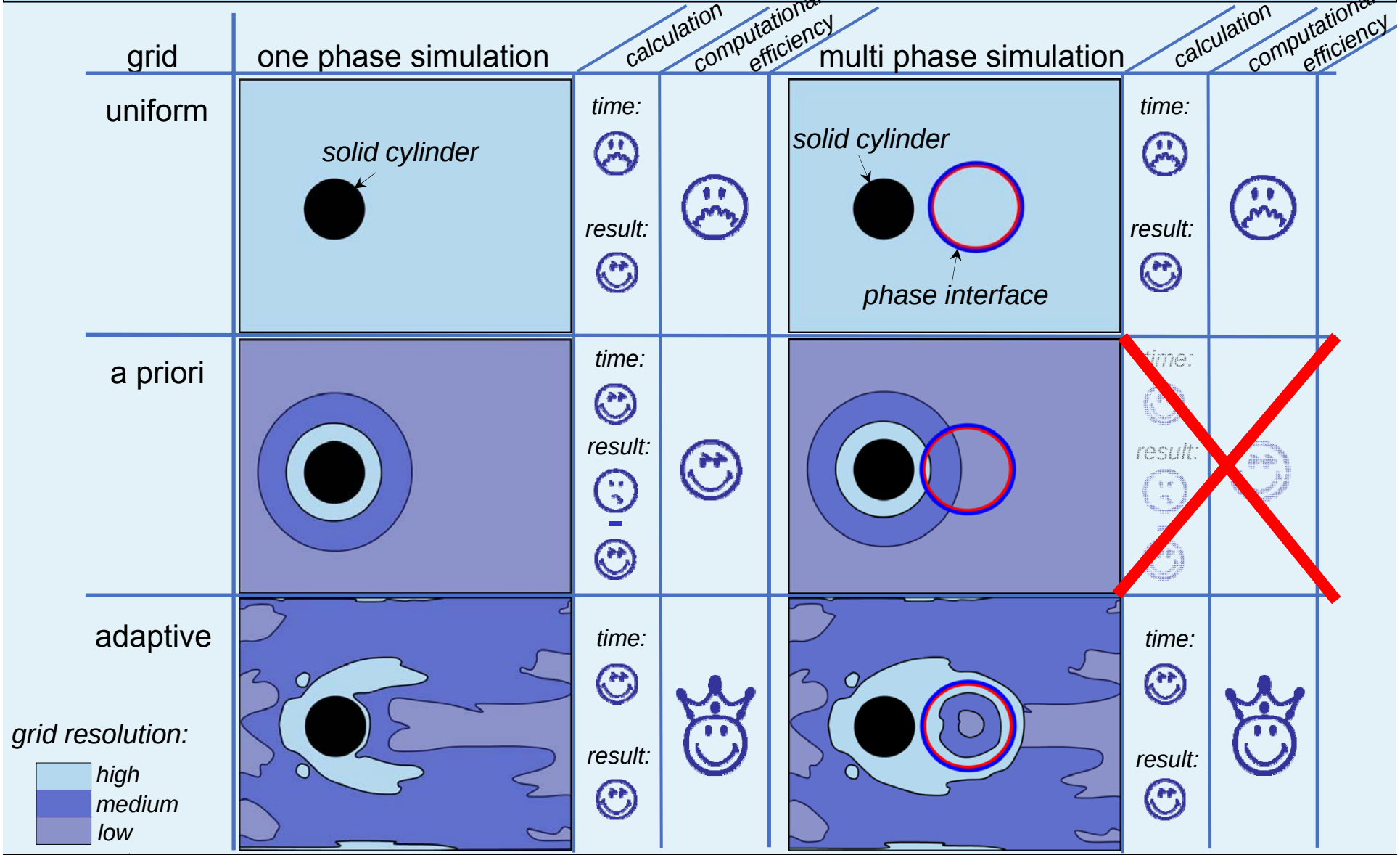

multiphase simulations on a priori refined grids (phase interface crosses grid interface) I

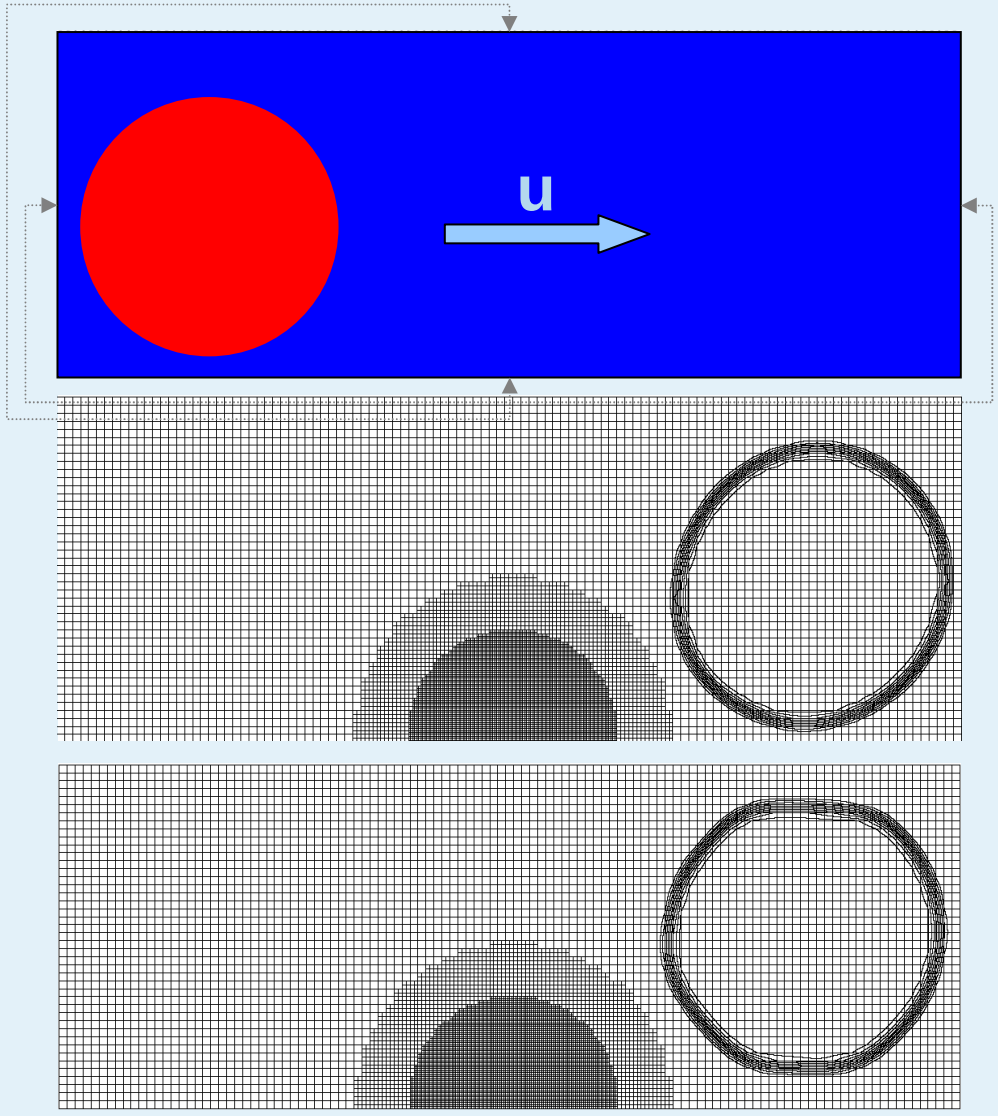

$u = 0.05\ m/s,\ \sigma = 0.01\ N/m$

$u = 0.05\ m/s,\ \sigma = 0.1\ N/m$

$u = 0.05\ m/s,\ \sigma = 0.00\ N/m$

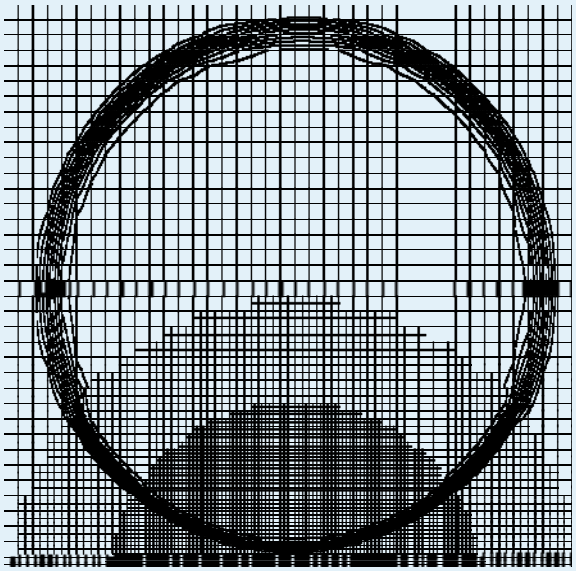

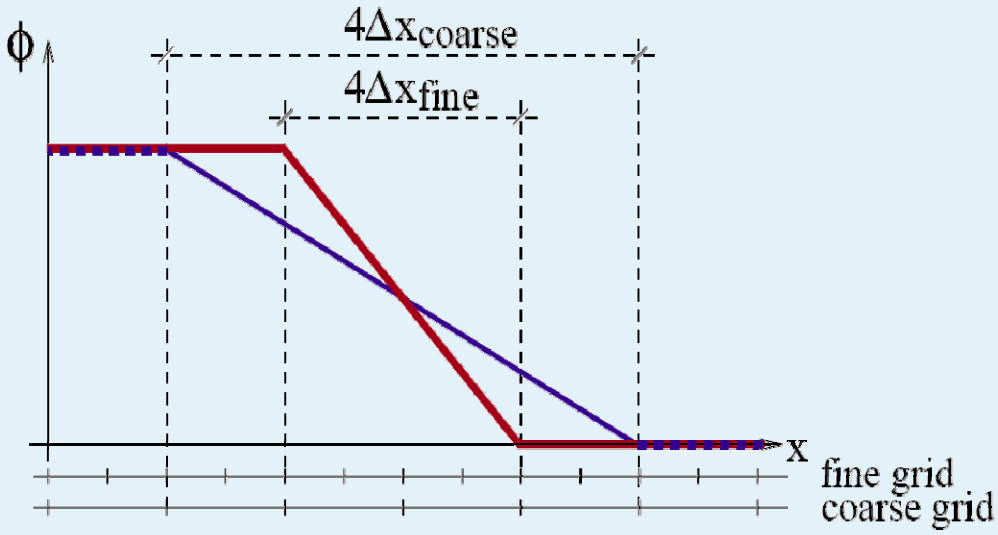

phase field gradient depends on grid level

conclusion I

multiphase simulations with phase interface crossing grid levels

- *possible with limitations*
- *stable parameter range is limited*
- *different width of phase interface on different grid levels*

fundamental idea of non uniform grids:

local resolution of gradients

→ relating to multiphase flow simulations: resolving the phase interface

implementation possible at

- *a priori grid refinement?* 
- *adaptive grid refinement?* 

validation I – surface tension

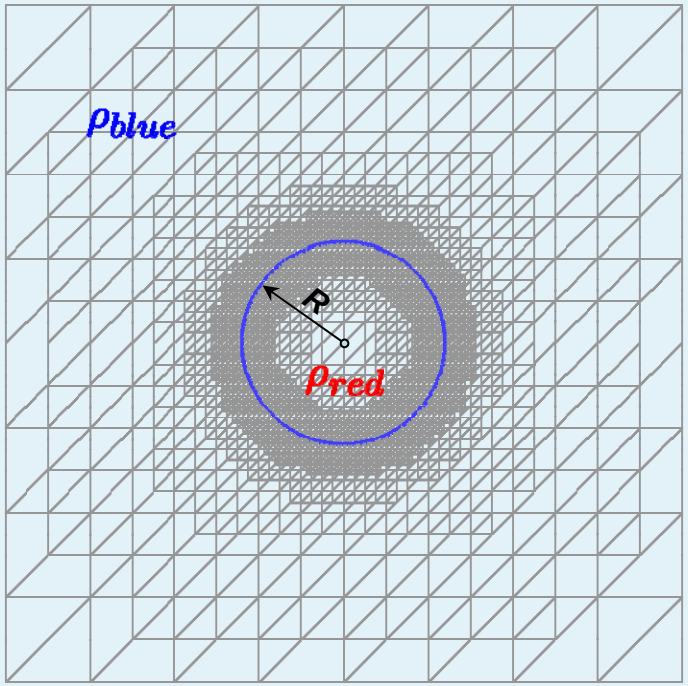

boxed bubble (128x128x128)
6 level refinement
$\vec{v} = 0$

Laplace law: $\sigma = \frac{\Delta p R}{2}$

ν	ρ_b	ρ_r	R	σ	$rel.error$
0.06	1.0	1.0	19	0.1	$1.0E$-5
0.06	1.0	1.0	19	0.01	$1.9E$-5
0.06	2.0	0.5	19	0.1	$1.5E$-5
0.06	2.0	0.5	19	0.01	$1.3E$-5
0.25	1.0	1.0	19	0.1	$1.0E$-5
0.25	1.0	1.0	19	0.01	$2.3E$-5
0.25	2.0	0.5	19	0.1	$2.1E$-5
0.25	2.0	0.5	19	0.01	$1.6E$-5

non uniform calculation is ~8 times faster than the uniform calculation

raising bubble in infinite expanded space - validation II

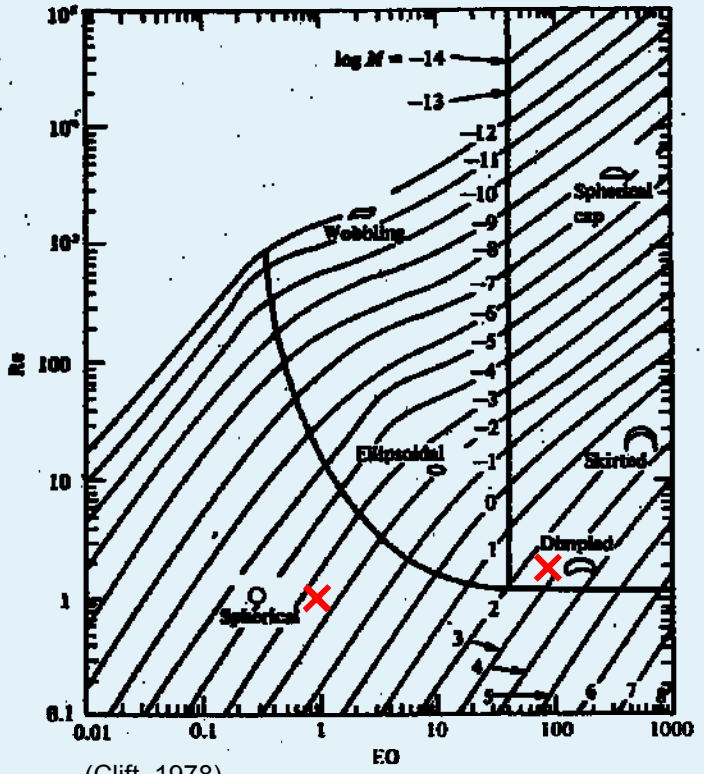

(Clift, 1978)

Eötvös number $$Eo = \frac{g\,\Delta\rho d_e^2}{\sigma}$$

Reynolds number $$Re = \frac{U_T\, d_e\, \rho}{\mu}$$

Morton number $$M = \frac{g\,\mu^4\,\Delta\rho}{\rho^2\,\sigma^3}$$

dimpled regime: $$2Re^2 + 6Re^2\,\frac{2+3\frac{\mu_r}{\mu_b}}{1+\frac{\mu_r}{\mu_b}} - E_o^{\frac{2}{3}} M^{-\frac{1}{2}} = 0$$

spherical regime: $$u = \frac{1}{6}\frac{g d_e^2 \Delta p}{\mu_b}\,\frac{\frac{\mu_r}{\mu_b}+1}{3\frac{\mu_r}{\mu_b}+2}$$

raising bubble (spherical regime) - validation II

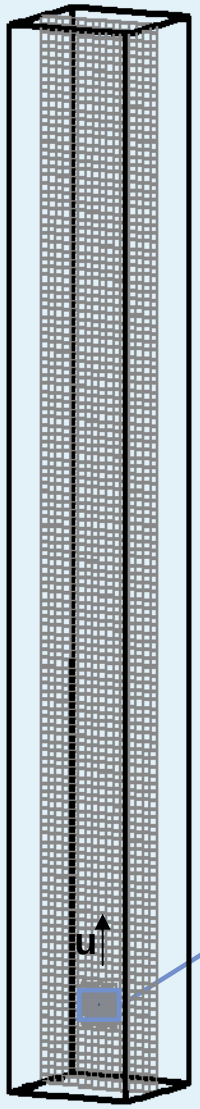

(2049x2049x16392)

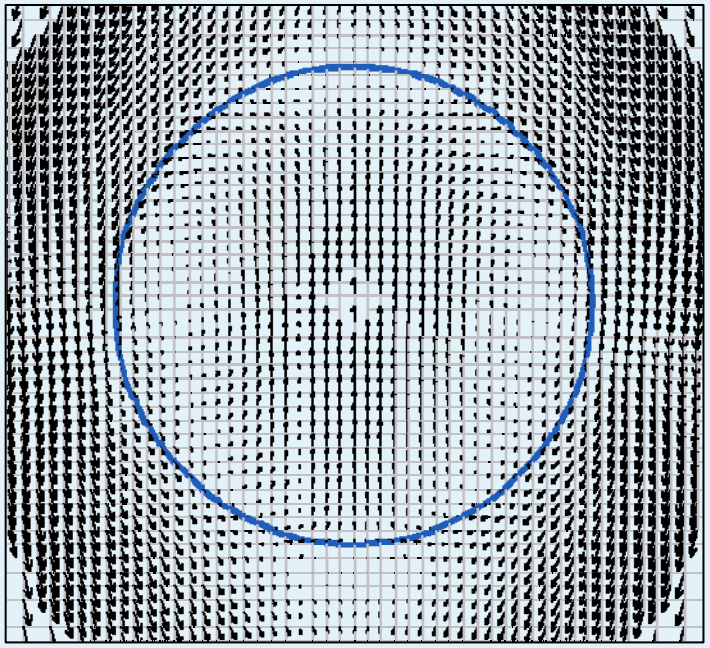

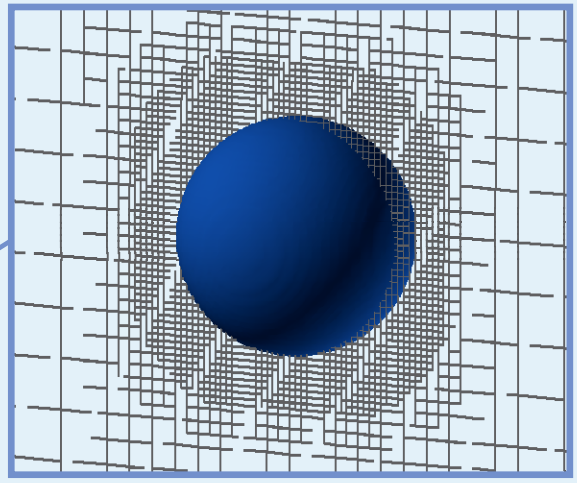

ρ_b	ρ_T	d	ν	σ	g
1.0	1.0	35	0.25	0.01	$2.14E{-}5$

Eo	M	Re	u_t	u_{num}
2.63	0.083	0.98	0.007	0.006

non uniform calculation is ~5 orders of magnitude faster than uniform calculation

	#nodes (*)	level	#nodes per level	%
uniform	$\sim 8.8E12$	11	$6.9E10$	100.0 %
adaptive	$\sim 1.7E07$	11	128270	68.3 %
		10	11799	6.2 %
		9	4237	2.2 %
		8	2541	1.4 %
		7	1238	0.7 %
		6	1181	0.7 %
		5	1206	0.7 %
		4	37156	19.8 %

(*) required node updates for 128 time steps = refinement interval

raising bubble (dimpled regime) - validation II

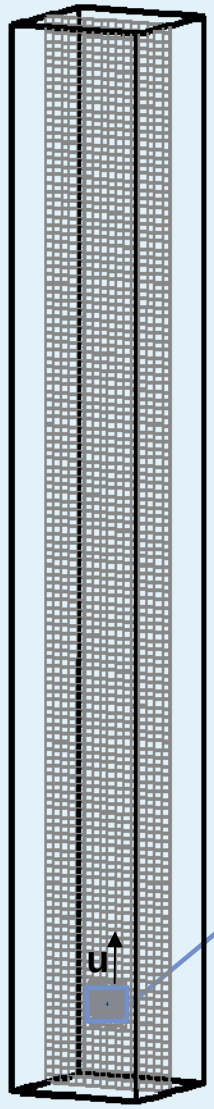

(2049x2049x16392)

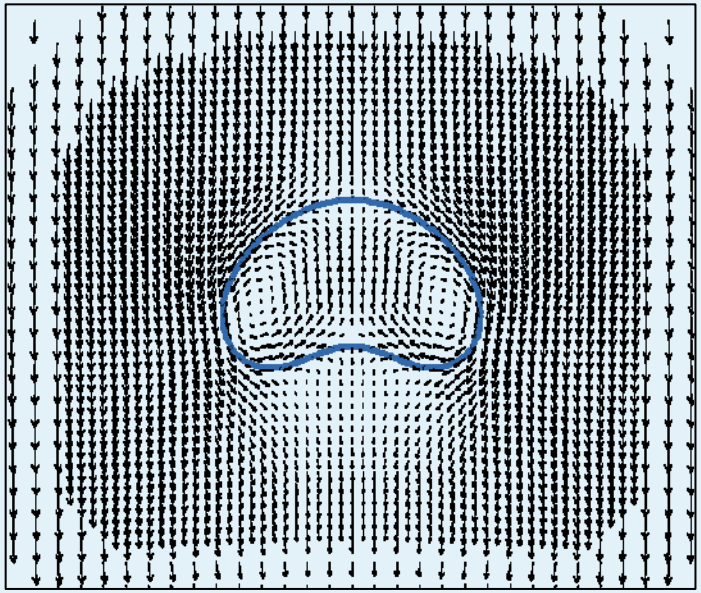

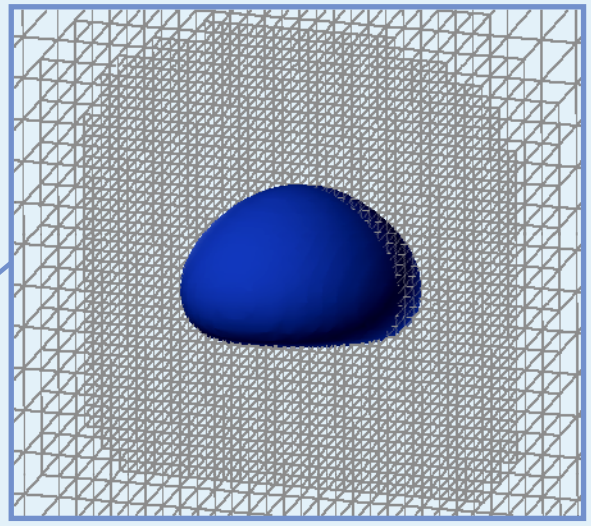

ρ_b	ρ_r	d	ν	σ	g
2.0	0.5	20	0.25	0.003	$1.35E{-}3$

Eo	M	Re	u_t	u_{num}
90	390	2.4	0.03	0.035

non uniform calculation is ~5 orders of magnitudes faster than the uniform calculation

	#nodes (*)	level	#nodes per level	%
uniform	$\sim 8.8E12$	11	$6.9E10$	100.0 %
adaptive	$\sim 1.3E07$	11	97013	70.0 %
		10	10369	7.0 %
		9	3692	2.6 %
		8	2249	1.6 %
		7	1041	0.8 %
		6	964	0.7 %
		5	989	0.7 %
		4	23309	16.6 %

(*) needed node updates for 128 time steps = refinement interval

conclusion II and outlook

- *adaptive grid refinement fulfills fundamental idea for non uniform (multiphase) simulations*
- *encouraging first results*
- *present implementation of mesh refinement is still time-consuming*

To Do

- *improvement of adaptive algorithms*
- *parallelization of the program for:*
  - *uniform grids*
  - *a priori grids*
  - ***adaptive grids***
- *extending program for other simulation models (e. g. LES, Free Surface)*

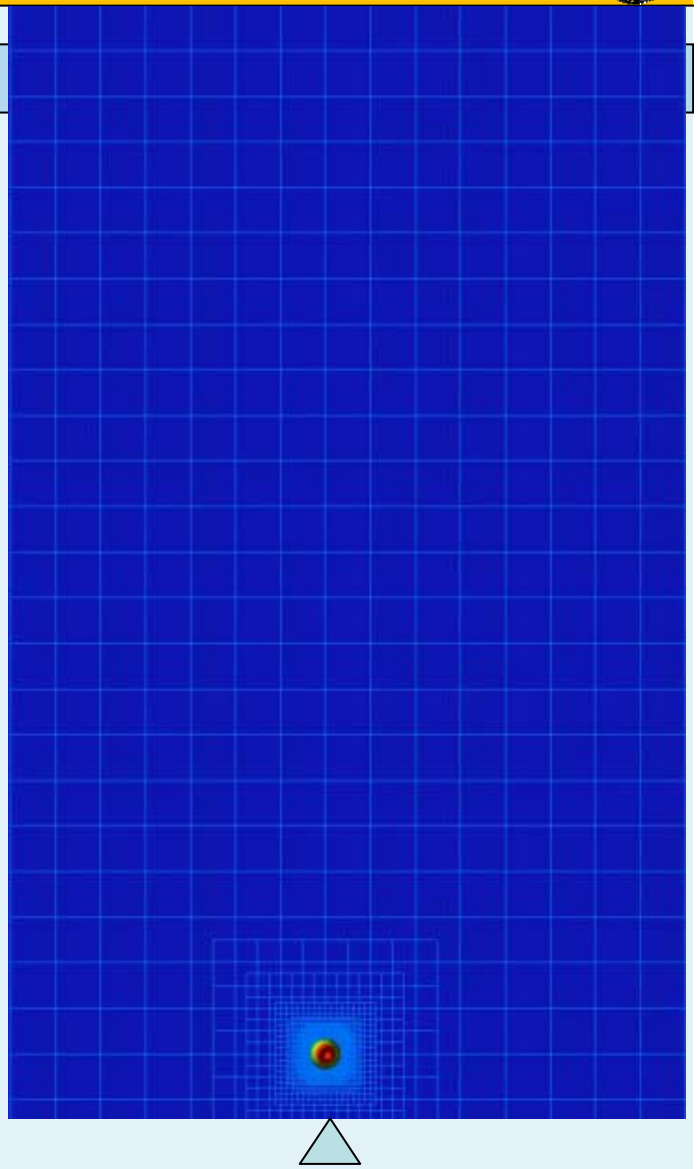

don't try this with uniform grids (YES, it is mass conservative)

Simulation of turbulent flows

	model credibility	computational effort	field of application
DNS	no modelling	extremely high, all scales resolved	low Re flows
LES	modelling of small scales only	medium and large scales resolved	often too complex for engineering applications
RANS	critical closure assumptions	low, only mean flow is calculated	method of choice for engineering applications

Large Eddy Simulation (LES) for LBGK

Eggels, 1998
Teixeira, 1998

algebraic approach:

$$\nu = \nu_0 + \nu_T \qquad \nu_T \propto l^2 \left| S_{\alpha\beta} \right|$$

based on filterwidth / mixing length l
and stress / strain rate tensor S

S is a local quantity ! $$S_{\alpha\beta} \propto \sum_i e_{i\alpha} e_{i\beta} (f_i - f_i^{(eq)})$$

Smagorinsky: $$\nu_T = (C_s \Delta x)^2 \left\| \bar{\varepsilon} \right\| \qquad C_s \in \{0.05, 0.2\}$$

Turbulence: RANS and turbulent viscosity

With $u_i = \underbrace{U_i}_{\text{mean}} + \underbrace{u_i'}_{\text{fluctuating}}$,

the Reynolds averaged momentum equation becomes

$$\frac{\partial U_i}{\partial t} + \frac{\partial}{\partial x_j}(U_i U_j + \overline{u_i' u_j'}) = -\frac{\partial p}{\rho \partial x_i} + \nu \frac{\partial}{\partial x_j}\left(\frac{\partial U_i}{\partial x_j} + \frac{\partial U_j}{\partial x_i}\right)$$

Using the turbulent-viscosity hypothesis (Boussinesq 1877), we obtain

$$\frac{\partial U_i}{\partial t} + \frac{\partial}{\partial x_j}(U_i U_j) = -\frac{\partial p}{\rho \partial x_i} + (\nu + \nu_T) \frac{\partial}{\partial x_j}\left(\frac{\partial U_i}{\partial x_j} + \frac{\partial U_j}{\partial x_i}\right)$$

Turbulence: two equation models

$$\frac{\partial k}{\partial t}+\frac{\partial (U_j k)}{\partial x_j}=\text{sourceterms}+\frac{\partial}{\partial x_j}\left[(\nu+\sigma_k \nu_t)\frac{\partial k}{\partial x_j}\right]$$

$$\frac{\partial \omega}{\partial t}+\frac{\partial (U_j \omega)}{\partial x_j}=\text{sourceterms}+\frac{\partial}{\partial x_j}\left[(\nu+\sigma_\omega \nu_t)\frac{\partial \omega}{\partial x_j}\right]$$

$$\boxed{\nu_t=\frac{k}{\omega}}$$

Turbulence: two equation models

$$\frac{\partial k}{\partial t}+\frac{\partial (U_j k)}{\partial x_j}=\text{sourceterms}+\frac{\partial}{\partial x_j}\left[(\nu+\sigma_k \nu_t)\frac{\partial k}{\partial x_j}\right]$$

$$\frac{\partial \omega}{\partial t}+\frac{\partial (U_j \omega)}{\partial x_j}=\text{sourceterms}+\frac{\partial}{\partial x_j}\left[(\nu+\sigma_\omega \nu_t)\frac{\partial \omega}{\partial x_j}\right]$$

$$\nu_t=\frac{k}{\omega}$$

$$\frac{\partial k}{\partial t}+\frac{\partial\left(U_j k+\sigma_k \frac{\partial \nu_t}{\partial x_j} k\right)}{\partial x_j}=\text{sourceterms}+\frac{\partial}{\partial x_j}\left[\frac{\partial[(\nu+\sigma_k \nu_t)k]}{\partial x_j}\right]$$

$$\frac{\partial \omega}{\partial t}+\frac{\partial\left(U_j \omega+\sigma_\omega \frac{\partial \nu_t}{\partial x_j} \omega\right)}{\partial x_j}=\text{sourceterms}+\frac{\partial}{\partial x_j}\left[\frac{\partial[(\nu+\sigma_\omega \nu_t)\omega]}{\partial x_j}\right]$$

"apparent velocity"

Two equation turbulence models on hierarchical grids

LB methods can be used for solving two-equation turbulence models such as

- k-ε-model (Jones, Launder 1973)
- k-ω-model (Wilcox)
- zonal models (Shear-Stress-Transport-Model (SST) [Menter, 1992])

- for the source terms, numerical differentiation is necessary

The SST model

- combining k-ω-model near walls and k-ε-model in the free stream
- using smart switching function
- able to integrate through the boundary layer without wall functions
- suitable for adverse pressure gradient boundary-layer flows

The SST model: Boundary conditions

at no-slip walls (u=0):

$$k = 0,$$

$$\omega = \frac{2500\nu}{k_s^{\,2}} \quad (\text{"slightly-rough-surface"-BC, Wilcox}), \quad k_s < 5\delta_v$$

=> multireflection for Dirichlet boundary conditions (Ginzburg 2005)

$$f_{\bar{i}}(\vec{r}_b, t+1) = (0.5-\delta_i)\tilde{f}_i(\vec{r}_b, t) + (\delta_i - 1)\tilde{f}_i(\vec{r}_b - \vec{e}_i, t) + 0.5\tilde{f}_{\bar{i}}(\vec{r}_b, t) + f_i^{eq}(\text{wall})$$

Turbulent channel flow: The law of the wall

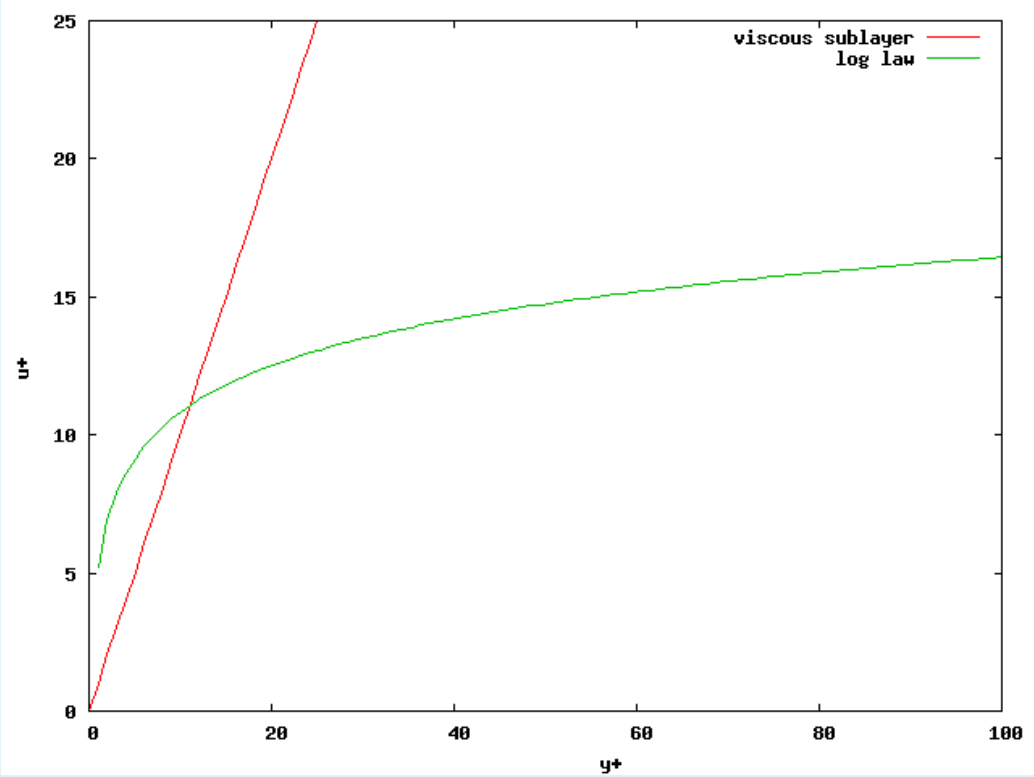

$$u^+ = \frac{\bar{u}}{u_\tau}, \quad y^+ = \frac{y}{\delta_v}$$

$$u_\tau = \sqrt{\frac{\tau_W}{\rho}}, \quad \delta_v = \frac{\upsilon}{u_\tau}$$

Refinement of near wall region

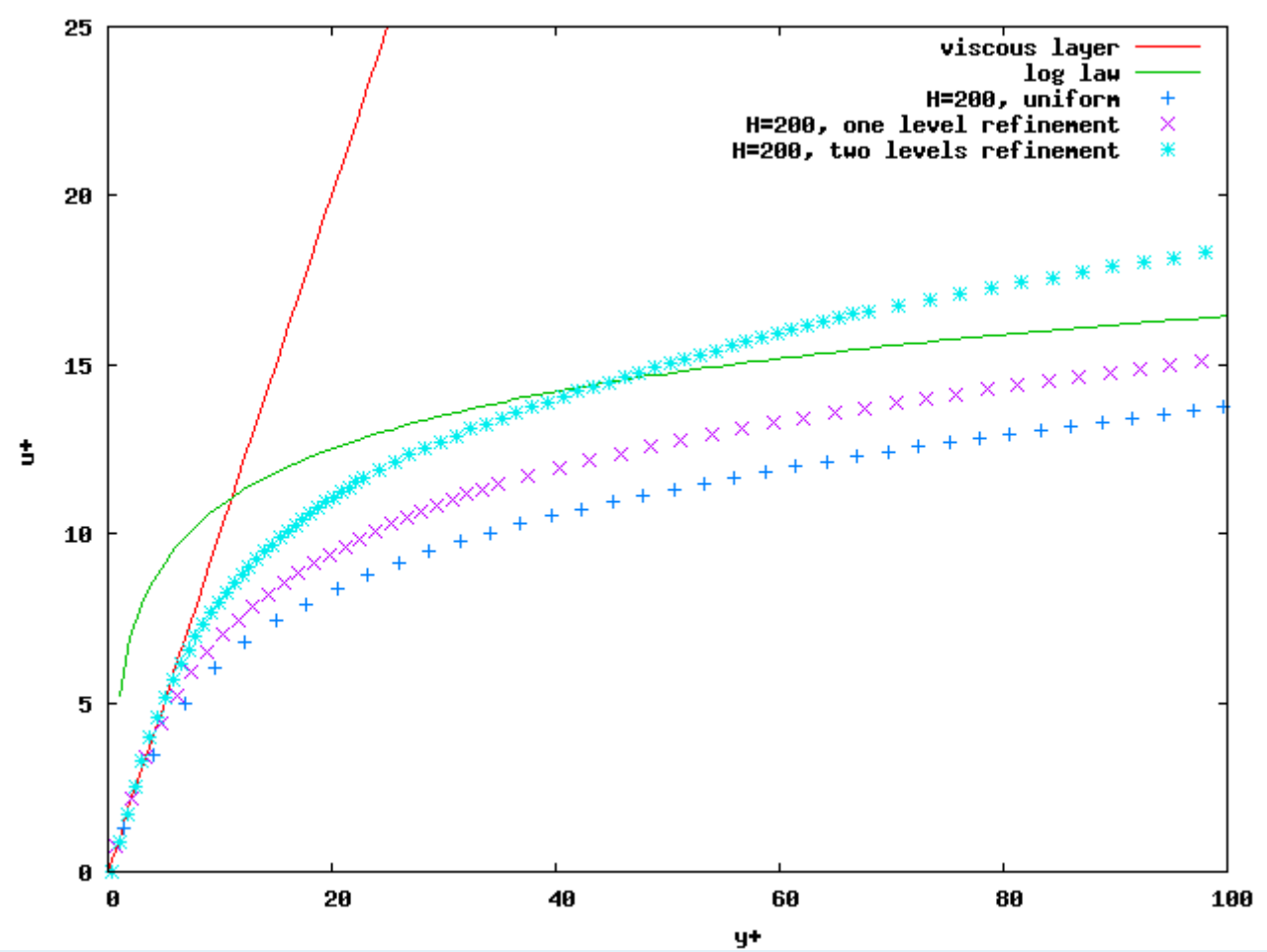

Re=11.000

Influence of wall roughness

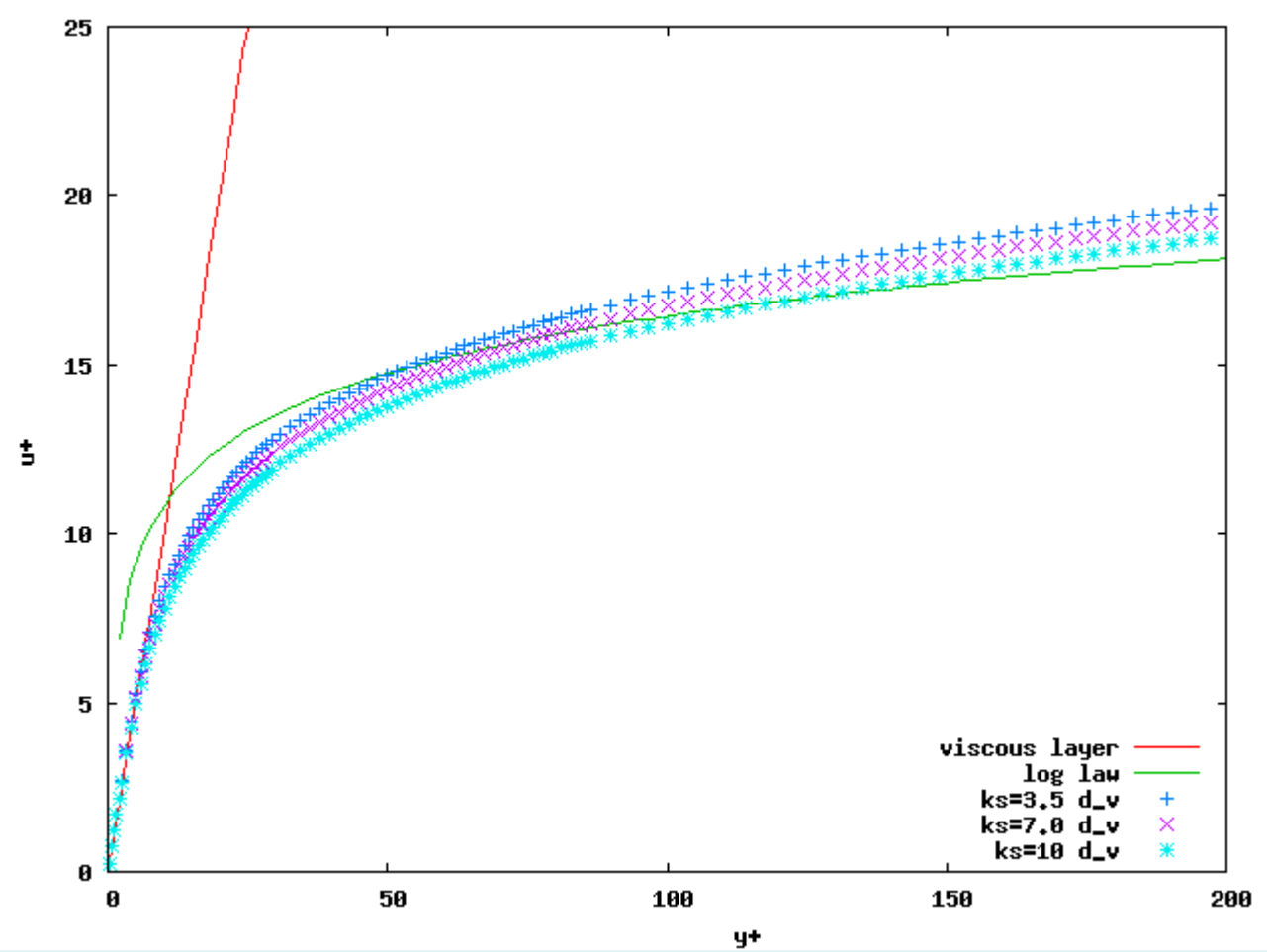

Re=15.000,
Ma=0.07

Channel flow at different Re numbers

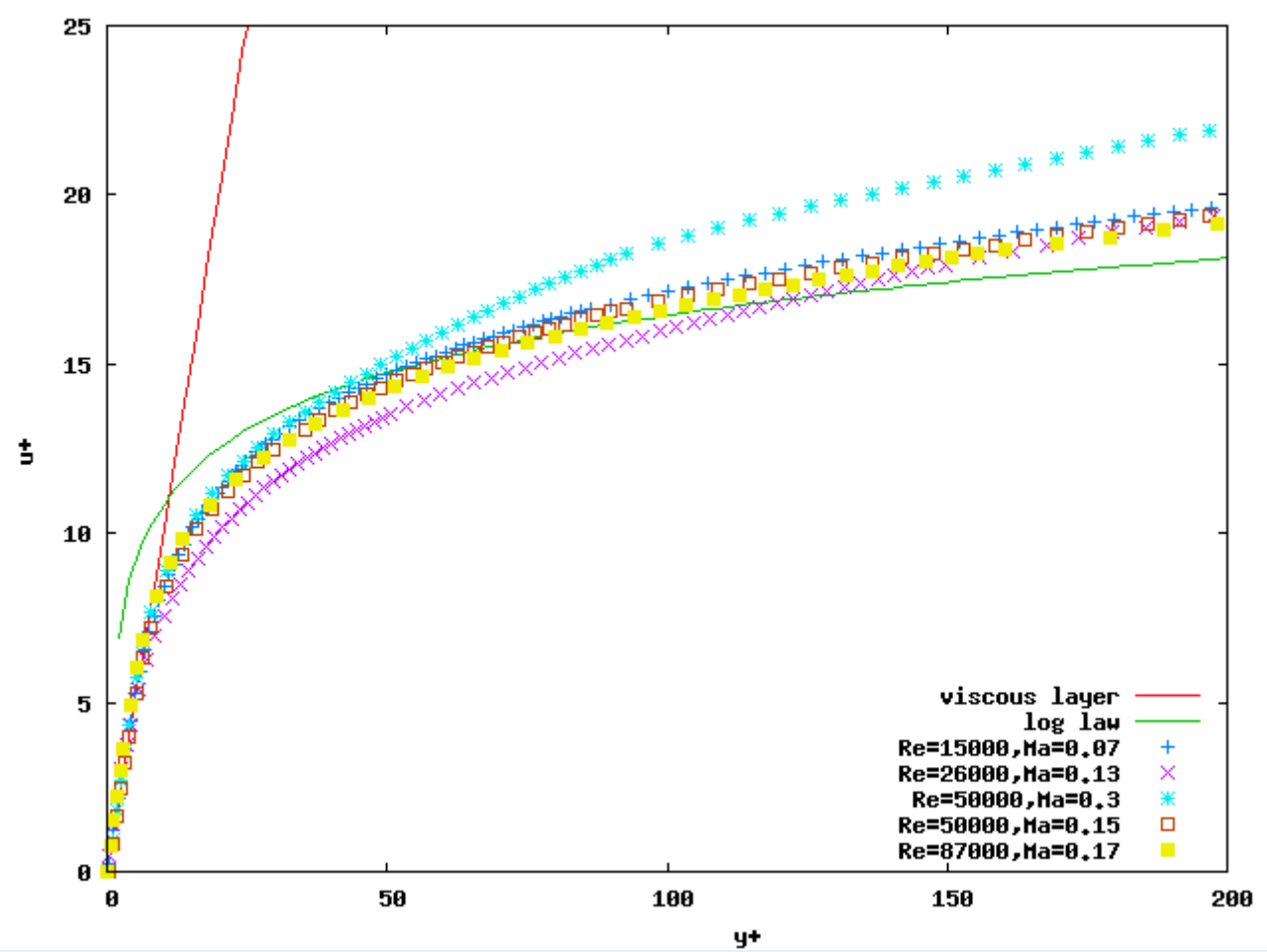

Channel flow at different Ma numbers

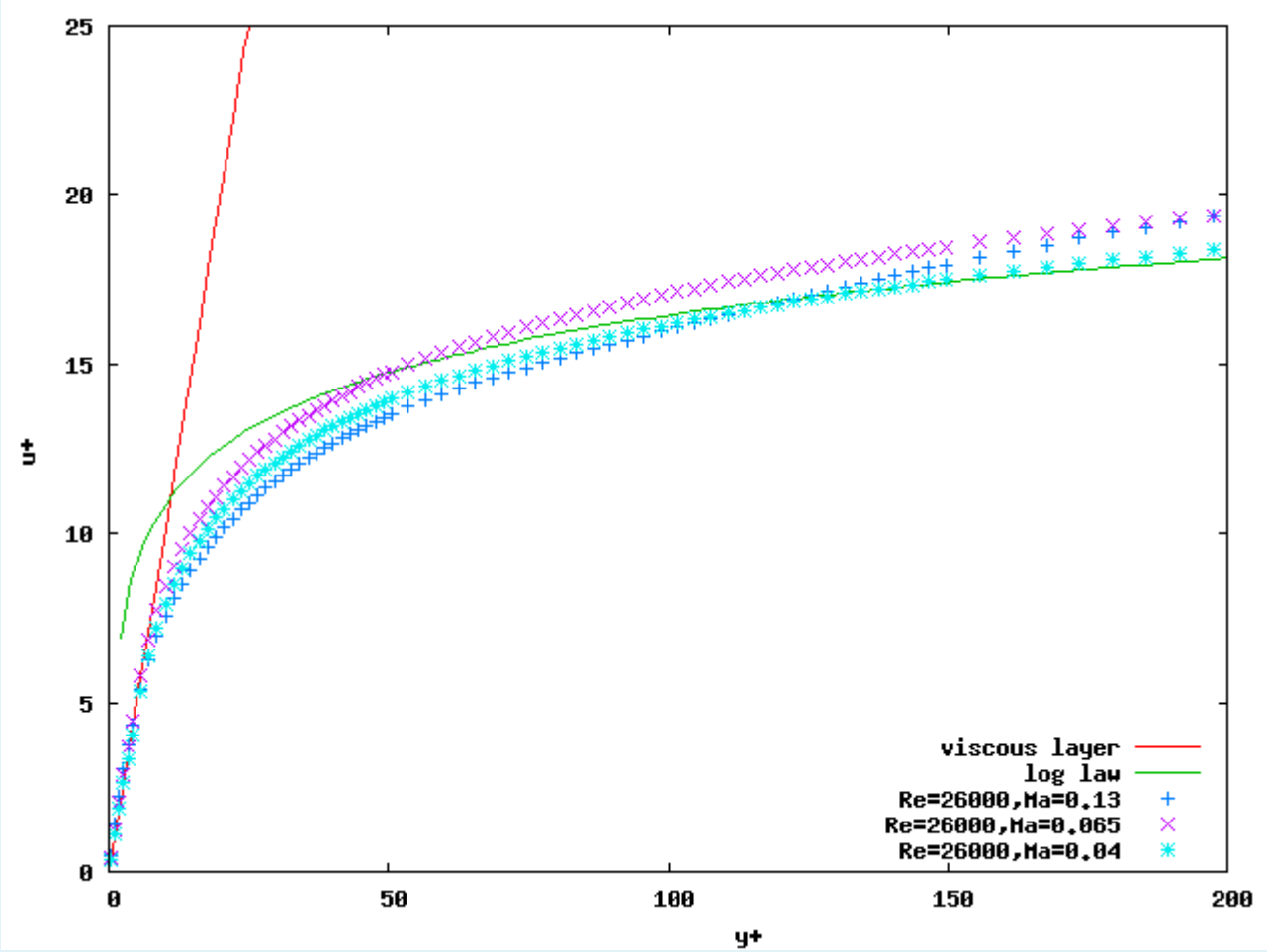

Re=26.000

kinetic turbulence modelling

the vast majority of LB simulations of turbulent flows are based on

LES or other classical closure models.

Recently so-called entropic models have been developed (S. Ansumali et al. Physica A 338 (2004) 379-394, Bruce M. Boghosian et al., Physica D 193 (2003) 169-181).

These schemes are unconditionally stable due to a built-in „H-function“.

Yet, the unresolved scales do not yet show the correct wave number spectrum.

Thus at present these models can only be regarded as numerical limiters.

A genuinely kinetic turbulence model is yet to be developed.

Another line to substantially improve the stability of LB-methods is the so-called cascaded LB approach by Geier (PRE 2006). A specific sequence of MRT-type relaxations in combination with improved Galilean invariance of third order moments allows
A substantial increase in cell Reynolds numbers